Steel Diaphragms in Prestressed Concrete Girder Bridges

Iowa DOT Project TR-424
CTRE Project 99-36

Sponsored by
the Iowa Department of Transportation
and the Iowa Highway Research Board

Iowa Department of Transportation

CTRE
Center for Transportation Research and Education

Department of Civil, Construction and Environmental Engineering

Iowa State University

Final Report • September 2004

CTRE's mission is to develop and implement innovative methods, materials, and technologies for improving transportation efficiency, safety, and reliability while improving the learning environment of students, faculty, and staff in transportation-related fields.

Technical Report Documentation Page

1. Report No. TR-424	2. Government Accession No.	3. Recipient's Catalog No.	
4. Title and Subtitle Steel Diaphragms in Prestressed Concrete Girder Bridges		5. Report Date September 2004	
		6. Performing Organization Code	
7. Author(s) Robert E. Abendroth, Fouad S. Fanous, and Bassem O. Andrawes		8. Performing Organization Report No.	
9. Performing Organization Name and Address Center for Transportation Research and Education Iowa State University 2901 South Loop Drive, Suite 3100 Ames, IA 50010-8634		10. Work Unit No. (TRAIS) 11. Contract or Grant No.	
12. Sponsoring Organization Name and Address Iowa Department of Transportation 800 Lincoln Way Ames, IA 50010		13. Type of Report and Period Covered Final Report, January 1999 to September 2004 14. Sponsoring Agency Code	
15. Supplementary Notes This report is available in color at www.ctre.iastate.edu.			

16. Abstract

Over the years, bridge engineers have been concerned about the response of prestressed concrete (PC) girder bridges that had been hit by over-height vehicles or vehicle loads. When a bridge is struck by an over-height vehicle or vehicle load, usually the outside and in some instances one of the interior girders are damaged in a bridge. The effect of intermediate diaphragms in providing damage protection to the PC girders of a bridge is not clearly defined. This analytical study focused on the role of intermediate diaphragms in reducing the occurrence of damage in the girders of a PC-girder bridge that has been struck by an over-height vehicle or vehicle load. The study also investigated whether a steel, intermediate diaphragm would essentially provide the same degree of impact protection for PC girders as that provided by a reinforced-concrete diaphragm.

This investigation includes the following: a literature search and a survey questionnaire to determine the state-of-the-art in the use and design of intermediate diaphragms in PC-girder bridges. Comparisons were made between the strain and displacement results that were experimentally measured for a large-scale, laboratory, model bridge during previously documented work and those results that were obtained from analyses of the finite-element models that were developed during this research for that bridge. These comparisons were conducted to calibrate the finite element models used in the analyses for this research on intermediate diaphragms. Finite-element models were developed for non-skewed and skewed PC-girder bridges. Each model was analyzed with either a reinforced concrete or two types of steel, intermediate diaphragms that were located at mid-span of an interior span for a PC-girder bridge. The bridge models were analyzed for lateral-impact loads that were applied to the bottom flange of the exterior girders at the diaphragms location and away from the diaphragms location. A comparison was conducted between the strains and displacements induced in the girders for each intermediate-diaphragm type.

These results showed that intermediate diaphragms have an effect in reducing impact damage to the PC girders. When the lateral impact-load was applied at the diaphragm location, the reinforced-concrete diaphragms provided more protection for the girders than that provided by the two types of steel diaphragms. The three types of diaphragms provided essentially the same degree of protection to the impacted, PC girder when the lateral-impact load was applied away from the diaphragm location.

17. Key Words bridges, collisions, damage, diaphragms, finite-element, girders, impacts, prestressed		18. Distribution Statement No restrictions.	
19. Security Classification (of this report) Unclassified.	20. Security Classification (of this page) Unclassified.	21. No. of Pages 151	22. Price NA

STEEL DIAPHRAGMS IN PRESTRESSED CONCRETE GIRDER BRIDGES

Iowa DOT Project TR-424

Principal Investigators
Robert E. Abendroth
Associate Professor of Civil Engineering

Fouad S. Fanous
Professor of Civil Engineering
Iowa State University

Research Assistant
Bassem O. Andrawes

Preparation of this report was financed in part
through funds by the Iowa Department of Transportation
through its research management agreement with the
Center for Transportation Research and Education, Project 99-36.

Center for Transportation Research and Education
Iowa State University
ISU Research Park
2901 South Loop Drive, Suite 3100
Ames, IA 50010-8634
Phone: 515-294-8103
Fax: 515-294-0467
www.ctre.iastate.edu

Final Report • September 2004

TABLE OF CONTENTS

LIST OF FIGURES v

ACKNOWLEDGEMENTS xi

1. INTRODUCTION 1

1.1. Background 1
1.2. Problem statement 2
1.3. Objective and scope 3
1.4. Literature review 4
1.5. Review of current department of transportation practice 9

2. EXPERIMENTAL BRIDGE MODEL 13

2.1. Introduction 13
2.2. Model description 13
2.3. Intermediate diaphragms 16
2.4. Loading mechanisms 18

3. FINITE ELEMENT MODEL OF AN EXPERIMENTAL BRIDGE 19

3.1. Introduction 19
3.2. Model description 19
3.3. Support conditions 21
3.4. Intermediate diaphragms 23
3.4.1. Preliminary models 24
3.4.1.1. Reinforced concrete intermediate diaphragm 24
3.4.1.2. Steel channel intermediate diaphragm 25
3.4.1.3. Steel X-braced with horizontal strut intermediate diaphragm 26
3.4.2. Refined models 27
3.4.2.1. Reinforced concrete intermediate diaphragm 27
3.4.2.2. Steel channel intermediate diaphragm 28
3.4.2.3. Steel X-braced with horizontal strut intermediate diaphragm 32
3.5. Load cases 33
3.5.1. Preliminary models 33
3.5.2. Refined models 35
3.6. Sub-models 35
3.6.1. Introduction 35
3.6.2. Steel channel intermediate diaphragm sub-model 36
3.6.3. Steel X-braced with horizontal strut intermediate diaphragm sub-model 40
3.7. Comparison of analytical and experimental results 43
3.7.1. Comparison of displacements 43
3.7.2. Comparison of strains 45

4. FINITE ELEMENT MODELS OF PROTOTYPE PC GIRDER BRIDGES....47

4.1. Introduction....47
4.2. Bridges selected for the analyses....47
4.2.1. Non-skewed bridge....47
4.2.2. Skewed bridge....51
4.3. Finite-element models of a non-skewed bridge....54
4.3.1. Description of the finite-element model....54
4.3.1.1. Four-span finite-element model....54
4.3.1.2. Single-span finite-element model....58
4.3.2. Intermediate diaphragms....59
4.3.2.1. Reinforced concrete intermediate diaphragm....59
4.3.2.2. Steel X-braced with horizontal strut intermediate diaphragm....64
4.3.2.3. Steel K-braced with horizontal strut intermediate diaphragm....69
4.3.3. Load cases....69
4.4. Finite element model of the skewed bridge....74
4.4.1. Model description....74
4.4.2. Intermediate diaphragms....75
4.4.3. Load cases....76

5. ANALYSIS RESULTS....79

5.1. Introduction....79
5.2. Four-span and one-span finite element models....79
5.3. Non-skewed bridge model....81
5.3.1. Strains....81
5.3.1.1. Reinforced concrete intermediate diaphragms....83
5.3.1.2. Steel X-braced with horizontal strut intermediate diaphragms....91
5.3.1.3. Steel K-braced with horizontal strut intermediate diaphragms....97
5.3.2. Displacements....101
5.3.3. Strain and displacement comparisons....112
5.3.3.1. Strain comparisons....112
5.3.3.2. Displacement comparisons....124
5.3.4. Four foot load case....127
5.4. Skewed bridge model....129
5.5. Maximum principal-tensile strain locations....134

6. CLOSING REMARKS....137

6.1. Summary....137
6.2. Conclusions....140
6.3. Recommendations for future work....144

REFERENCES....145

APPENDIX A: DESIGN AGENCY QUESTIONNAIRE RESULTS....147

LIST OF FIGURES

Figure 2.1. Experimental bridge 14

Figure 2.2. PC-girder cross section 15

Figure 2.3. Abutment and end diaphragm 16

Figure 2.4. Reinforced concrete intermediate diaphragm 17

Figure 2.5. Steel channel intermediate diaphragm 17

Figure 2.6. Steel X-braced with horizontal strut intermediate diaphragm 18

Figure 3.1. Finite element model of an experimental bridge 20

Figure 3.2. Supports condition of the finite element model of the experimental bridge 22

Figure 3.3. Reinforced concrete diaphragm for the preliminary finite element model 24

Figure 3.4. Steel channel diaphragm for the preliminary finite element model 26

Figure 3.5. Steel X-braced with horizontal strut diaphragm for the preliminary finite element model 27

Figure 3.6. Reinforced concrete diaphragm for the refined finite element model 29

Figure 3.7. Steel channel diaphragm for the refined finite element model 30

Figure 3.8. Steel X-braced with horizontal strut diaphragm for the refined finite element model 32

Figure 3.9. The load locations considered in the analysis 34

Figure 3.10. Vertical and horizontal load locations considered in the preliminary and refined finite element models 34

Figure 3.11. Steel channel diaphragm sub-model 37

Figure 3.12. Steel X-braced diaphragm sub-model 41

Figure 3.13. Horizontal load versus horizontal displacement at Point 1 for the no diaphragm condition 44

Figure 3.14. Horizontal load versus horizontal displacement at Point 1 for the RC diaphragms 44

Figure 4.1. Longitudinal section at centerline of the roadway for the Marshall County Bridge (Adapted from the Iowa DOT-Highway Division design details).....48

Figure 4.2. Cross section of Marshall County Bridge (Adapted from the Iowa DOT-Highway Division design details, File no. 27498, Sheet no. 8).....50

Figure 4.3. Cross section of an Iowa "Type-D" PC girder.....51

Figure 4.4. Diaphragms at the abutments and piers (Adapted from the Iowa DOT-Highway Division design details, File no. 27498, Sheet no. 9).....52

Figure 4.5. Longitudinal section at centerline of the roadway for the Johnson County Bridge (Adapted from Iowa DOT-Highway Division design details, file no. 26197, sheet no. 2).....53

Figure 4.6. Cross section of the four-span, non-skewed, finite-element bridge model.....55

Figure 4.7. Cross section of the roadway passing beneath the bridge.....56

Figure 4.8. Boundary conditions considered in the analysis of the four-span finite element model.....57

Figure 4.9. Iowa DOT reinforced concrete diaphragms (adapted from the Iowa DOT standard details).....60

Figure 4.10. Connection between the RC diaphragms and the PC girders.....63

Figure 4.11. Iowa DOT X-braced with horizontal strut diaphragm (adapted from the Iowa DOT standards).....65

Figure 4.12. Finite element model of a cross bracing member (view looking along the member length).....67

Figure 4.13. Iowa DOT K-braced with horizontal strut diaphragm (adapted from the Iowa DOT standards).....70

Figure 4.14. Load locations.....72

Figure 4.15. Force versus time relations used in simulating lateral-impact loads.....73

Figure 4.16. Arrangement of the intermediate diaphragms in the skewed bridge.....74

Figure 4.17. Load locations of the skewed bridge model.....76

Figure 5.1. Maximum principal-tensile strain versus time for the four-span and one-span models without diaphragms (load and strains at the mid-span of Beam BM1).....80

Figure 5.2. Horizontal displacement versus time for the four-span and one-span models (load and displacement at the mid-span of Beam BM1).....81

Figure 5.3. Maximum principal-tensile strain versus time for the RC diaphragms (no load offset on Beam BM1) 83

Figure 5.4. Maximum principal-tensile strain distribution along a portion of Beam BM1 for the RC diaphragms (no load offset on Beam BM1) 84

Figure 5.5. Maximum principal-tensile strain versus time for the RC diaphragms (no load offset on Beam BM5) 85

Figure 5.6. Maximum principal-tensile strain distribution along a portion of Beam BM5 for the RC diaphragms (no load offset on Beam BM5).....88

Figure 5.7. Maximum principal-tensile strain versus time for the RC diaphragms (16-ft load offset on Beam BM1).....89

Figure 5.8. Maximum principal-tensile strain versus time for the RC diaphragms (16-ft load offset on Beam BM5).....90

Figure 5.9. Maximum principal-tensile strain versus time for the X-braced diaphragms (no load offset on Beam BM1).....92

Figure 5.10. Maximum principal-tensile strain distribution along a portion of Beam BM1 for the X-braced diaphragms (no load offset on Beam BM1) 92

Figure 5.11. Maximum principal-strain versus time for the X-braced diaphragms (no load offset on Beam BM5) 94

Figure 5.12. Maximum principal-tensile strain distribution along a portion of BM5 for the X-braced diaphragms (no load offset on Beam BM5) 96

Figure 5.13. Maximum principal-tensile strain versus time for the X-braced diaphragms (16-ft offset load on Beam BM1).....96

Figure 5.14. Maximum principal-tensile strain versus time for the X-braced diaphragms (16-ft load offset on Beam BM5).....97

Figure 5.15. Maximum principal-tensile strain versus time for the K-braced diaphragms (no load offset on Beam BM1) 98

Figure 5.16. Maximum principal-tensile strain distribution along a portion of BM1 for the K-braced diaphragms (no load offset on Beam BM1) 99

Figure 5.17. Maximum principal-tensile strain versus time for the K-braced diaphragms (no load offset on Beam BM5) 99

Figure 5.18. Maximum principal-tensile strain distribution along a portion of BM5 for the K-braced diaphragms (no load offset on Beam BM5) 100

Figure 5.19. Maximum principal-tensile strain versus time for the K-braced diaphragms (16-ft load offset on Beam BM1)....102

Figure 5.20. Maximum principal-tensile strain versus time for the K-braced diaphragms (16-ft load offset on Beam BM5)....102

Figure 5.21. Horizontal displacement versus time for the RC diaphragms (no load offset on Beam BM1)....104

Figure 5.22. Horizontal displacement versus time for the X-braced diaphragms (no load offset on Beam BM1)....104

Figure 5.23. Horizontal displacement versus time for the K-braced diaphragms (no load offset on Beam BM1)....105

Figure 5.24. Horizontal displacement versus time for the RC diaphragms (no load offset on Beam BM5)....106

Figure 5.25. Horizontal displacement versus time for the X-braced diaphragms (no load offset on Beam BM5) 107

Figure 5.26. Horizontal displacement versus time for the K-braced diaphragms (no load offset on Beam BM5) 107

Figure 5.27. Horizontal displacement versus time for the RC diaphragms (16-ft load offset on Beam BM1)....108

Figure 5.28. Horizontal displacement versus time for the X-braced diaphragms (16-ft load offset on Beam BM1)....109

Figure 5.29. Horizontal displacement versus time for the K-braced diaphragms (16-ft load offset on Beam BM1)....109

Figure 5.30. Horizontal displacement versus time for the RC diaphragms (16-ft load offset on Beam BM5)....110

Figure 5.31. Horizontal displacement versus time for the X-braced diaphragms (16-ft load offset on Beam BM5)....111

Figure 5.32. Horizontal displacement versus time for the K-braced diaphragms (16-ft load offset on Beam BM5).....111

Figure 5.33. Maximum principal-tensile strain in Beam BM1 versus time for the diaphragm conditions (no load offset on Beam BM1).....113

Figure 5.34. Maximum principal-tensile strain distribution along a portion of Beam BM1 for the diaphragm conditions (no load offset on Beam BM1).....114

Figure 5.35. Maximum principal-tensile strains in Beams BM1 and BM2 for the diaphragm conditions in the non-skewed bridge (no load offset on Beam BM1 116

Figure 5.36. Forces in the X-braced and K-braced diaphragms for the simplified models 117

Figure 5.37. Maximum principal-tensile strains in BM5 versus time for the diaphragm conditions (no load offset on Beam BM5).....119

Figure 5.38. Maximum principal-tensile strain distribution along a portion of BM5 for the diaphragm conditions (no load offset on Beam BM5).....120

Figure 5.39. Maximum principal-tensile strains in Beams BM5 and BM4 for the diaphragm conditions in the non-skewed bridge (no load offset on Beam BM5).....121

Figure 5.40. Maximum principal-tensile strain in Beam BM1 versus time for the diaphragm conditions (16-ft load offset on Beam BM1).....122

Figure 5.41. Maximum principal-tensile strain in Beam BM5 versus time for the diaphragm conditions (16-ft load offset on Beam BM5).....123

Figure 5.42. Horizontal displacement of Beam BM1 versus time for the diaphragm conditions (no load offset on Beam BM1).....124

Figure 5.43. Horizontal displacement of Beam BM5 versus time for the diaphragm conditions (no load offset on Beam BM5).....125

Figure 5.44. Horizontal displacement of Beam BM1 versus time for the diaphragm conditions (16-ft offset on Beam BM1).....126

Figure 5.45. Horizontal displacement of Beam BM5 versus time for the diaphragm conditions (16-ft offset on Beam BM5).....126

Figure 5.46. Maximum principal-tensile strain in Beam BM1 versus time for the diaphragm conditions (4-ft load offset on Beam BM1).....128

Figure 5.47. Maximum principal-tensile strains in Beams BM1 and BM2 for the diaphragm conditions in the skewed bridge (no load offset on Beam BM1) 129

Figure 5.48. Maximum principal-tensile strains in Beams BM5 and BM4 for the diaphragm conditions in the skewed bridge (no offset load on Beam BM5) 131

Figure 5.49. Maximum principal-tensile strains in Beam BM1 for the diaphragm conditions in the skewed bridge (16-ft offset load on Beam BM1).....133

Figure 5.50. Locations for maximum principal-tensile strains 135

ACKNOWLEDGEMENTS

The Iowa Highway Research Board of the Iowa Department of Transportation (Iowa DOT) provided funding for the research project (Project No. TR-424). The members of the research advisory board were Norm McDonald, Bridge Engineer with the Iowa DOT, Darren Moon, Assistant Bridge Engineer with the Story County Engineering Office, Ray Andrews with Andrews Prestressed Concrete, and Dan Timmons with Jensen Construction Company. The authors wish to acknowledge their input and guidance. Also, the authors extend their appreciation to Denise Wood, Structures Secretary, for her typing of this final report.

1. INTRODUCTION

1.1. Background

Over the years bridge engineers have been concerned about the response of prestressed concrete (PC) girder bridges that have been hit by over-height vehicles or vehicle loads. According to (Shanafelt and Horn, 1980), for each year, about 200, PC-girder bridges in the United States are damaged. About 162 of these bridges are damaged by over-height vehicles or vehicle loads. The actual number of impacts was expected to be significantly higher than these numbers since many minor collisions are not reported. When a bridge is struck by an over-height vehicle, usually the outside and in some instances one or more of the interior bridge girders are damaged.

Historically, engineers with the Office of Bridges and Structures of the Iowa Department of Transportation (Iowa DOT) have required the use of reinforced concrete (RC), intermediate diaphragms in all PC-girder bridges that cross over highways. The use of RC intermediate diaphragms by the Iowa DOT is based on an intuitive damage assessment of the PC bridge girders that is caused by impacts from over-height traffic beneath the bridge. Bridge engineers with the Iowa DOT believe that the larger mass, stiffness and damping characteristics of a RC, intermediate diaphragm, when compared to those characteristics of a steel, intermediate diaphragm, provide a greater degree of impact protection for the bridge girders.

Bridge contractors have always expressed a desire to substitute steel, intermediate diaphragms for the RC, intermediate diaphragms in order to reduce the construction time and to simplify the construction process for PC girder bridges. With the continued use of PC sub-deck panels for the bridge decks that are constructed in Iowa, precast-concrete manufacturers have renewed their desire to have the current-design policy regarding intermediate diaphragms

changed to permit the use of a simpler configuration for a steel intermediate diaphragm in place of a RC intermediate diaphragm.

In July of 1989, the Iowa Highway Research Board sponsored a research project whose objective was to investigate the behavior of steel and RC, intermediate diaphragms. Design alternatives for a steel, intermediate diaphragm that could be used in place of a RC, intermediate diaphragm were documented in the final report (Abendroth et al., 1991) of that work. One configuration for a steel, intermediate diaphragm was reported to essentially provide the same behavioral response to statically applied, lateral forces as that provided by the RC, intermediate diaphragm. However, the recommended steel diaphragm was not used by bridge contractors due to the complexity of the steel bracket assembly that was needed to match the profile of a PC girder.

The Office of Bridges and Structures of the Iowa DOT recently developed a steel, intermediate diaphragm that was a modification of the suggested diaphragm (Abendroth et al., 1991). The modified steel diaphragm was used for the West Town Parkway Bridge in West Des Moines that has Iowa LXD girders and in the Mason City bypass bridge that has 72-in.-deep, bulb-tee PC girders. The configuration of this diaphragm is presented later in this report. Both of these two bridges have highway traffic beneath them; however, the height clearance beneath these bridges is greater than usual. Therefore, the possibility of impacts to the PC girders of these two bridges by an over-height vehicle is minimal.

1.2. Problem statement

Intermediate diaphragms for PC girder bridges provide stability to the girders during bridge construction, contribute to the lateral distribution of vertical wheel loads that are applied to the bridge deck of multi-girder bridges, and help to distribute lateral-impact forces from over-

height vehicles or vehicle loads. Previous research and publications regarding girder stability and vertical-load distribution have adequately addressed these two topics. Very few publications have discussed the behavior of PC girder bridges with different types of intermediate diaphragms when a bridge is subjected to lateral loads. The work presented in this report addresses this concern, and discusses whether a steel, intermediate diaphragm with simple connections to the PC girders provides essentially the same degree of damage protection as that provided by the RC, intermediate diaphragm currently being used by the Iowa DOT.

1.3. Objective and scope

The overall objectives of this work involve extensive and detailed analytical studies. No experimental work was conducted during this research program. However, published test results for similar structures were used to calibrate the theoretical findings. The following research objectives have been identified:

- Review and evaluate the state-of-the-art regarding the role of intermediate diaphragms in distributing lateral loads through out PC girder bridges.
- Investigate the performance of different types and configurations of intermediate diaphragms in PC girder bridges.
- Recommend an efficient type of steel, intermediate diaphragm that can be used as an alternate for a RC, intermediate diaphragm in Iowa, PC-girder bridges. The selected steel diaphragm should essentially maintain the same degree of damage protection for the PC girders as that provided by a RC diaphragm, when over-height vehicles or vehicle loads impact against the bottom flange of the bridge girders.

Verification of the accuracy of any analytical analysis, such as a finite-element analysis, is necessary to gain confidence in the modeling technique that is used for the finite-element

method. Thus, a comparison was made by the ISU researchers between the measured strain and displacement results that were obtained for an experimental bridge, which was tested during the earlier ISU research (Abendroth et al., 1991), and those predicted results that were obtained from the finite-element model, which was developed during this new research, for the same bridge. Several types of intermediate diaphragm were modeled and studied in the comparison. The finite-element models were analyzed for the same cases of loading that were used for the testing the experimental-bridge model. A description of the experimental bridge model, finite-element model, and experimental and analytical results are presented in this report.

The finite-element-modeling techniques that were applied during the verification study were then used to analyze two in service bridges. Each model represented a PC girder bridge with similar properties and dimensions that were used by the Iowa DOT for this type of a bridge. One of the models was for a skewed bridge and the other model was for a non-skewed bridge. Each of these bridge models was analyzed considering different types of intermediate diaphragms. Complete descriptions of the finite-element models and the loading cases used in the analysis are presented in this report. Predicted strain and displacement responses of the bridges were calculated and compared for each of the different diaphragm types.

1.4. Literature review

A literature review was conducted on the topics related to the behavior of PC-girder bridges that were subjected to lateral-impact loads. The search also covered the topics related to the effectiveness of intermediate diaphragms in distributing lateral load. The search focused on the use of RC or steel diaphragms in resisting lateral-impact loads that might result from an over-height vehicle or vehicle load passing beneath a bridge. In addition, the available publications

discussing the crash tests (crashworthiness) conducted on vehicles were reviewed to study the techniques used in modeling the impact load resulting from collisions.

Several domestic and international databases were utilized in this search. Among the domestic databases were the NTIS (National Technical Information Service), EI Compendex, GSCI (General Science Abstract), ASTI (Applied Science and Technology Abstracts), the ASCE civil engineering database, Journal of Structural Engineering, the Northwest Transport Catalog, and the Iowa State University Catalog. Although there was a large number of publications that discuss the existence of intermediate diaphragms in bridges, a very few number of these publications were concerned about the role of diaphragms in distributing lateral loads. Most of the literature found was discussing the effectiveness of diaphragms when a bridge is subjected to normal traffic load. Very few publications discussed the use of steel diaphragms in conjunction with PC girder bridges.

Different opinions were noticed in the publications discussing whether the intermediate diaphragms are essential in the PC-girder bridges. Although Article 9.10.2 in the Standard Specifications for Highway Bridges (AASHTO, 1996) requires the use of intermediate diaphragms at the points of maximum moments for spans over than 40 ft, clear reasons for such requirements were not given.

Wei (1959) conducted an analytical study of a simple-span, non-skewed, I-beam bridge, which had a concrete roadway slab that was continuous over steel stringers. Steel, intermediate diaphragms, which may be in the form of steel channel, a WF-beam, or a built-up section were inserted in the bridge at different locations. The study was conducted under several types of vertical loading including a single load, a standard-truck load, and a four-wheel-truck load. Wei found that in the case of the single and standard-truck load, the addition of diaphragms reduces

the maximum moments in the interior beams. On the contrary, when the diaphragms are used in the case of the four-wheel-truck load, the maximum moment increased in the girders.

The effectiveness of diaphragms in distributing the load was investigated by Sithichaikasem and Gamble (1972) and Wong and Gamble (1973). These investigations involved analytical studies to determine the effectiveness of diaphragms in distributing loads in simple and continuous, PC-girder and slab, highway bridges. Sithichaikasem and Gamble focused on a simple-span bridge case. Some of their results were:

- Diaphragms cause an increase in the maximum moment in the bridge girders in the case when the outer line of the wheels can fall directly over the exterior girders. Thus, their recommendation was to eliminate intermediate diaphragms.
- The location and spacing of diaphragms should not be a function of the span length alone. In many cases diaphragms are more effective in short bridges than longer ones.
- The flexural stiffness of the diaphragms should be carefully selected. Diaphragms that have a flexural stiffness greater than an optimum value may increase the moments in the girders.

Wong and Gamble, 1973, conducted a similar analysis for a continuous bridge. Some of their results were:

- An improvement of the load-distribution characteristics was noticed in the case of bridges that have a large, beam-spacing-to-span-length ratio.
- In most cases, intermediate diaphragms are harmful to PC girders.

There appears to be conflicting evidence as to whether the diaphragms are damage-limiting or damage-spreading members. Sithichaikasem and Gamble (1972) and Wong and Gamble (1973)

suggested that the diaphragms currently being used in bridges are probably the wrong shape and size and are usually in the wrong locations.

Sengupta and Breen (1973) studied the effectiveness of using diaphragms in PC-girder and slab bridges. The cast-in-place, concrete diaphragm was the only type of diaphragm that was discussed in this research. Their experimental research was conducted by testing four, 1/5.5-scale, micro-concrete, simple-span, model bridges with a series of vertical and lateral loads. The variables that were considered for their tests were the length of the bridge, the skew angle, and the locations for intermediate diaphragms. These authors tested four models with and without intermediate diaphragms under cyclic and impact loads. Several simplified analytical models were used to complete the objectives of their work. The following findings were documented by these authors:

- The use of diaphragms increased the design moments for the exterior girders and reduced the design moment for interior girders. The diaphragms were found to be more effective in reducing the girder moments in the case of bridges with large, girder-spacing-to-span ratios and large, girder-stiffness-to-slab-stiffness ratios.
- Vertical, static-load tests revealed that bridges of this type can carry considerable overloads without causing any considerable damage to the girders.
- End diaphragms greatly increase both the ultimate and concrete-cracking loads.
- When bridges were subjected to sustained-cyclic load, diaphragms did not influence the dynamic amplifications (natural frequency) of the bridges and no effect was observed on the damping coefficient of bridge vibration.

- Testing with a lateral-impact load hitting the bottom flange of an exterior girder, revealed that the diaphragms reduce the energy-absorption capacity of the girders, which makes the girders more vulnerable to be damaged from the lateral impact.

Based on these conclusions, Sengupta and Breen (1973) recommended the removal of intermediate diaphragms in PC-girder bridges. End diaphragms were recommended to be provided in bridges unless an alternative can be used such as a thickening of the end slab or providing additional reinforcement in the slab for the approach-span zone.

Kostem and Decasto (1977) performed a finite-element analysis for two existing, simple-span, non-skewed, PC-girder bridges. The analysis focused on the effect that diaphragms had on the lateral distribution of vertical live loads. An HS20-44 truck was placed near the mid-span of the bridge to produce maximum bending moment at the mid-span. The load was moved laterally to simulate the effect of different lane loading. The following results were documented by Kostem and DeCastro:

- Mid-span diaphragms are not fully effective in the lateral distribution of live load for PC girder bridges.
- Increasing the number of diaphragms along the length of the bridge does not necessarily correspond to a more uniform distribution of the load at the maximum-moment sections.
- When all bridge lanes were loaded, diaphragms do not noticeably contribute to the lateral distribution of live load.

Cheung, et al. (1986) reported that there was a disagreement on the effectiveness of intermediate diaphragms in laterally distributing the vertical load. The economic impact on the bridge cost with and without intermediate diaphragms was also addressed in some literature such

as McCathy, et al. (1979). These authors determined that if the intermediate diaphragms are omitted, a reduction of three to five percent is expected in the costs of bridge superstructures.

Analytical investigations that addressed vehicle collisions were also conducted using a number of finite-element, computer programs that have several, dynamic-analysis capabilities, which are not available in ANSYS (DeSalvo and Swanson, 1985). Because of these programming differences, these publications were not very useful in providing a guide for techniques to model an impact load that results from a vehicle striking an object. Several crashworthiness publications (Abdullatif, et al., 1996; Nalepa, 1960; Doong and Cheng, 1994; Omar, et al., 1998; and Johnson, et al., 1992) provided some information regarding the properties and duration time of an impact load.

1.5. Review of current department of transportation practice

In addition to the literature search, a survey was conducted of the departments of transportation in several states to obtain information related to the design and use of intermediate diaphragms for bridges. A copy of the questionnaire that was used in the survey and the responses to the questionnaire are presented in Appendix A. The questionnaire addressed the following topics:

- Whether a bridge-design agency is currently using or has ever used intermediate diaphragms in PC girder bridges.
- Types of intermediate diaphragms that are currently used by each agency when a bridge is passing over a highway, navigable waterway, railway, or a grade separation that has no traffic beneath the bridge.
- Design criteria used for intermediate diaphragms.

- Design criteria used for the connections between diaphragms and the bridge deck or and/or girders.
- Performance evaluation of each diaphragm type in minimizing the damage to PC girders that is caused by a lateral impact from an over-height load passing beneath the bridge.

Approximately 75 percent of the agencies that were contacted responded to the survey. Almost 95 percent of the respondents said that they are currently using intermediate diaphragms in PC girder bridges. Less than 40 percent of these agencies use structural-steel intermediate diaphragms in PC girder bridges. The reason for using structural-steel diaphragms varied between agencies. About 40 percent of them claimed that bridge contractors have not chosen to use a reinforced concrete diaphragm, while 70 percent of the agencies use steel diaphragms for different reasons. The most common reasons given by agencies for using steel diaphragms were that they were faster, easier and cheaper to install than cast-in-place RC diaphragms. One of the reasons of using steel diaphragms was to provide stability for the structure during construction.

About 95 percent of the respondents said that their agencies permit using cast-in-place RC diaphragms in PC girder bridges passing over highways, while 75 percent of the respondents claimed that their agencies permit the use of different types of steel diaphragms for the same type of bridges in the same situation. In the case of a PC bridge crossing a navigable waterway, almost 90 percent of the agencies said they permit using cast-in-place RC diaphragms, while about 65 percent of the agencies permit the use of different types of steel diaphragms. The agency responses for diaphragm use when a bridge is over a railroad right-of-way were almost the same as those given for a bridge crossing a highway. Approximately 90 percent of the agencies permit using the cast-in-place RC diaphragm when a PC-girder bridge passes over a

grade separation that has no traffic (highway, water or rail), while 70 percent of the agencies said they permit the use of steel diaphragms in the same case.

When the agencies were asked whether intermediate diaphragms are used for temporary lateral support of the PC girders during the bridge construction, about 90 percent of the respondents gave a positive answer. About 70 percent of the respondents said they do not use intermediate diaphragms to minimize the damage to PC girders that could be caused by an impact from an over-height vehicle or vehicle load passing beneath the bridge. Although 25 percent of the agencies said they have developed a structural-steel diaphragm that can be used as an alternate to a RC or PC diaphragms in PC-girder bridges, almost none of these agencies have any specific criteria in designing these steel diaphragms or their connections with the bridge deck and/or girders. The bridge-design agencies were asked to rate each intermediate- diaphragm type based on its overall performance in minimizing the damage to the PC girders caused by a lateral impact from an over-height load passing beneath the bridge. About 80 percent of the respondents, which rated a cast-in-place, RC diaphragm, rated this type of a diaphragm as good or excellent. Among the respondents, which rated the steel diaphragms, 90 percent of these respondents rated steel diaphragms as average and good.

Each bridge-design agency was asked to attach a copy of the standard details and specifications that they use for all types of intermediate diaphragms for PC-girder bridges. About 75 percent of the respondents included a copy of their standard details and specifications for the types of diaphragms that are currently used by their agencies in PC-girder bridges. The majority of the details were for cast-in-place concrete diaphragms. The types of steel diaphragms included steel-channel diaphragms, bent-plate (channel shape) diaphragms, and

cross-braced diaphragms with or without a horizontal strut. These drawings were reviewed for information that might be helpful in conducting this research.

2. EXPERIMENTAL BRIDGE MODEL

2.1. Introduction

The advancements in computer technology and finite-element programs has permitted the analysis of complex structures. However, the accuracy of the results of any finite-element analysis depends on the knowledge and experience of the person conducting such an analysis. Therefore, a comparison of finite-element results to published experimental-test results or to well-documented, analytical work is strongly recommended. Based on this recommendation a finite-element model was developed for the experimental-bridge model that was previously tested in the earlier research by Abendroth, et al. (1991). This chapter briefly describes the experimental-bridge model that was used in earlier research work.

2.2. Model description

Figure 2.1 shows the bridge model that was used in the previous research (Abendroth, et al., 1991) to study the characteristic behavioral responses of the bridge when subjected to a load applied at the girder bottom flange. The loads applied to the model were either horizontal or vertical or a combination of vertical and horizontal loads. The experimental-bridge model consisted of three, PC girders that were spaced at 6 ft – 0 in. on center. Figure 2.2 shows the PC-girder cross section and its dimensions. The girders were the Iowa DOT, LXA38 beams. The three girders supported a 4-in. thick, reinforced-concrete deck that was 40 ft – 4 in. long and 18-ft wide. The deck had a 3-ft-wide overhang that was measured from the center of each exterior girder. At each end of the bridge model, a 42-in. deep by 18-in. wide, reinforced-concrete abutment supported the ends of the PC girders. The abutments rested on the laboratory floor.

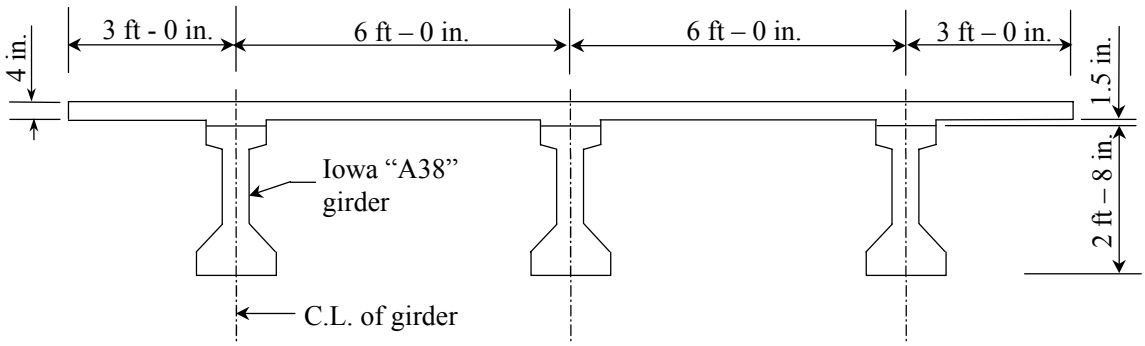

a. Section A-A

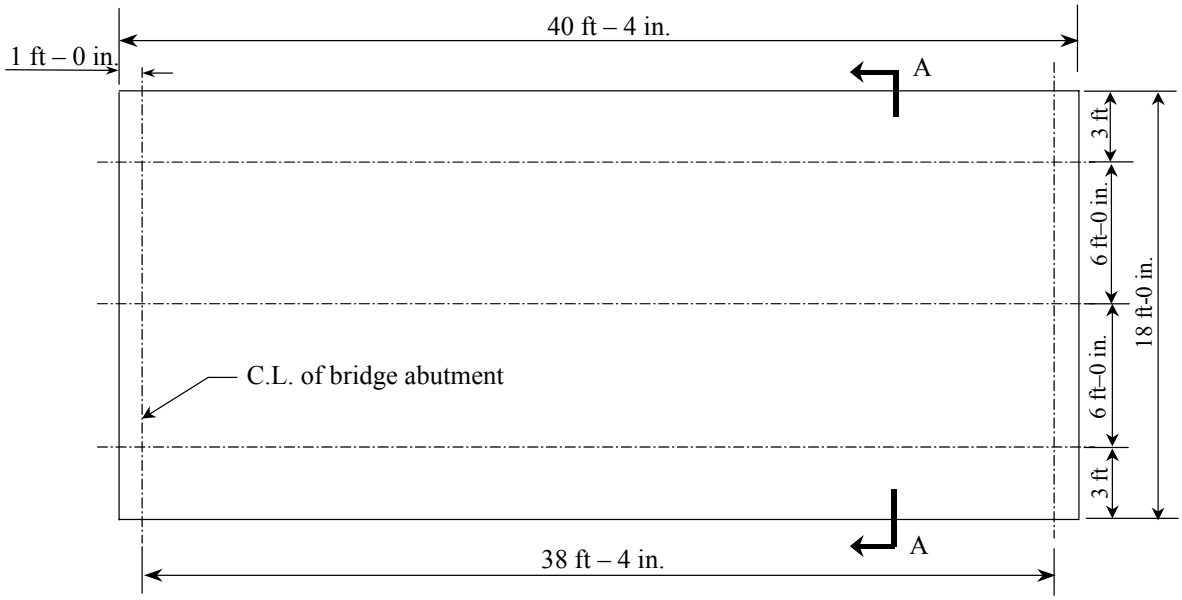

b. Plan view

Figure 2.1. Experimental bridge

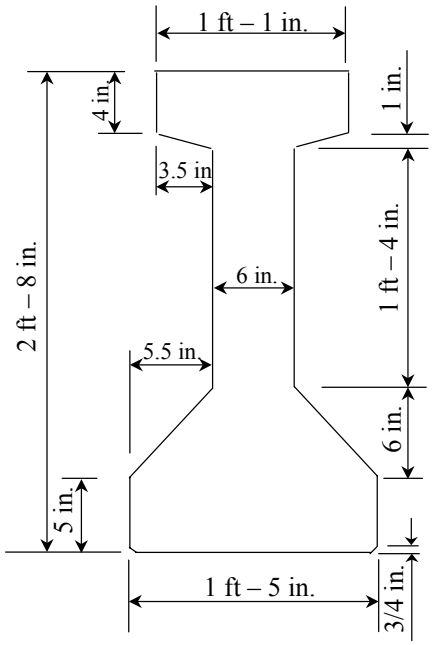

Figure 2.2. PC-girder cross section

The end of each girder was placed on an elastomeric, bridge-bearing pad. The distance between the centerline of the bridge abutments was 38 ft – 4 in. An 8-in. thick, reinforced-concrete, end diaphragm was cast at each end of the PC girders. Figure 2.3 shows the full-depth, RC, end diaphragm. To provide a structural connection between the end diaphragms and the abutments, No.5 reinforcing bars were extended from the abutment into the end diaphragm. The No.5 reinforcing bars were also used to provide a monolithic joint between the RC, end diaphragms and the bridge deck.

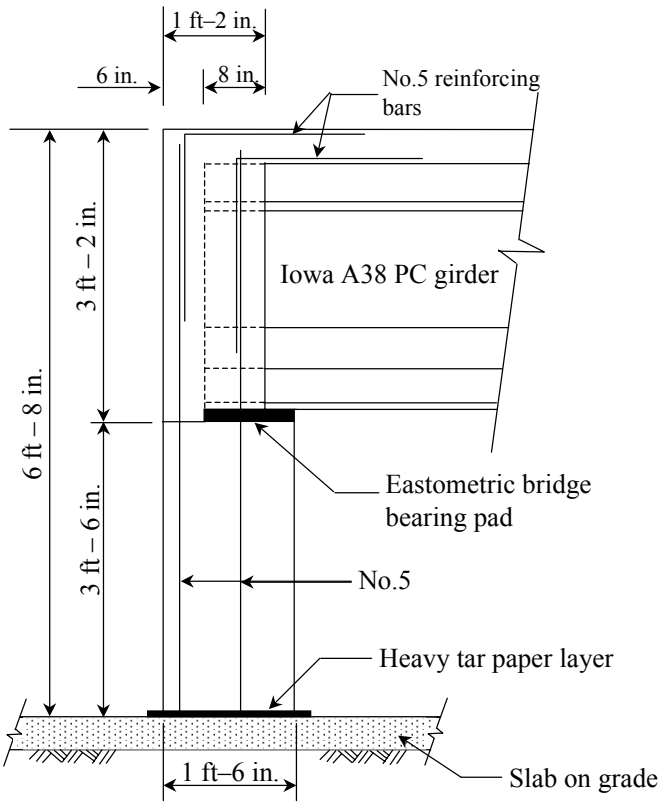

Figure 2.3. Abutment and end diaphragm

2.3. Intermediate diaphragms

The diaphragm types that were used in the bridge model were a reinforced concrete (RC) diaphragm, two sizes (deep and shallow) of steel-channel diaphragms, and a steel X-braced diaphragm with and without a horizontal strut. Figures 2.4 through 2.6 show the different diaphragm types that were used in the experimental bridge. Two diaphragm locations were considered in the tests: diaphragm located at mid span and diaphragms located at the third points of the bridge. In addition, tests were conducted on the bridge model without any intermediate diaphragms. Abendroth et al. (1991), gives the complete details for these three types of intermediate diaphragms and for the tests that were conducted using the experimental-bridge model.

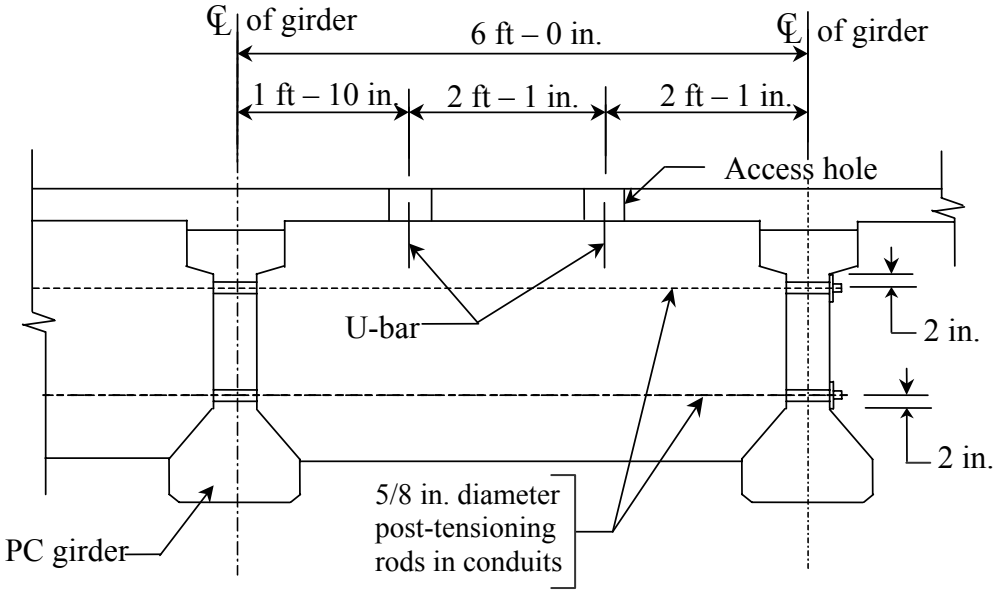

Figure 2.4. Reinforced concrete intermediate diaphragm

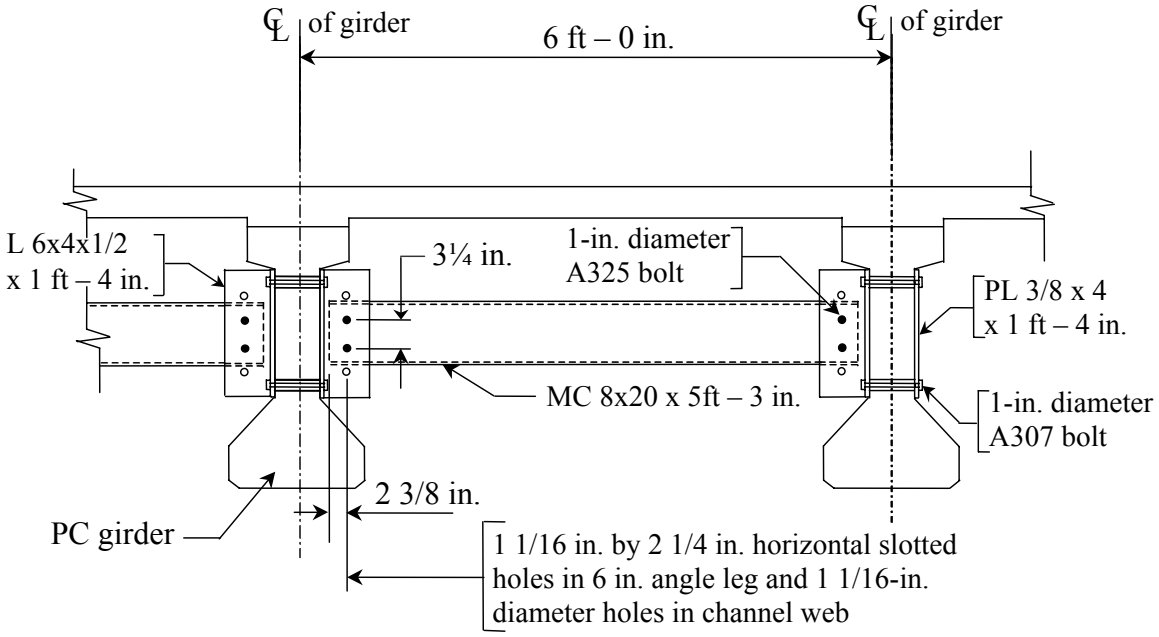

Figure 2.5. Steel channel intermediate diaphragm

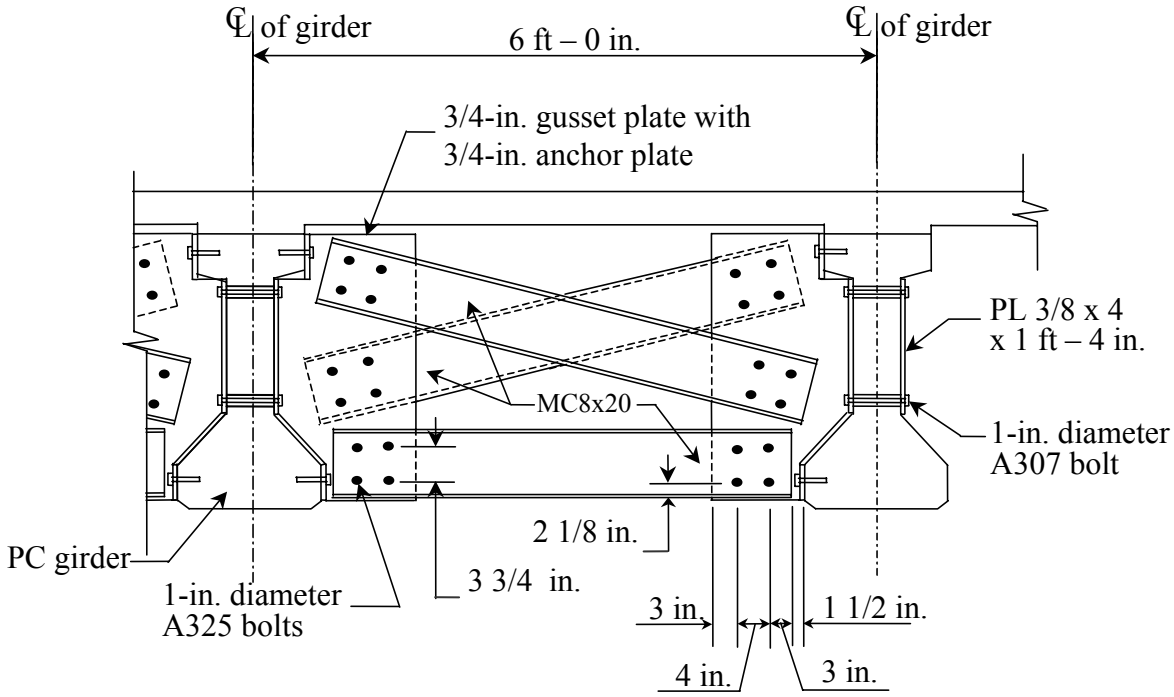

Figure 2.6. Steel X-braced with horizontal strut intermediate diaphragm

2.4. Loading mechanisms

In the experimental tests (Abendroth et al., 1991), vertical and horizontal loads were applied either separately or simultaneously to the bottom flanges of the PC girders. The vertical loads were applied with a hydraulic cylinder and measured with a load cell. The vertical loads were only applied in the upward direction. Horizontal loads were applied at various locations on the bottom flange of any of the three, PC girders. A self-resisting, load mechanism was used to apply the horizontal loads. Horizontal loads were applied as a pressure on two, small, vertical areas that were located on one side of the bottom flange for a girder to avoid interference with the diaphragms when the horizontal load was applied at a diaphragm location. A more complete description of the loading mechanisms is provided in Abendroth et al. (1991)

3. FINITE ELEMENT MODEL OF AN EXPERIMENTAL BRIDGE

3.1. Introduction

The ANSYS (DeSalvo and Swanson, 1985) finite-element program was selected to analyze the work, primarily because of its convenient preprocessing (i.e., for data input), and for its post-processing capabilities (i.e., formulated results). ANSYS is a large-scale, user-oriented, general purpose finite-element program for linear and nonlinear systems with analysis capabilities including static, dynamics, creep, buckling, heat transfer and fluid flow. The program contains a library of more than 70 different elements. One of the main advantages of ANSYS is the integration of the three phases of finite-element analysis: preprocessing, solution and post-processing.

Preprocessing routines in ANSYS define the model, boundary conditions, and loadings. Displays may be created interactively on a graphics terminal as the data are input to assist the model verification. Post-processing routines may be used to retrieve analysis results in a variety of ways. Plots of the structure's deformed shape and stress or strain contours can be obtained in the post-processing stage.

3.2. Model description

Figure 3.1 shows an overall view and a cross section of the finite-element model that was developed for an experimental-bridge model (Abendroth et al., 1991) without intermediate diaphragms. The deck and the PC girders were modeled using solid elements (brick elements) with eight nodes (SOLID45 in the ANSYS element library). This element has three translation degrees of freedom at each node. The end diaphragms and the abutments were modeled using shell elements (SHELL63 in ANSYS element library). Each node of the shell element has six degrees of freedom: three translations and three rotations.

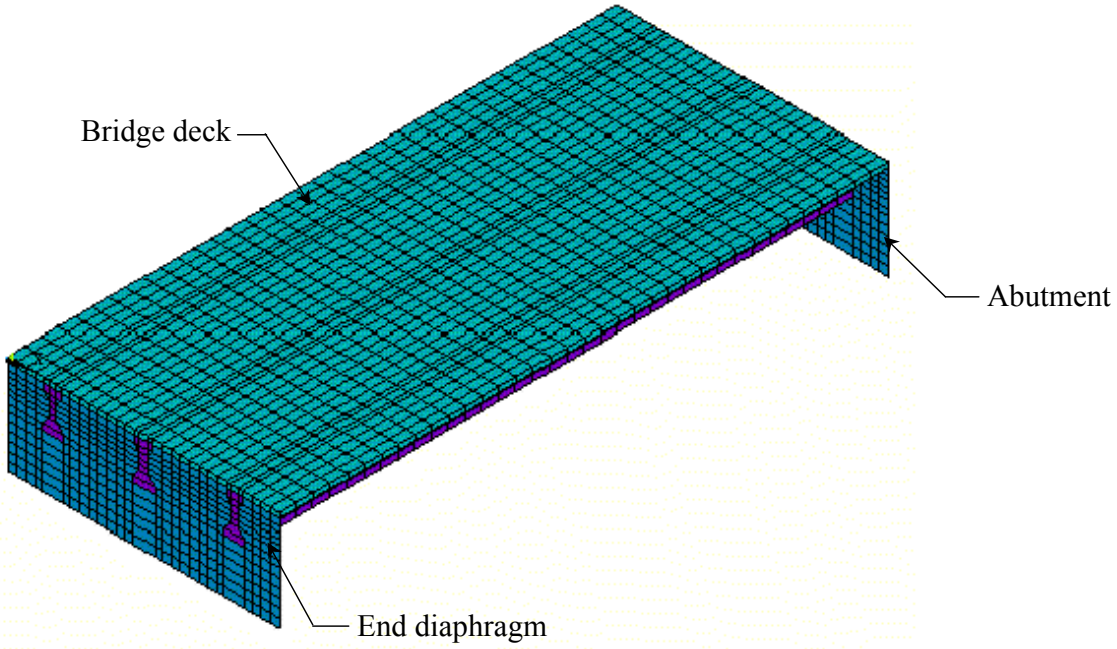

a. Overall view

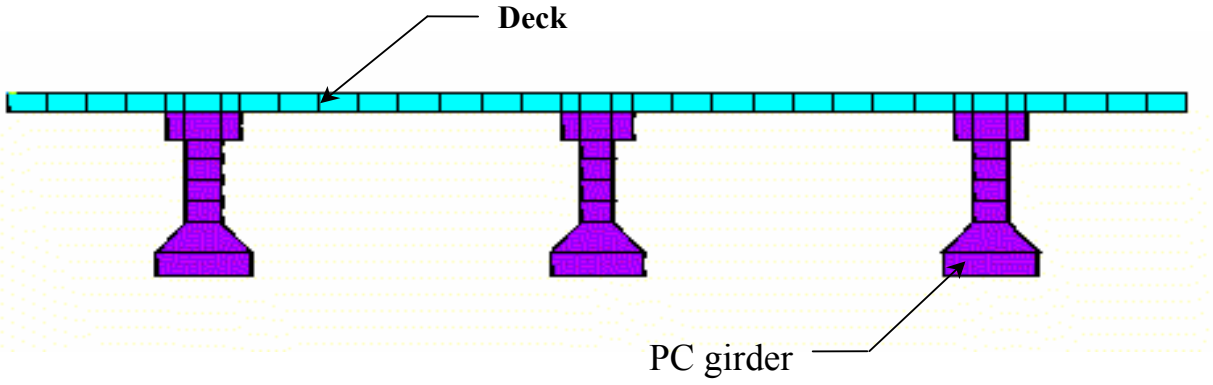

b. Cross section

Figure 3.1. Finite element model of an experimental bridge

The analytical model for the experimental bridge consisted of 4,949 nodes and 2,921 elements. The deck was modeled with 1,188 solid elements (SOLID45), which were arranged in one layer that contained 36 rows of elements in the longitudinal direction of the bridge (see Fig. 3.1a) and 33 rows of elements across the width of the bridge (see Fig.3.1b). The modulus of elasticity of the deck was set equal to 3,908 ksi, which corresponds to a concrete-compressive strength, f'_c, of about 4700 psi when the bridge was tested in the laboratory. The girders were modeled with 972 solid elements; such that each girder contains 9 elements in a cross section (see Fig.3.1b). Since the concrete haunches between the top flange and the underside of the slab for a girder were small in size, they were not included in the model.

Each abutment consisted of 162 shell elements (SHELL63) that had a thickness equal 18 in. Each end diaphragm contained 172 shell elements. The thickness of the end diaphragms was 14 in. The modulus of elasticity of the abutments and end diaphragms was set equal to 4,084 ksi, which corresponds to a f'_c-strength of about 5,100 psi.

Each concrete abutment and the end diaphragm were assumed to have common nodes, since reinforcing bars were provided for monolithic behavior. Also, a similar idealization was used to model the connections between the bridge deck, bridge girders, and the end diaphragms.

3.3. Support conditions

The two, 18-in. thick, abutments that supported the bridge rested on the floor of the laboratory. Thus, all the nodes on the bottom of the abutment were restrained in the vertical (y-axis) direction (see Fig.3.2). In addition, lateral supports were added only at one end of the finite-element model, while the other end was modeled as a roller. As shown in Fig.3.2, the edge nodes along each side and at the bottom of the laterally-supported abutment were prevented from

a. Side view

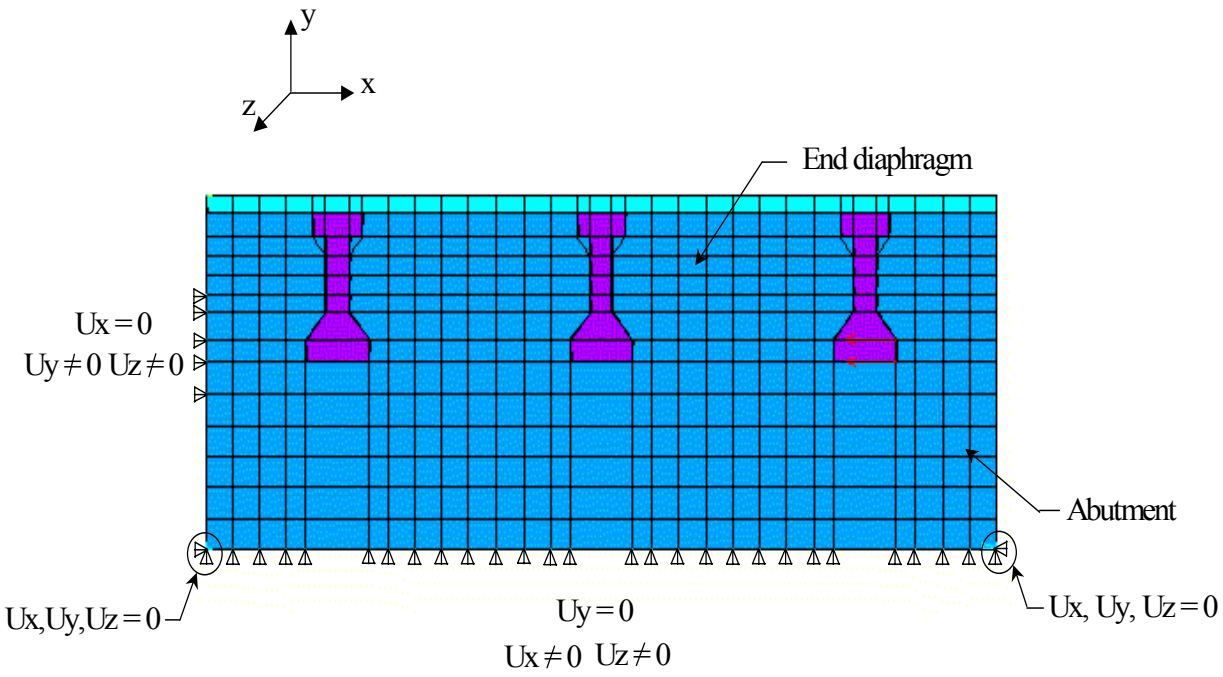

b. End view

Figure 3.2. Supports condition of the finite element model of the experimental bridge

translation (the displacements Ux,Uy and Uz that are along the x-axis, y-axis, and z-axis, respectively, are equal to zero). The figure also shows that one side of the end diaphragm for each abutment was restrained from moving in the x-direction at the location of the self-restraining, load mechanism that was used to apply the horizontal loads to the experimental bridge.

3.4. Intermediate diaphragms

The effect of using different types of intermediate diaphragms on the overall behavior of the bridge model was investigated. This was accomplished using two analytical steps. For the first analytical step, the bridge model was idealized using a coarse size of elements to model the bridge deck, girders, abutments and concrete end diaphragms. In addition, three-dimensional, truss elements were used to model the different types of steel diaphragms. This step included two types of models. The first models were the preliminary models, and the second models were the refined models. For the refined models, some modifications were added to the modeling of the diaphragms. In the second analytical step, the sub-modeling option that is available in the ANSYS (DeSalvo and Swanson, 1985) was used in the vicinity of the diaphragms. At these locations, smaller-size elements and a detailed idealization of each diaphragm and its connection with the bridge girders were used to improve the accuracy of the predicted strains and displacements for the bridge girders. The input data for displacements at the boundaries of these sub-models were obtained from the analysis conducted in the first analytical step. More details regarding these analytical procedures is given in the following sections.

3.4.1. Preliminary models

3.4.1.1. Reinforced concrete intermediate diaphragm.

The analytical model for the mid-span, RC diaphragm was developed using shell elements (SHELL63). Figure 3.3 shows a cross-sectional view of the analytical bridge model with the 6-in. thick, RC diaphragms. Each diaphragm consisted of 50 shell elements. The coordinates of the nodes located at the edges of the RC diaphragms were created to match the coordinates of the corresponding nodes for the PC girders and deck of the bridge. This matching of nodes was necessary for creating a bond between the RC diaphragms and the bridge. According to the experimental research (Abendroth et al., 1991), the RC diaphragms and the bridge deck had the same strength. Their modulus of elasticity was set equal to 3900 ksi.

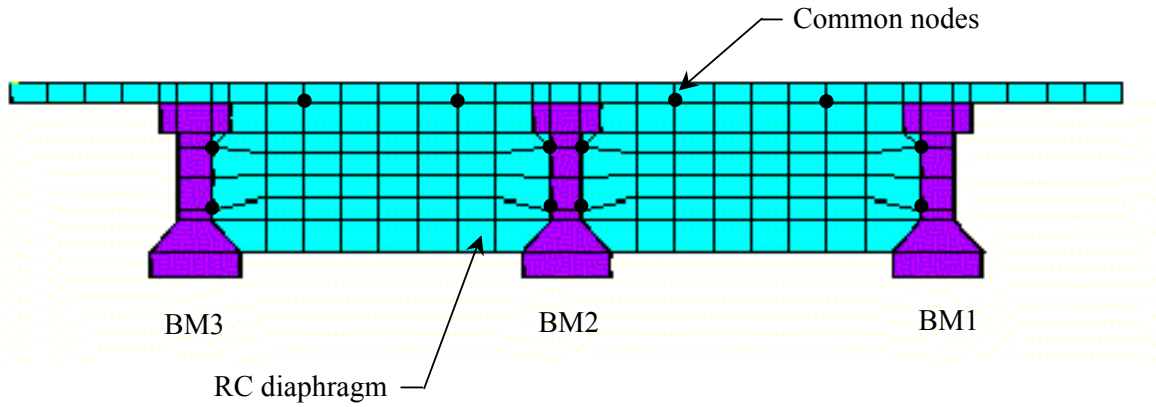

Figure 3.3. Reinforced concrete diaphragm for the preliminary finite element model

Since the RC diaphragms were cast after the bridge deck already existed, the diaphragms were not monolithically connected to the bridge. However, U-shaped (hair-pin) dowel bars were placed through the access holes in the deck that were used in casting each diaphragm. At these locations, the RC diaphragms were connected to the bridge deck. The connection between the RC diaphragms and the PC girders were developed by the two, 5/8-in. diameter, post-tensioning

tendons that were placed through 3/4-in. diameter, pipe sleeves that were cast into and along the mid-thickness of the diaphragms. Since the post-tensioning force was not noted in the experimental tests, an assumption was made that the PC girders and the RC diaphragms were fully connected at the location of the two, post-tensioning tendons. These connections were modeled using common nodes between these elements. The solid circles that are shown in Fig. 3.3 represent the common nodes in the model for the RC diaphragm. At all other locations along the interface surface between a diaphragm and the bridge, two coinciding rows of nodes were used. Independent nodes along a boundary between the bridge members permitted the RC diaphragms and the bridge to displace independently of each other at those locations.

Independent displacements between the diaphragms and the bridge were only required when the surfaces between a RC diaphragm and a PC girder and between a RC diagram and the RC deck moved away from or parallel to each other. When these surfaces moved towards each other, the RC diaphragm and the PC girders and the RC diaphragm and the RC deck will have an effect on each other. To satisfy these displacement conditions at the coinciding nodes, a three-dimensional, node-to-node, contact element was added to the model at the locations of the coinciding nodes. A description of this contact element and its properties is presented in Section 3.7.1.

3.4.1.2. Steel channel intermediate diaphragm.

Figure 3.4 shows a cross section of the analytical bridge with the steel-channel diaphragm. Each steel channel was modeled by a three-dimensional, truss link (LINK8 in the ANSYS element library) that was located at mid-height of the webs for the PC girders. This truss link has three, translation degrees-of-freedom at each end, which allowed the member to resist only axial tension or compression. The use of slotted holes in the outstanding, 6-in. leg for

the angle that was connected to the diaphragm web with two, A325, high-strength bolts caused forces to be transferred only by friction between PC girder and a steel-channel diaphragm. The experimental results (Abendroth et al. 1991), showed that slippage occurred between the web for a steel-channel diaphragm and a connection-angle leg. This type of slippage was neglected for

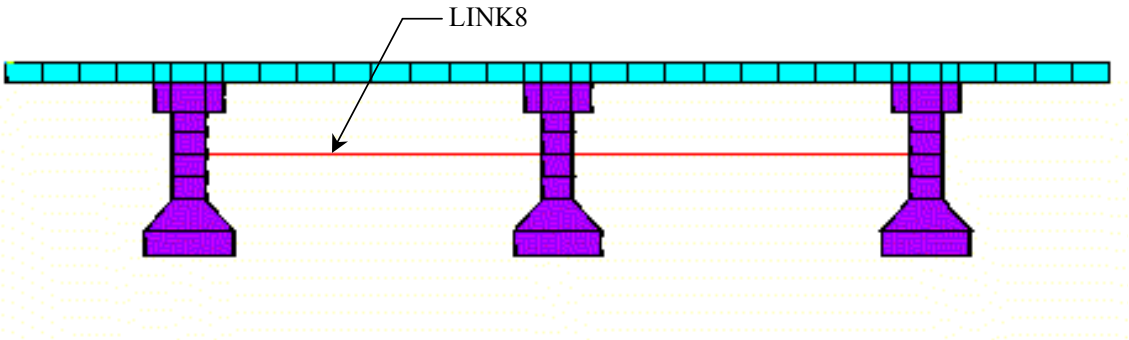

Figure 3.4. Steel channel diaphragm for the preliminary finite element model

the analytical of the preliminary model of the channel-shaped diaphragm. Therefore, a thrust-only-type connection was assumed between the steel-channel diaphragms and the webs of the PC girders.

3.4.1.3. Steel X-braced with horizontal strut intermediate diaphragm.

Figure 3.5 shows the cross section of the analytical bridge model with the X-braced plus horizontal strut diaphragm. Both, the cross brace and the horizontal struts were idealized using three-dimensional, truss links (LINK8). As was mentioned for the steel-channel diaphragm, modeling the MC8x20 channels as truss links prevented the transfer of bending moment between the PC girders and the steel channels, as well as neglecting the effect of the shape of a steel channel on the analytical results. Although the holes that were drilled in the 3/4-in. thick, gusset plate and in the webs of the steel channels were not slotted, slippage between a steel-channel web and a gusset plate might occur because of the required clearance between the bolt and the

standard-sized, drilled hole for this bolt diameter. Any slippage between these steel parts was neglected for this preliminary model. Therefore, relative displacements were assumed not to occur between the PC girders and the steel, X-braced plus horizontal-strut diaphragms.

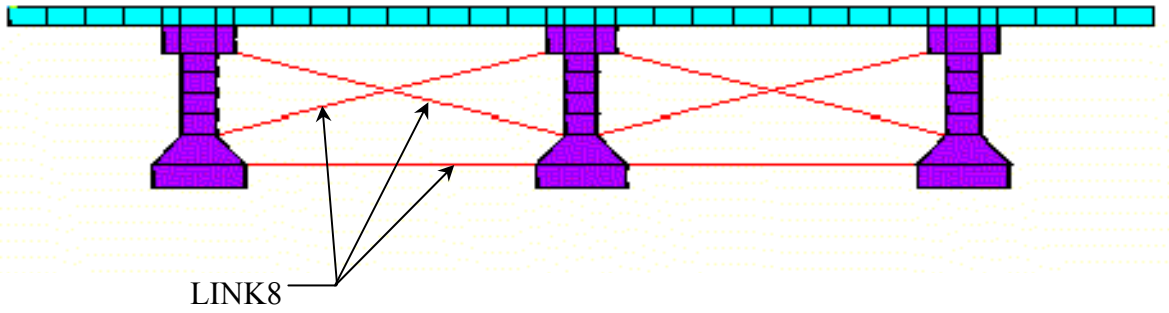

Figure 3.5. Steel X-braced with horizontal strut diaphragm for the preliminary finite element model

3.4.2. Refined models

A review of the displacement results for these preliminary models, which are discussed in Chapter 4, revealed significant differences between the predicted and measured displacements. More accurate finite-element models (the refined models) were developed to account for the actual geometric configurations of the two, steel diaphragms and for the connection details between the diaphragms and the PC girders.

3.4.2.1. Reinforced concrete intermediate diaphragm.

When the bottom flange of Beam BM2 (see Fig. 3.6) was horizontally loaded, a tension force was predicted by the preliminary model at the surface between Beam BM2 and the RC diaphragm that was located between Beams BM1 and BM2. Even though the tightening force of the post-tensioning tendons was not recorded in the experimental test (Abendroth et al., 1991), a

complete structural connection was assumed between the PC girders and the RC diaphragms in the preliminary model at the locations of the post-tensioning tendons. This connection assumption produced a prediction of a smaller horizontal displacement for Beam BM2 compared to that which was experimentally measured. This difference in the displacement was expected to be caused by a non-integral connection between the girders and the adjacent diaphragms that allowed a gap to open between Beam BM2 and the intermediate diaphragm that was located between Beams BM1 and BM2.

To allow Beam BM2 to displace more when this beam is horizontally loaded, the common nodes on the interface between Beam BM2 and the diaphragm located between Beams BM1 and BM2 were replaced by two coinciding nodes. One set of these nodes was located on the web for Beam BM2 and the other set of nodes was located on the adjacent edge of the diaphragm. A three-dimensional, node-to-node, contact element was placed between each of the coinciding nodes. Figure 3.6 shows the refined model with the common nodes shown as solid circles. The refined model was used only when Beam BM2 was horizontally loaded towards the left (as viewed in Fig. 3.6). The preliminary model shown in Fig.3.3 was used when a horizontal load was applied towards the left (as viewed in Fig. 3.3) on Beam BM1.

3.4.2.2. Steel channel intermediate diaphragm.

A refined model for the steel-channel, intermediate diaphragm was developed to consider the effect of slippage between the web of a steel channel and the 6-in., outstanding leg of the angle that was connected to the web of the PC girders and to consider the effect of the configuration for the steel-channel diaphragm. As shown in Fig. 3.7, the finite-element, bridge

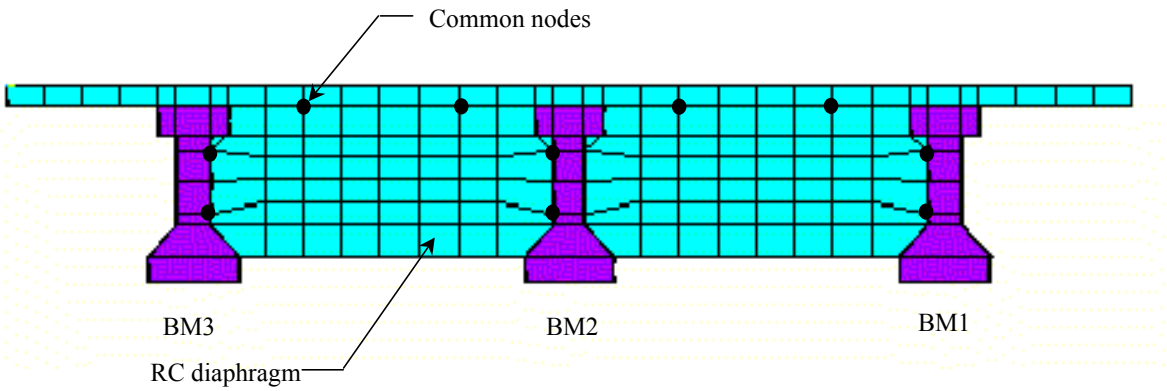

Figure 3.6. Reinforced concrete diaphragm for the refined finite element model

model was similar to the preliminary model. Shell elements (SHELL63) were used to model the steel-channel diaphragm in the refined model. The 6-in., outstanding leg of the steel angle that connected the steel channel to the PC-girder web was modeled using four, 1/2-in. thick elements. The horizontal top and bottom edges of this modeled angle leg were not connected to a PC girder. The vertical edge of this modeled angle leg that corresponded with the heel of an angle that was adjacent to the web of a PC girder was connected to the nodes for the web of the girder. The angle leg that was attached to the web of a PC girder for the experimental bridge was neglected in this analytical model. The web of a steel channel was modeled using eleven rows of elements in the longitudinal direction of the channel and two rows of elements in the depth direction of the channel. The twenty-two shell elements that were used to model the channel web had a thickness equal to 0.4 in. The flanges for a steel channel were modeled using eleven rows of shell elements in the longitudinal direction, and one row of element across the width of a flange. The flange thickness was decreased from the actual 0.5-in. thickness to a 0.4-in. thickness to account for an increase in the modeled depth for the channel above that for the

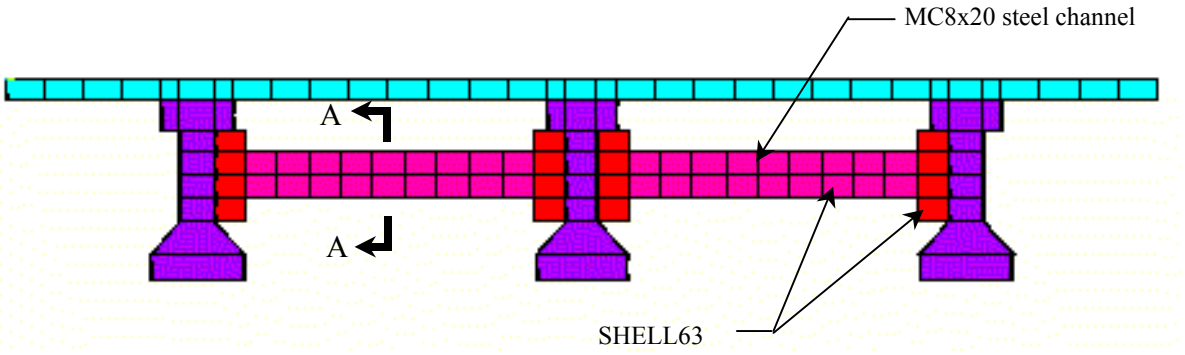

a. Cross section

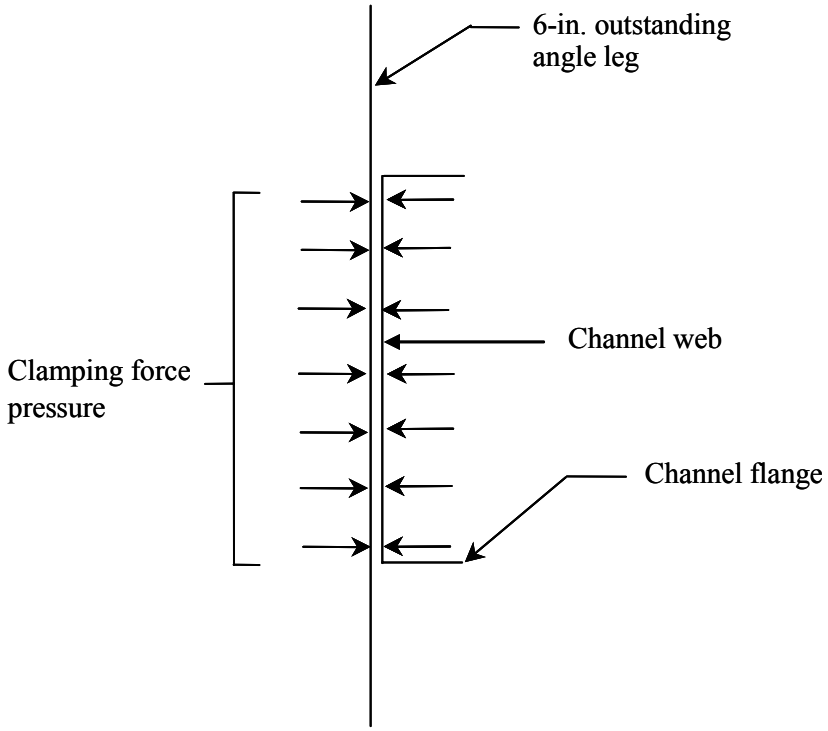

b. Section A-A

Figure 3.7. Steel channel diaphragm for the refined finite element model

actual channel. The modeled channel depth was established so that the nodes for channel would match those for a PC girder web.

In the area where a steel-channel web and an outstanding, angle leg were attached, coinciding nodes and coinciding shell elements were used for the web and the angle leg. To develop a friction resistance between the coinciding elements that was equal to that which is provided by fully-tensioned, 1-in. diameter, A325, bolts and to avoid overlapping between the elements, contact surfaces with coefficient of friction, μ, equal to 0.33 were used between the channel-web elements and the outstanding-leg elements. Since the force that was used to tighten the high-strength bolts was not recorded in the experimental test (Abendroth et al., 1991), an initial force of 51 kips was applied as a clamping force for each bolt at each channel-to-angle connection. This force was equal to the minimum, bolt-tension force for a 1-in. diameter, A325 bolt (AISC, 2002).

Finite-element analyses were conducted for different magnitudes of the clamping force that was provided by the high-strength bolts to investigate the sensitivity of the predicted strain and displacement results to this assumed clamping force. These clamping forces were applied as pressures (see Fig. 3.7b) at the inner surface of the channel web and at the outer surface of the outstanding leg for the connection angle. Equal pressures on both surfaces acted towards each other and their magnitude was equal to the clamping force that is induced by two, fully-tensioned, 1-in. diameter, A325 bolts divided by the contact area. This magnitude for the clamping force, which was equal to 32 kips, produced an average, axial force in the steel-channel diaphragm that was close to that measured for the experimental model.

3.4.2.3. Steel X-braced with horizontal strut intermediate diaphragm.

For the reasons mentioned in the previous section, the refined model shown in Fig. 3.8 was created for the X-braced, with the horizontal strut, intermediate diaphragm. The diaphragm consisted of three, steel-channel members (two cross braces and one horizontal strut). Shell elements were used in creating the entire diaphragm. The web of the three, steel channels was modeled using eight element rows along the channel length and two element rows for the channel depth. The flanges for the channels were modeled with a single row of eight elements along the channel length. The web thickness was 0.4 in., and the flange thickness was 0.5 in. The total depth and flange width for each channel were 8 in. and 3.025 in., respectively.

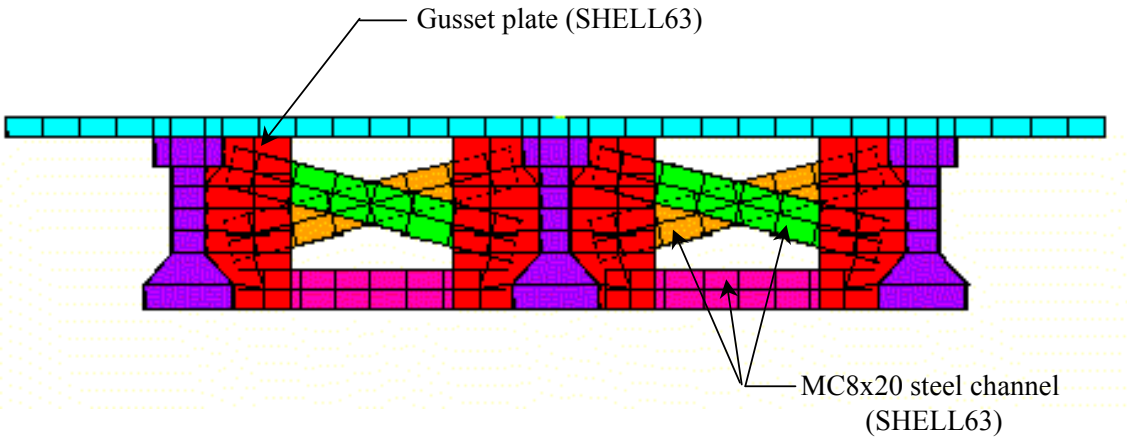

Figure 3.8. Steel X-braced with horizontal strut diaphragm for the refined finite element model

The gusset plate that connected the channel webs to the PC girders were modeled using fifteen, ¾-in. thick, shell elements. The top and bottom, horizontal edges of a gusset plate were free. The nodes for the vertical edge of the gusset plate, which was adjacent to a PC girder, were common with nodes for a girder. The modeling approach discussed in the previous section was used to develop the connection between the steel-channel web and the gusset plate. Contact

elements that were similar to those used for the steel-channel diaphragm were used in this model. Because of the inclination of the X-braced channels the nodes of both the channel web and the gusset plate did not coincide with each other. Therefore, the elements for both pieces did not match with each other. A 32-kip, clamping force was applied as two, equal-in-magnitude and opposite-in-direction, concentrated forces that were applied at the two, coinciding nodes between a channel web and a gusset plate.

3.5. Load cases

3.5.1. Preliminary models

The purpose of developing and studying the preliminary models was to predict the behavior of the bridge model under different cases of loading even when some of the construction details were neglected in the finite-element model. To accomplish this goal, horizontal and vertical loads were applied to the preliminary bridge models with loads equal to that which were used in the experimental tests. The load locations shown in Fig. 3.9 were considered in this study. Loads were only applied at the mid-span of Beams BM1 and BM2. The responses for Beam BM3 were not included in the comparison study.

Vertical loads were applied as concentrated loads in an upward direction and at the two points shown in Fig. 3.10. Each concentrated load started at 5 kips and was gradually increased to 25 kips. Horizontal loads were applied as two, equal, concentrated loads toward Beam BM3 and at the points shown in Fig. 3.10. The three, diaphragm configuration cases and the no diaphragm case were loaded at Points 1 and 2 (see Fig. 3.9) with a horizontal load that started at 10 kips and increasing to 75 kips (the maximum load for the no diaphragm case was 60 kips).

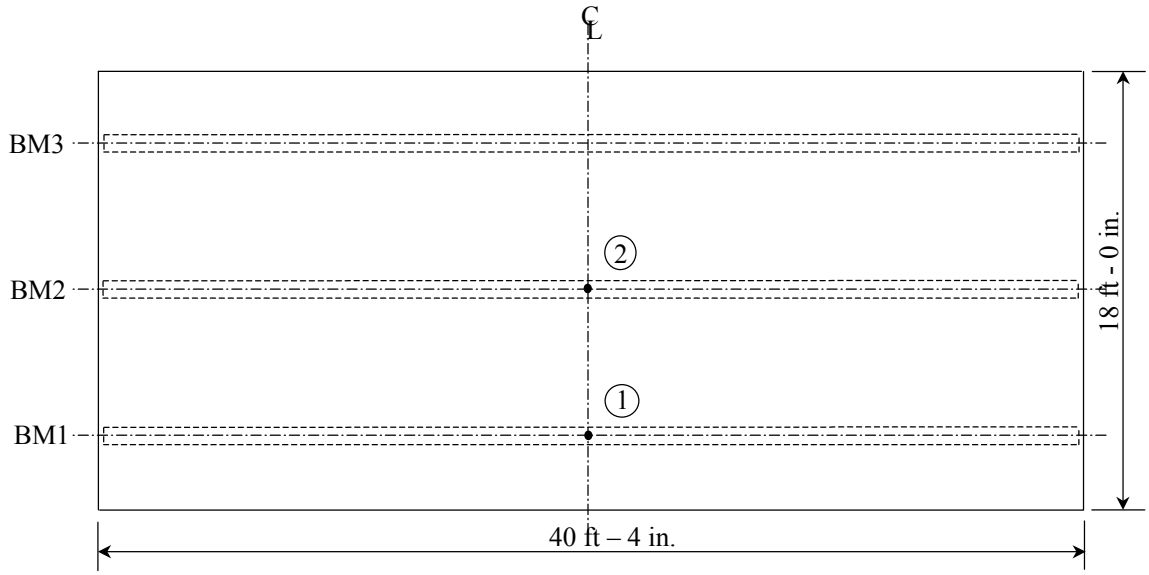

Figure 3.9. The load locations considered in the analysis

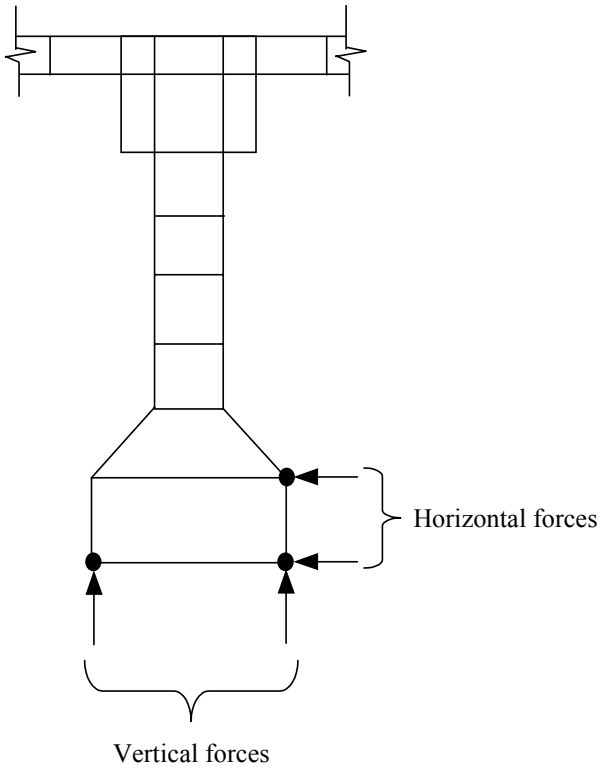

Figure 3.10. Vertical and horizontal load locations considered in the preliminary and refined finite element models

3.5.2. Refined models

After the displacements that were predicted by the preliminary model were compared with those experimental displacements, the refined models were developed to improve the displacement predictions. Since the intermediate diaphragms had a minor effect on the bridge behavior for vertical loads, vertical loads were not applied to the refined models.

A maximum, horizontal load of 75 kips was applied for each type of intermediate diaphragm. This load was applied at Point 1 for both types of the steel diaphragms and at Point 2 for the RC diaphragms (see Fig. 3.9). The horizontal loads were applied to the analytical models using the procedure described in Section 3.5.1.

3.6. Sub-models

3.6.1. Introduction

The refined models that were developed for the different diaphragm configurations gave approximate results for the strains and stresses in the bridge deck and girders. The mesh size used in modeling of the bridge elements and intermediate diaphragms and the excluded details, such as the exact locations of the A325 bolts and the existence of the A307 bolts that connected the steel diaphragms, to the PC girders, were among the factors that affected the finite-element results.

To more accurately predict the stress and strain distributions in the intermediate diaphragms and their connections, a finite-element sub-model was developed for each steel-diaphragm configuration. A sub-model was not developed for the reinforced-concrete diaphragm because predicted strain results for both the preliminary and refined models that are shown in Fig.3.3 and Fig.3.6, respectively were in acceptable agreement with the experimentally

measured strains in the bridge deck, girders, and intermediate diaphragms. One of the main elements used in creating and developing the sub-models was the surface-to-surface contact element that was used to model the connections between the diaphragm elements and the bridge.

An available option in ANSYS (DeSalvo and Swanson, 1985) referred to as "sub-modeling" was used to analyze the portion of the bridge in the vicinity of the intermediate diaphragms. In general, sub-modeling is a tool that allows the analyst to study the behavior of a certain part of a structure without modeling the entire model with a fine-mesh size. In this technique, cut boundaries are defined that are far enough away from the area of interest. Boundary conditions (displacements) are calculated first from the analysis of a coarse model representing the entire structure. These boundary displacements are then applied as displacement conditions to the cut boundary of the sub-model.

3.6.2. Steel channel intermediate diaphragm sub-model

This sub-model was created to study the strain distribution in the steel-channel, intermediate diaphragm and its connections. To avoid affecting the results at the diaphragm location, cut boundaries were taken at a 3-ft distance along the longitudinal direction of the bridge, at each side of the diaphragm. Figure 3.11 shows the sub-model that was developed for the steel-channel, intermediate diaphragm. Solid elements (SOLID45) were used in creating the entire sub-model, including the steel-channel diaphragm and its connections. The same material properties that were used for the steel-channel, intermediate-diaphragm, refined model were used for this sub-model.

The bridge deck contained 96 elements in a cross section. These elements were divided into two equal layers with 22 element rows along the longitudinal direction for the bridge. Each PC-girder, cross section was modeled using 32 elements. The steel channel was modeled with 234 elements. Three layers of 26 solid elements were used to model the channel web. Each channel flange had 26 element rows along the length of a channel and 3 element rows across the

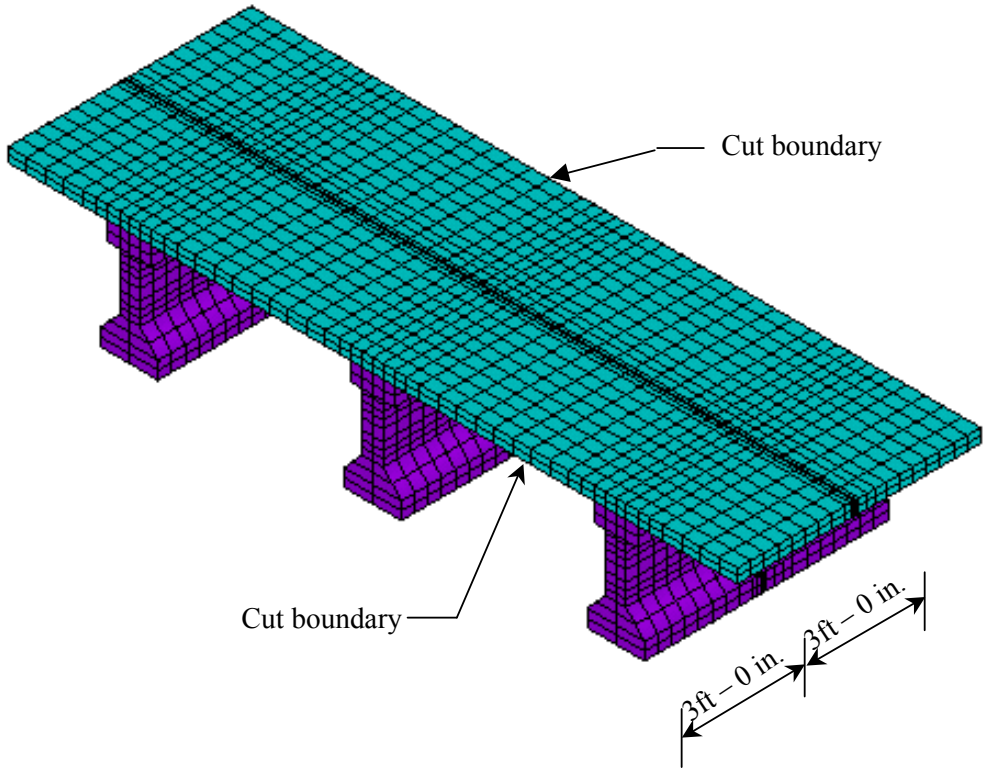

a. Overall view

Figure 3.11. Steel channel diaphragm sub-model

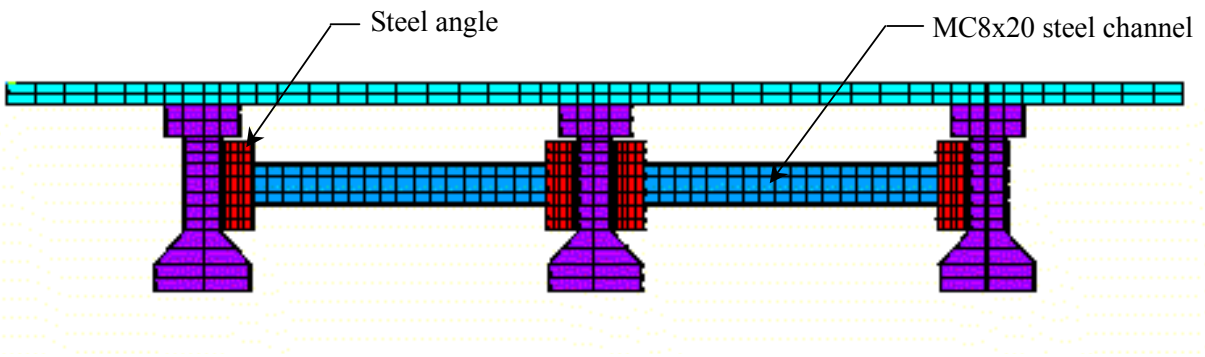

b. Cross section

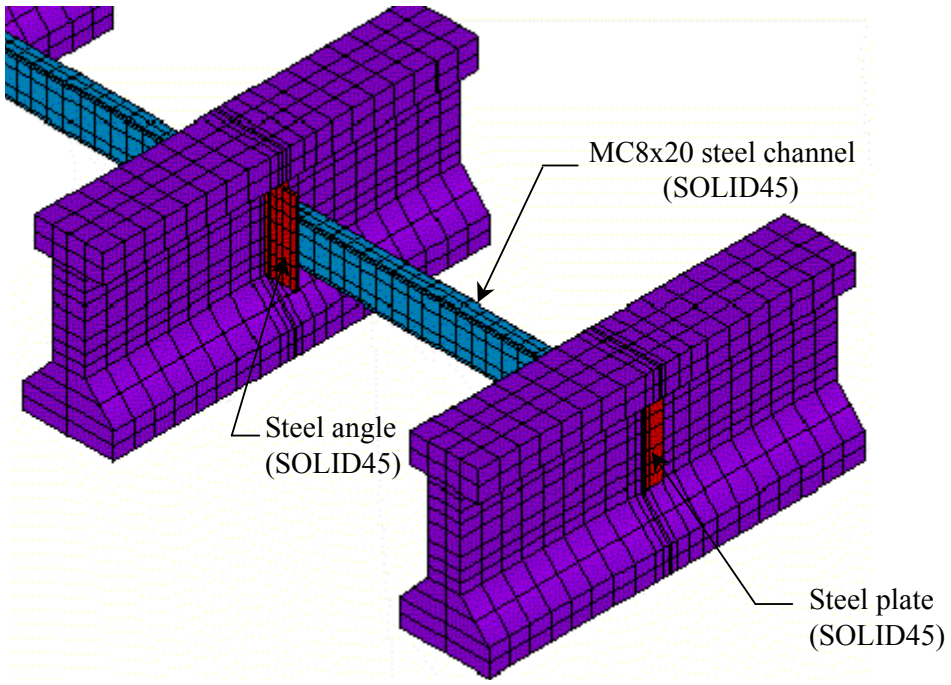

c. Overall view with no deck

Fig. 3.11. (Continued)

flange width. Each of the 16-in. long, steel angles that connected one end of a channel diaphragm to a PC girder was modeled using 56 elements. The outstanding leg for an angle was divided to 5 element rows in its short direction and 7 element rows in its long direction. The angle leg that was attached to the PC-girder web was divided to 3 element rows in its short direction and 7 element rows in its long direction. The 3/8-in. thick, steel plate that was attached to the outer side of the web for an exterior, PC girder was modeled using 3 element rows in its short direction and 7 element rows in its long direction.

Separate nodes were used for the PC girders, steel channel, steel angle, and outside steel plate that occurred in the area of contact between these bridge elements. Therefore, common nodes were not used for any two, adjacent members. This type of element modeling allowed for sliding and for gaps to open between the finite elements when loads were applied to the bridge model. Two types of contact surfaces were used in this sub-model. One surface was a sliding-contact surface, and the other surface was a sticking-contact surface. The sliding-contact surface was created to attach the channel web to the outstanding angle leg. For a contact surface, one surface must be designated as the target and the other surface must be designated as the contact. Since the adjacent surfaces of the channel web and the angle leg are steel, the hardness of each surface was the same. Therefore, either the channel web or the angle leg can be designated as target. The coefficient of friction was set equal to 0.33, which applies for a Class A surface (unpainted, clean-mill scale, steel surfaces), as defined by AISC (2002).

The joint-clamping forces were applied as two equal, 32-kip, but oppositely directed, compressive, concentrated forces. The clamping forces were applied at the exact location of the bolts. The two nodes at the application points for these forces had the same x and y- coordinates

but different z-coordinates. One of the two nodes was on the side of the channel web toward the flanges. The other node was on the surface of the angle leg that was away from the channel.

Two sticking contact surfaces were used for the adjacent surfaces between a PC-girder web and the 4-in. angle leg and the outside steel plate. The sticking-contact surfaces prevented any relative displacement along the surface of contact between these portions of the bridge. Since a concrete girder surface is softer than a steel surface, the target was attributed to the steel plates and the contact was attributed to the PC girder.

Each of the two, A307 bolts that fastened the steel-angle leg and outside steel plate to a PC-girder web was modeled as a beam element. A beam element has two nodes with six degrees-of-freedom at each node. Three of the degrees-of-freedom are in translation and the other three degrees-of-freedom are in rotation. Each beam element was located at the exact location of the bolt in the experimental bridge. This beam element connected two corresponding nodes. At an exterior girder, one of the nodes was on the outer steel plate and the other node was on the angle leg. At the interior girder, the nodes for this beam element were on the angle leg on each side of the girder web. The nodes for this beam element were located on the two surfaces that were not directly attached to the PC girder web.

3.6.3. Steel X-braced with horizontal strut intermediate diaphragm sub-model

Figure 3.12 shows the sub-model that was developed using solid elements (SOLID45) for the X-braced, with horizontal-strut diaphragm. The material properties for this sub-model were the same as those for the refined model for this type of diaphragm. The cut boundaries were taken at the same locations as those for the sub-model of the steel-channel diaphragm. The concrete deck for this sub-model consisted of 96 solid elements in a cross section of the bridge and 18 element rows along the longitudinal direction of the bridge. The deck elements were

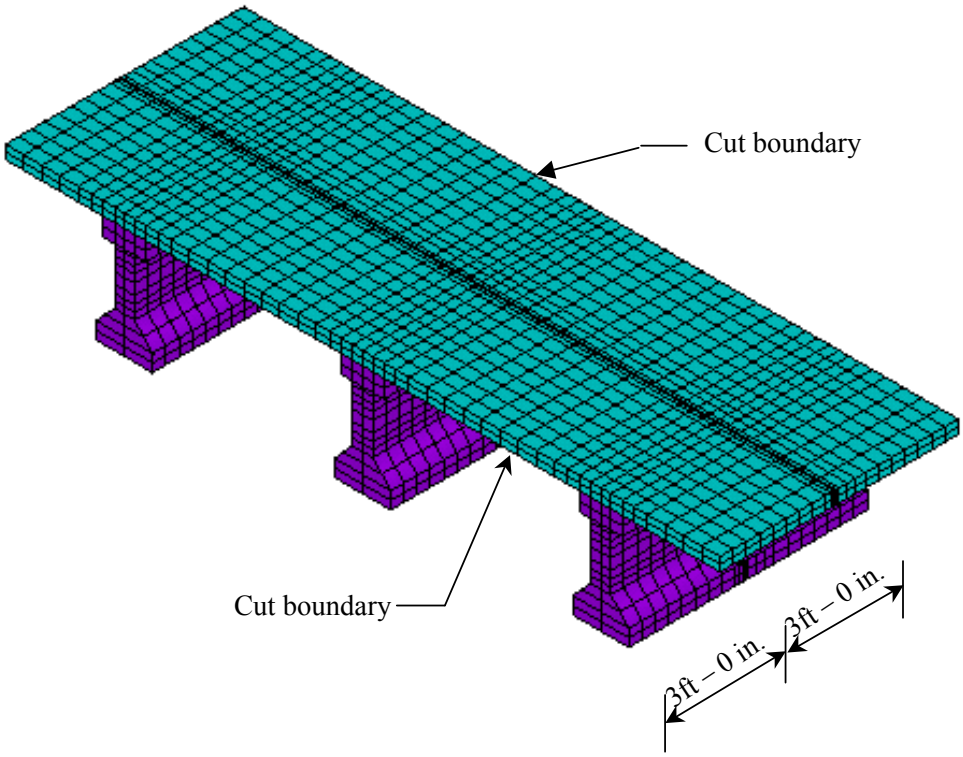

a. Overall view

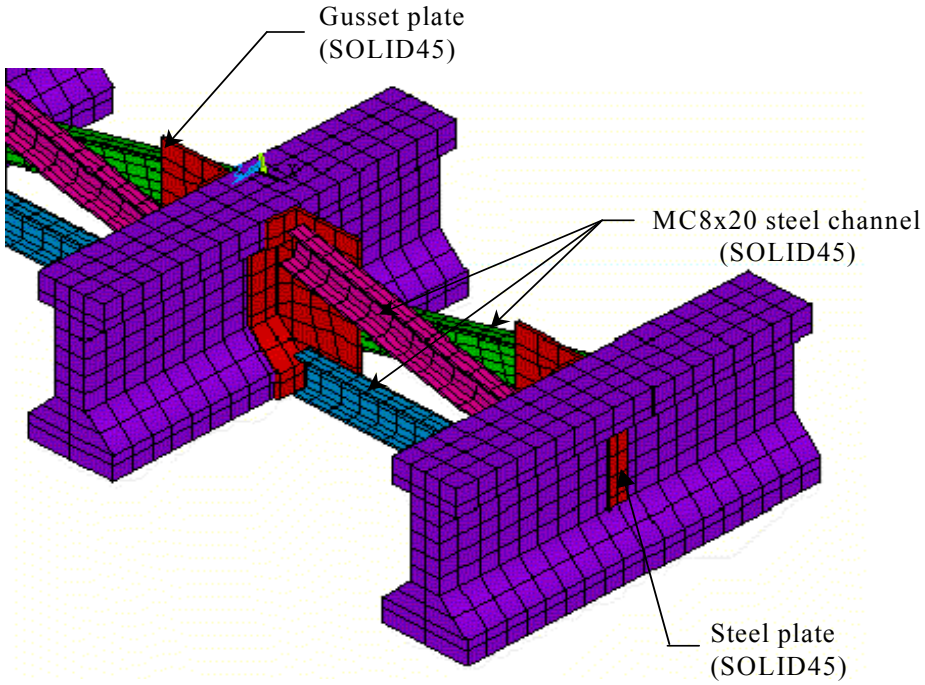

b. Overall view with no deck

Figure 3.12. Steel X-braced diaphragm sub-model

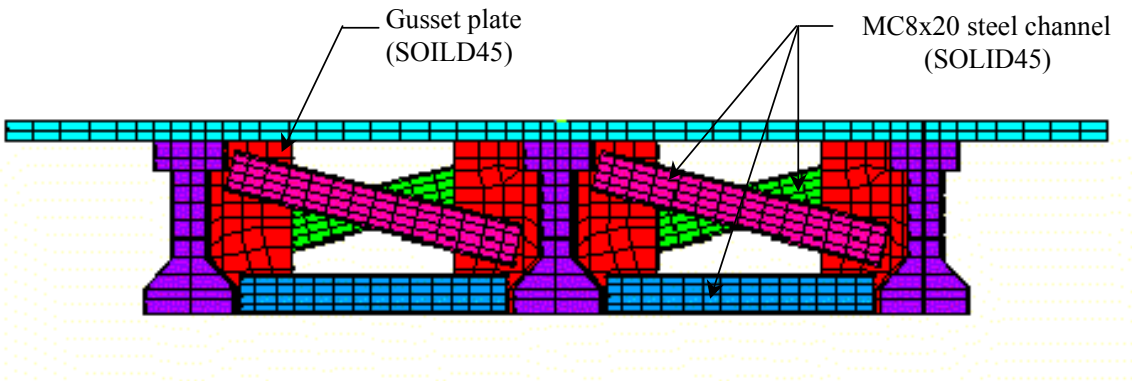

c. Cross section

Figure 3.12. Continued

modeled on two layers through the thickness of the deck. A PC-girder, cross section contained 26 elements. In the longitudinal direction of the bridge model, the girders were divided into 18 element rows. Displacements (boundary conditions) that were calculated from the finite-element analysis of the steel, X-braced diaphragm for the refined model that is shown in Fig. 3.8 were applied at the cut-boundary nodes of the sub-model.

The steel-channel cross braces and horizontal strut were modeled using the same number of elements. The channel web had 4 element rows along the channel depth and 14 element rows in the longitudinal direction of the channel. A steel-channel flange was modeled using 3 element rows along the flange width and 14 element rows along the flange length. The 3/4-in. thick, gusset plate was modeled using 40 elements. An element node occurred at each A325-bolt location. An edge plate that fastened a gusset plate to a PC girder was modeled using 3 element rows along the plate width and 11 element rows along the plate length. This edge plate consisted of two parts. The first part was attached to the top flange of a PC girder, and the second part was attached to the web and the bottom flange of a PC girder.

The method used to model the connections for the X-braced, intermediate diaphragm was the same as that used for the connections of the steel-channel, intermediate diaphragm. However, for the sub-model of the X-braced diaphragm, each end of a channel was fastened to

the gusset plate using four, A325 bolts. A clamping force of 32 kips per bolt was applied as described in Section 3.6.2.

3.7. Comparison of analytical and experimental results

The results obtained from analyzing the experimental-bridge model were compared to the laboratory-test results. These comparisons included the displacements and strains at the bottom flange of the PC girders that were induced by the vertical and horizontal loads, which were applied separately at Points 1 and 2, as shown in Fig. 3.10. The following sections briefly summarize some of these comparisons, however, for more detailed comparisons, the reader is referred to the thesis by Andrawes (2001).

3.7.1. Comparison of displacements

Figures 3.13 and 3.14 show the relationships between the horizontal load and the horizontal displacement at Point 1 for the bridge model without any intermediate diaphragms and with a RC, intermediate diaphragm, respectively. Similar results that are associated with the other diaphragm types were presented by Andrawes (2001). The no diaphragm case presented in Fig. 3.13 showed insignificant differences between the results obtained from the analytical and experimental models. On the other hand, the differences between the analytical and the experimental results were noticeable for the bridge model with different types of diaphragms (see Andrawes, 2001). For example, when a 75-kip, horizontal load was applied at Point 1, the differences between the predicted and measured, horizontal displacement at Point 1 were 11%, 26%, and 23% for the bridge with RC, steel channel, and X-braced, intermediate diaphragms, respectively. These displacement discrepancies were most likely caused by the presence of

concrete cracks in the experimental-bridge deck that were not included in the finite-element models.

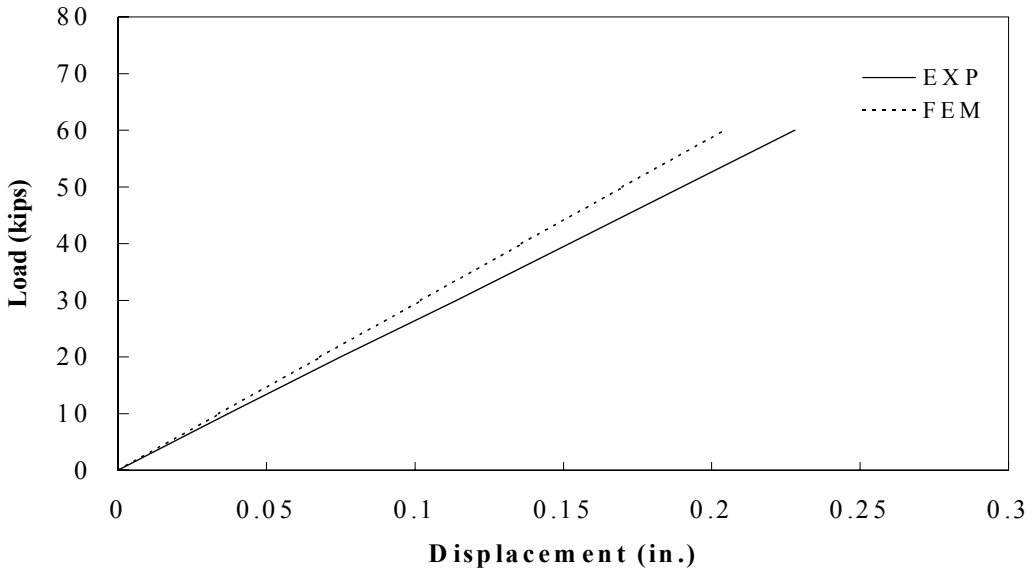

Figure 3.13. Horizontal load versus horizontal displacement at Point 1 for the no diaphragm condition.

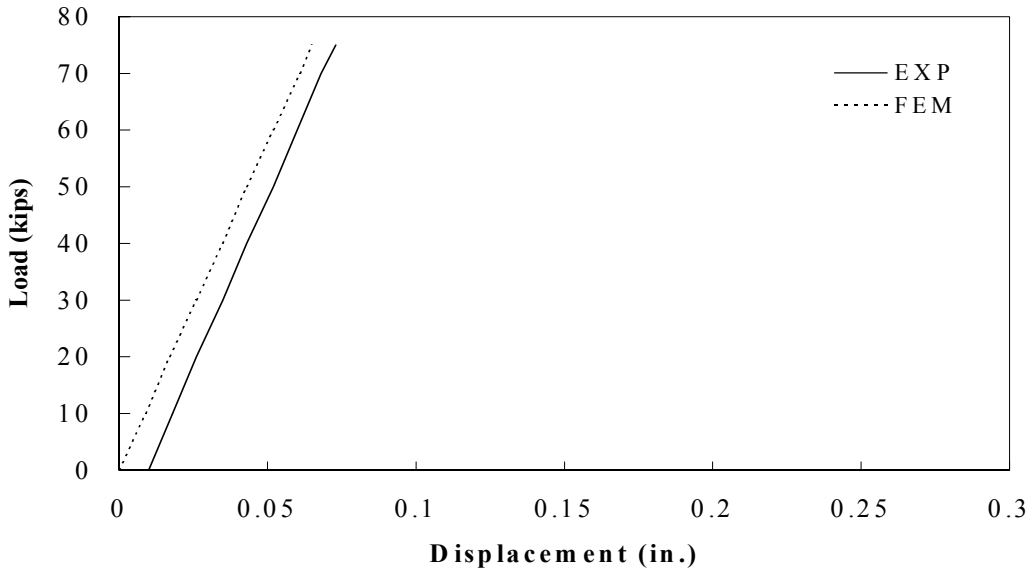

Figure 3.14. Horizontal load versus horizontal displacement at Point 1 for the RC diaphragms

3.7.2. Comparison of strains

Table 3.1 lists the experimental and analytical strains in the PC girders and in the diaphragms for the experimental bridge with reinforced-concrete, intermediate diaphragms. For the first-load case, a 75-kip, horizontal load was applied to the bottom flange of the exterior girder at Point 1. For the second-load case, that same load was applied to the bottom flange of the interior girder at Point 2.

The first column in the table lists the bridge member, and the second column in the table lists the location that was used for the comparison of the experimental and analytical strains. The numbers 1, 2, and 3 refer to Beams BM1, BM2, and BM3, respectively. The letters L and R refer to the left side and right side, respectively, of the bottom flange of the girder where the strains were measured. The diaphragm strains that are presented in this table are the average of the strains on each side of the diaphragm between the impacted girder and the next girder. Negative strains are compressive strains, and positive strains are tensile strains.

The results listed in Table 3.1 reveal that some of the predicted, PC-girder strains are significantly different from those strains that were recorded during the experimental tests (Abendroth et al., 1991). One explanation for these strain differences can be attributed to the presence of concrete cracks in the experimental-bridge deck that were not modeled for the finite-element analyses. Another reason for these strain differences could be related to the differences in the method that was used for the application of the horizontal load. In the experimental work, this load was applied as a pressure over a finite area on the outer face of the bottom flange of a PC girder. For the analytical models, this load was applied as a concentrated load at an element node. Similar strain comparisons for the other types of intermediate diaphragms were summarized by Andrawes (2001).

Table 3.1. Experimental strain results for the RC diaphragm case

Bridge member	Location	Experimental strains (Micro-strain)		F.E.M. strains (Micro-strain)	
		Point 1	Point 2	Point 1	Point 2
PC GIRDER	1R	-8.9	3.9	-22.0	11.0
	1L	110.7	21.8	91.0	26.0
	2R	-59.0	-42.5	-49.0	-38.0
	2L	12.1	140.2	18.0	124.0
	3R	-38.9	-90.6	-48.0	-90.0
	3L	7.8	-7.0	-9.0	-21.0
DIAPHRAGM		-159.9	3.9	-202.0	2.0

The discrepancies between the experimental and analytical results could have resulted from several other sources. One of these additional sources is the idealization of perfect, simple-support conditions that were used in the finite-element modeling. Also, any differences in the material properties of the experimental-bridge structure and those assumed in the analytical solution could have been another reason for the differences between the experimental and analytical result. Even though differences occurred between the predicted and measured bridge responses, the calibration study provided the ISU researchers with valuable, finite-element, modeling guidelines regarding element type and size, idealization of diaphragm-girder connections, and interface modeling for the parts of the intermediate diaphragms. The ISU researchers believe that these types of finite-element models can be utilized to analyze this type of a complex-bridge system.

4. FINITE ELEMENT MODELS OF PROTOTYPE PC GIRDER BRIDGES

4.1. Introduction

The finite-element guidelines that were discussed in Section 3.8 were used to develop and analyze PC girders bridges when the bottom flange of one of the PC girders was subjected to a lateral-impact force. Also, the bridge-skew angle was investigated regarding its effect on the response of PC-girder bridges to lateral impacts. For this purpose, two sets of finite-element models for a bridge were used in this analysis. The first set consisted of a straight (non-skew) bridge model, and the second set consisted of 30-deg., skewed-bridge models. All of the analyses were conducted for PC-girder bridges with the Iowa Department of Transportation (Iowa DOT) reinforced concrete (RC), intermediate diaphragm, as well as with different configurations of steel, intermediate diaphragms.

4.2. Bridges selected for the analyses

Engineering drawings for two PC girder bridges in the State of Iowa were obtained from the Iowa DOT to establish design parameters for two, prototype bridges. The geometric configurations, dimensions and material properties of each of these two representative bridges are presented in the following sections.

4.2.1. Non-skewed bridge

Figure 4.1 shows a longitudinal cross section for a PC girder bridge that was constructed over US Hwy. 30 in Marshall County, Iowa. This bridge will be referred to as the Marshall County Bridge. The bridge skewed angle is 1°-19`-17``, which is almost a non-skewed alignment. The bridge has four spans with three, intermediate, frame-type piers and two, integral abutments. Each end span is 35 ft – 9 in. long, and each interior span is 96 ft – 6 in. long.

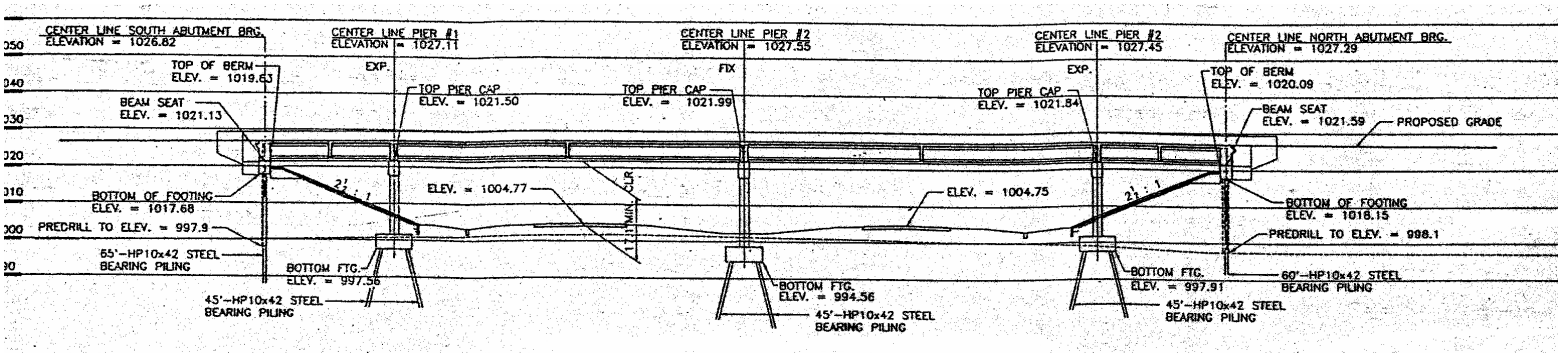

Figure 4.1. Longitudinal section at centerline of the roadway for the Marshall County Bridge (adapted from the Iowa DOT-Highway Division design details)

Figure 4.2 shows transverse cross sections of the bridge near the abutment, piers, and intermediate diaphragms. An 8-in. thick, RC-bridge deck is supported by five PC girders. The girders are spaced at 6 ft – 9 in. on center. A 3 ft-1 in. long, slab overhang that is measured from the centerline of the exterior girder to the edge of the deck was constructed along each longitudinal edge of the bridge. The total width of the bridge slab is 33 ft-2 in. The clear width of the bridge slab that is measured between the integral guardrails is 30 ft-0 in. Figure 4.3 illustrates the configuration and dimensions of the Iowa "Type D" PC girder used in this bridge.

At each of the integral abutments, a 3-ft wide, RC, end-diaphragm was constructed. Steel bearing plates are located underneath each of the five girders. A 3/4–in. diameter, coil rod passed through the bottom flange of each girder and extends into the end diaphragm. Bent bars extend from the diaphragm into the 8-in thick deck to provide a connection between the end-diaphragm and the deck.

The piers that support an end span and an interior span were constructed as expansion piers, and the pier that supports the two interior spans was constructed as a fixed pier. Figure 4.4 shows diaphragm details at an integral abutment, at an expansion pier, and at a fixed pier. An expansion pier is constructed such that the PC girders and the 26-in. thick, RC, pier diaphragm are supported by laminated-neoprene, bearing pads which permit relative displacement in longitudinal direction of the bridge between the girders and the pier. A fixed pier is constructed with formed keyways in the top surface of the pier cap beam. These keyways have 1-in. thick, strips of preformed, expansion-joint filler along the bottom, sides and ends of the keyways. Also at the fixed pier, a 1-in. thick, expansion-joint filler is used at all interface surfaces between the pier diaphragm and the pier cap beam. The PC girders are supported at this pier by 1-in. thick,

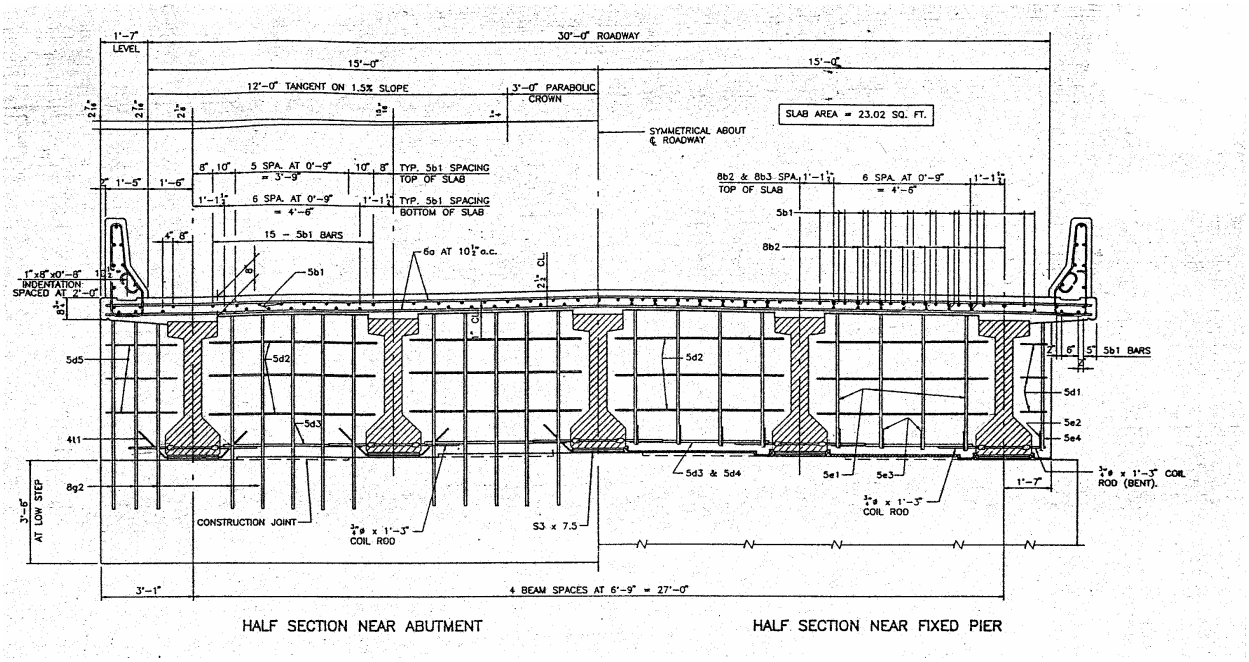

a. Cross section near abutment and fixed pier

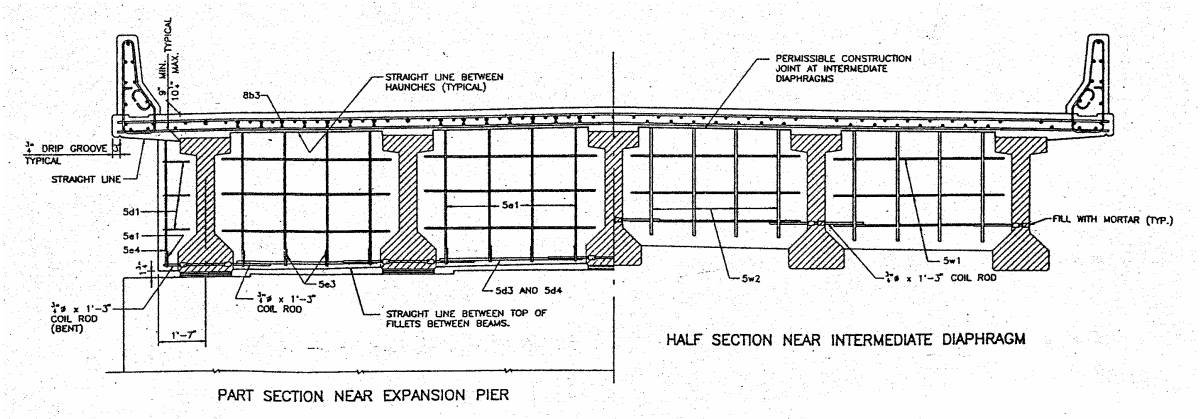

b. Cross section near expansion pier and intermediate diaphragm

Figure 4.2. Cross section of Marshall County Bridge (Adapted from the Iowa DOT-Highway Division design details, File no. 27498, Sheet no. 8)

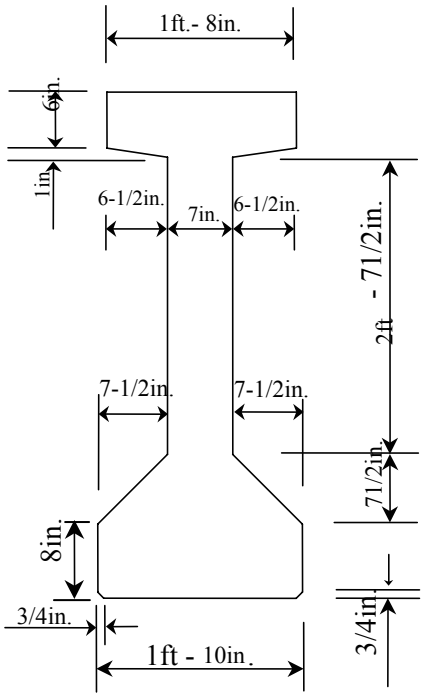

Figure 4.3. Cross section of an Iowa LXD PC girder

bearing pads. These construction details for a fixed pier minimized the relative displacement in the longitudinal direction of the bridge that can occur between the PC girders and the pier. The concrete that was specified for the PC girders and for the rest of the bridge had a 28-day, compressive strength of 5,000 psi and 3,500 psi, respectively.

4.2.2. Skewed bridge

Figure 4.5 shows a longitudinal cross section for a PC girder bridge that was constructed over US Hwy. 518 in Johnson County, Iowa. This bridge will be referred to as the Johnson County Bridge. The bridge-skew angle is 20°-24`-48``, and has four spans with three, intermediate, frame-type piers and two, integral abutments. The end span is 45 ft – 9 in. long, while the interior span is 96 ft – 6 in. long. The five, PC girders; bridge deck; and the two, expansion-type piers; and one, fixed-type pier are similar for the Marshall County Bridge.

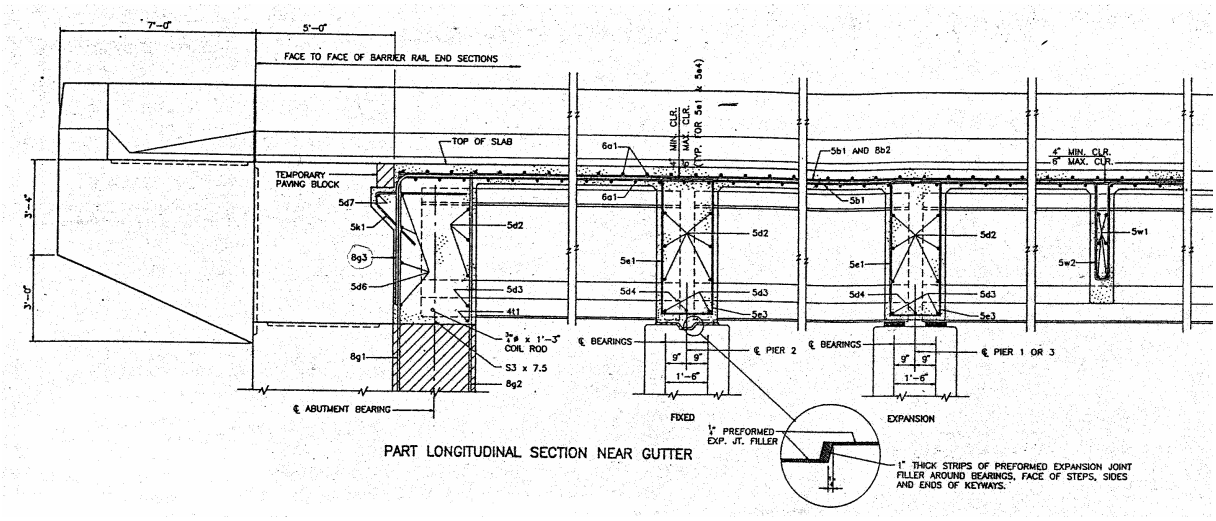

a. Cross section

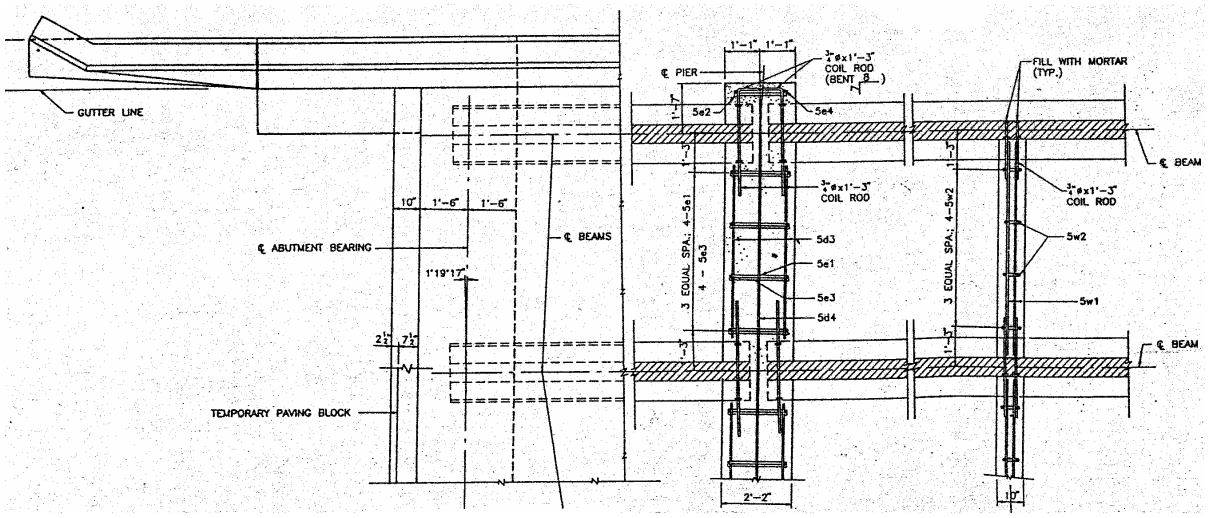

b. Plan

Figure 4.4. Diaphragms at the abutments and piers (Adapted from the Iowa DOT-Highway Division design details, File no. 27498, Sheet no. 9)

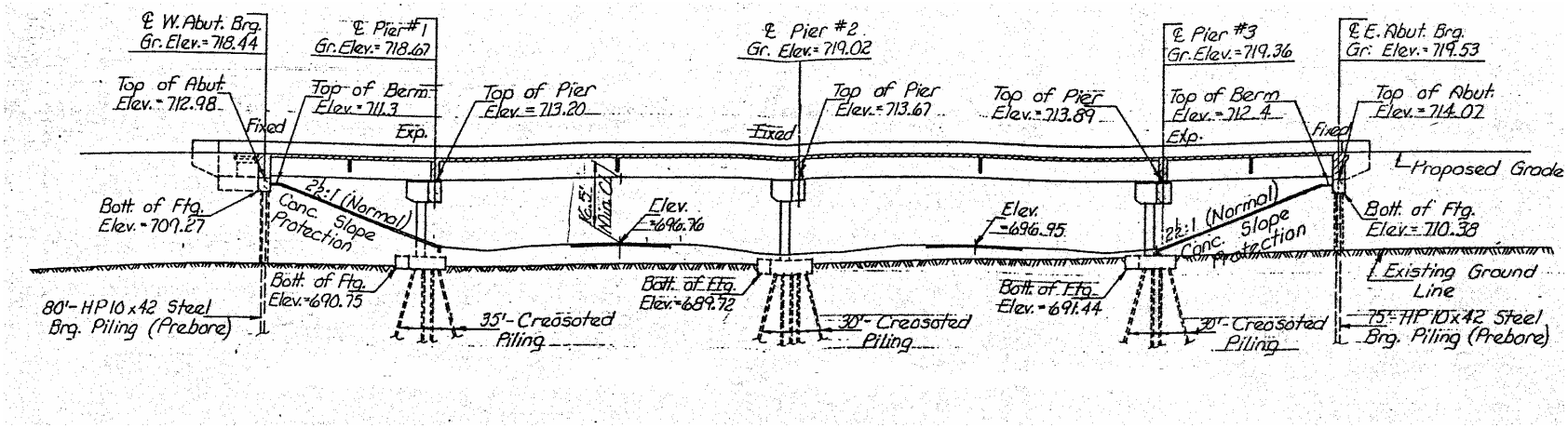

Figure 4.5. Longitudinal section at centerline of the roadway for the Johnson County Bridge (adapted from Iowa DOT-Highway Division design details, file no. 26197, sheet no. 2)

The two, RC, abutment diaphragms in the Johnson County Bridge had the same thickness as that for the Marshall County Bridge. For the Johnson County Bridge, the thickness of the RC, pier diaphragm is 32 in. The same type of connections between the abutment, pier diaphragms, bridge deck, and girders that were used in the Marshall County Bridge were also used in the Johnson County Bridge. The same material properties were applied in the finite-element analyses of the non-skewed and skewed bridges.

4.3. Finite-element models of a non-skewed bridge

This section describes the finite-element model developed for a non-skewed, PC- girder bridge. The bridge structure was analyzed twice: (1) by modeling the entire bridge structure and (2) by modeling only one of the interior spans. To decrease the complexity of the finite-element models, some slight modifications were made to the original, geometric configurations of the prototype bridge.

4.3.1. Description of the finite-element model

4.3.1.1. Four-span finite-element model

Figure 4.6 shows the transverse cross section of the four-span, finite-element model that was developed for a non-skewed, PC- girder bridge. To simplify building the finite-element model, the span lengths for the Marshall County Bridge described in Section 4.2 were slightly modified from the actual lengths. The end and interior span lengths were set equal to 46 ft and 97 ft, respectively. The bridge deck and girders were modeled using eight-node solid "brick" elements. A total number of 10,988 solid elements were used in the deck and girders of the bridge model. Complete details of the finite-element modeling of the bridge structure are discussed by Andrawes (2001).

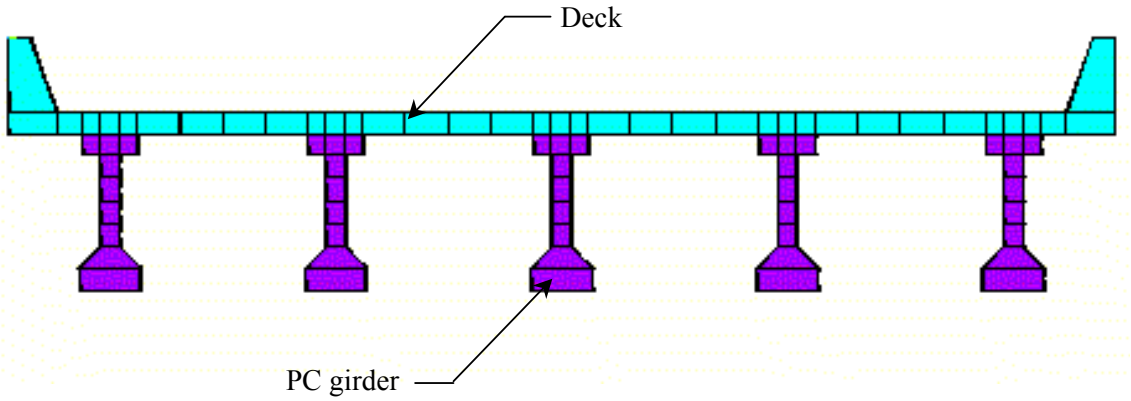

Cross section

Figure 4.6. Cross section of the four-span, non-skewed, finite-element bridge model

Based on the geometrical alignment of the Marshall County Bridge and the dimensions of the roadway beneath the bridge, the ISU researchers concluded that an over-height vehicle passing beneath the bridge could strike only an interior span of the bridge.

Figure 4.7 shows the cross section of the roadway beneath the bridge. The roadway profile has two, 12-ft wide, traffic lanes; a 10-ft-wide shoulder near the end span of the bridge; and a 6-ft-wide shoulder on the other side of the roadway. The intermediate diaphragms for an interior span of the bridge were assumed to be located at the center of the 24-ft-wide roadway beneath the bridge. As shown in the figure, two-load locations were initially considered in the analysis. The first-load location was at the location of the intermediate diaphragm, and the second-load location was at a point 16 ft away from the mid-span and towards the fixed pier. In the vicinity of the load, a finer-mesh size was used in the finite-element model for the bridge.

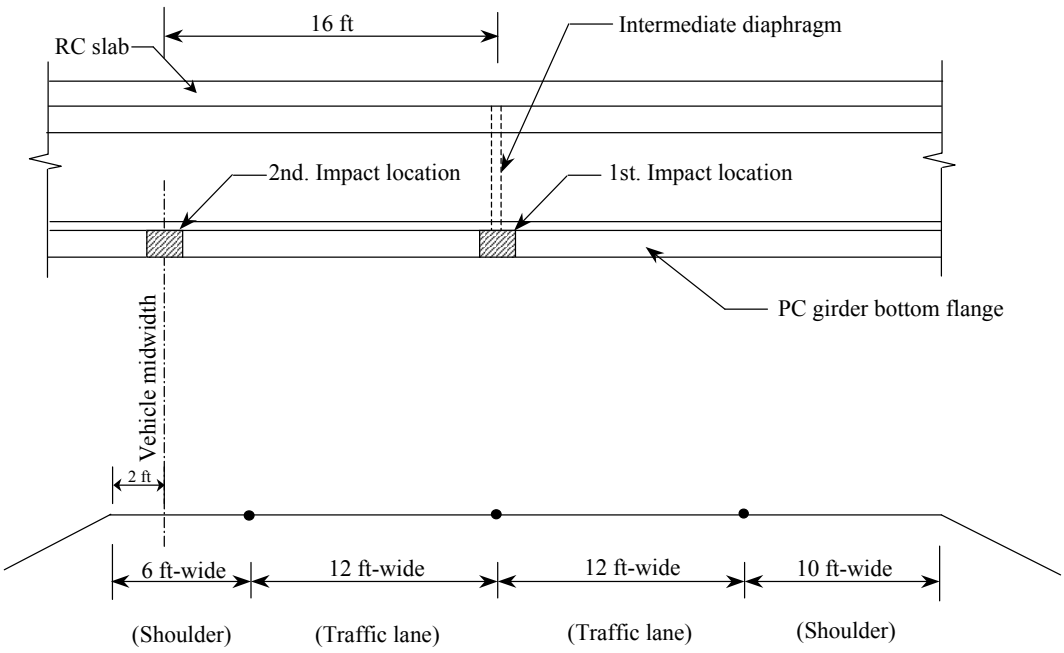

Figure 4.7. Cross section of the roadway passing beneath the bridge

The modulus of elasticity for the bridge deck and girders were calculated as 3370 ksi and 4030 ksi, respectively. The density of the concrete for the deck and girders was set equal to 150 lb/ft^3. Poisson's ratio for the concrete was set equal to 0.18.

The abutment-pile caps and abutment wingwalls were not included in the finite-element model; however, the abutment-end diaphragms were included in the analytical model. These 36-in. thick, end diaphragms were modeled using shell elements and were considered to be integrally connected to the bridge. The concrete material properties for these diaphragms were assumed to be the same as those for the concrete in the bridge deck.

For the purpose of simplifying the finite-element models without appreciably affecting the accuracy of predicted bridges responses, the three piers and their pile caps were not included

in the finite-element model. However, the 32-in. thick, pier diaphragms were modeled using shell elements, and they were assumed to act integrally with the girder and the deck.

The boundary conditions of the finite-element models were selected to represent the relative restraints of the prototype bridge. Figure 4.8 shows a schematic sketch of the boundary conditions that were used for the finite-element model. As shown in the figure, the boundary conditions were added to the model at the locations of the abutments and piers. Since the main contact between a bridge superstructure and substructure is at the bottom flange for each girder, the boundary conditions were added at each of the lower nodes for the bottom flange of each girder. At all the locations where boundary conditions were considered, the bridge was fully restrained from displacing in the vertical direction.

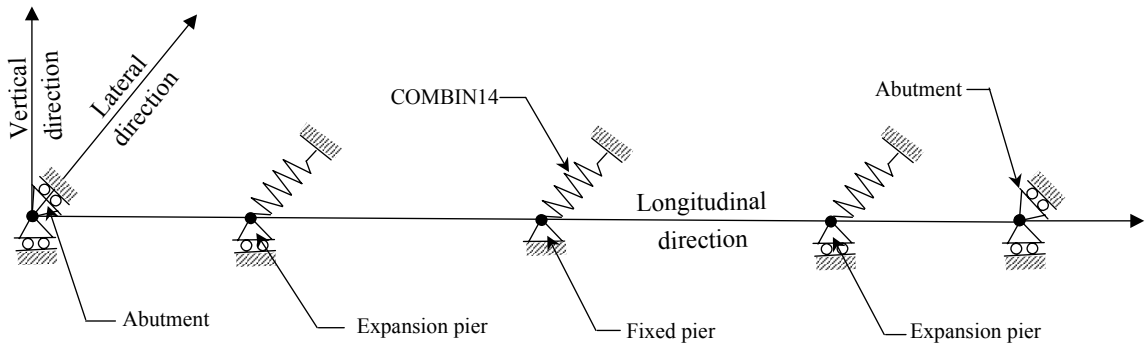

Figure 4.8. Boundary conditions considered in the analysis of the four-span finite element model

Because of the very large restraint provided by the abutments in the lateral direction (horizontal direction perpendicular to the bridge length) of a bridge, lateral translation was prevented at the bottom nodes of the bottom flange for each girder. Roller support conditions were assumed in the longitudinal direction of the bridge at the expansion piers and the abutments. The boundary conditions at the fixed pier did not permit longitudinal translation of the PC girders at this

location. To account for the in-plane lateral stiffness of the pier structures, linear-spring-type, finite elements were included in the analytical model at each pier location.

Each spring-type element had three, translational degrees-of-freedom, one for each of the three global X,Y, and Z-axis directions, and no damping capability. These elements, which were located in a horizontal plane, were connected at one end to a node on the bottom of a PC girder. The other end of each element was connected to a fixed node that was fully restrained from being displaced in any of the three orthogonal directions. The linear-spring stiffness for each of these elements was equal to a proportionate share of the lateral stiffness of the particular pier frame. The lateral stiffness of each pier frame was based on the flexural stiffness of the fixed-ended columns with sidesway.

4.3.1.2. Single-span finite-element model

An elastic analysis of the bridge structure using the four-span, finite-element model with static loads required a large amount of computer-file storage and computation time. If the bridge model is revised to incorporate the nonlinear behavior of the contact elements (discussed later in Section 4.3.2.1) and impact loading, the required computer-computational time and data-storage size became prohibitive for an analytical solution. To reduce the computational effort, the size of the finite-element model was reduced by modeling only the span of a bridge that experiences the impact load. The diaphragms at an expansion pier and at the fixed pier were included in this model. The results obtained from such an analysis must be verified to determine the effect of this simplification on the accuracy of the results. This verification was accomplished by comparing the results obtained from an analytical solution that involved the four-span, finite-element model with another analytical solution that involved the one-span, finite- element model. The single-span and the four-span bridge models were analyzed for the same loading conditions,

to establish specific strains and displacements. These results are presented and discussed in Chapter 5.

The finite-element, modeling guidelines that were discussed in Section 3.8 and the techniques and boundary conditions discussed in Section 4.3.1.1 were used to develop the single-span, finite-element model. For this model, all of the deck and girder nodes located at the two ends of the modeled span were restrained from displacing in the vertical direction, and the effect of continuity of the bridge in the longitudinal direction was not included in the model. The validity of this last assumption is based on the application of St. Venant principles.

4.3.2. Intermediate diaphragms

This section describes different types of intermediate diaphragms that were used in the theoretical study. One concrete diaphragm and two different configurations of steel diaphragms were considered in the analysis. The details are discussed for the three types of intermediate diaphragms, as well as for the finite-element models that were developed for the study of each diaphragm type.

4.3.2.1. Reinforced concrete intermediate diaphragm

Figure 4.9 shows the details of the standard, RC, intermediate diaphragm used by the Iowa DOT. The 10-in.-thick diaphragm starts from the underside of the bridge deck and extends down to the vertical face of bottom flange for the PC girders. The intermediate diaphragms can be cast either before or when the bridge slab is cast. Continuity between a diaphragm and the bridge deck is developed by using U-shape stirrups that extend from the diaphragm into the deck. To connect the bridge girders and the diaphragms, two, 3/4–in. diameter, steel-coil rods are inserted in the web of each girder at the location of the diaphragm. The two rods are positioned

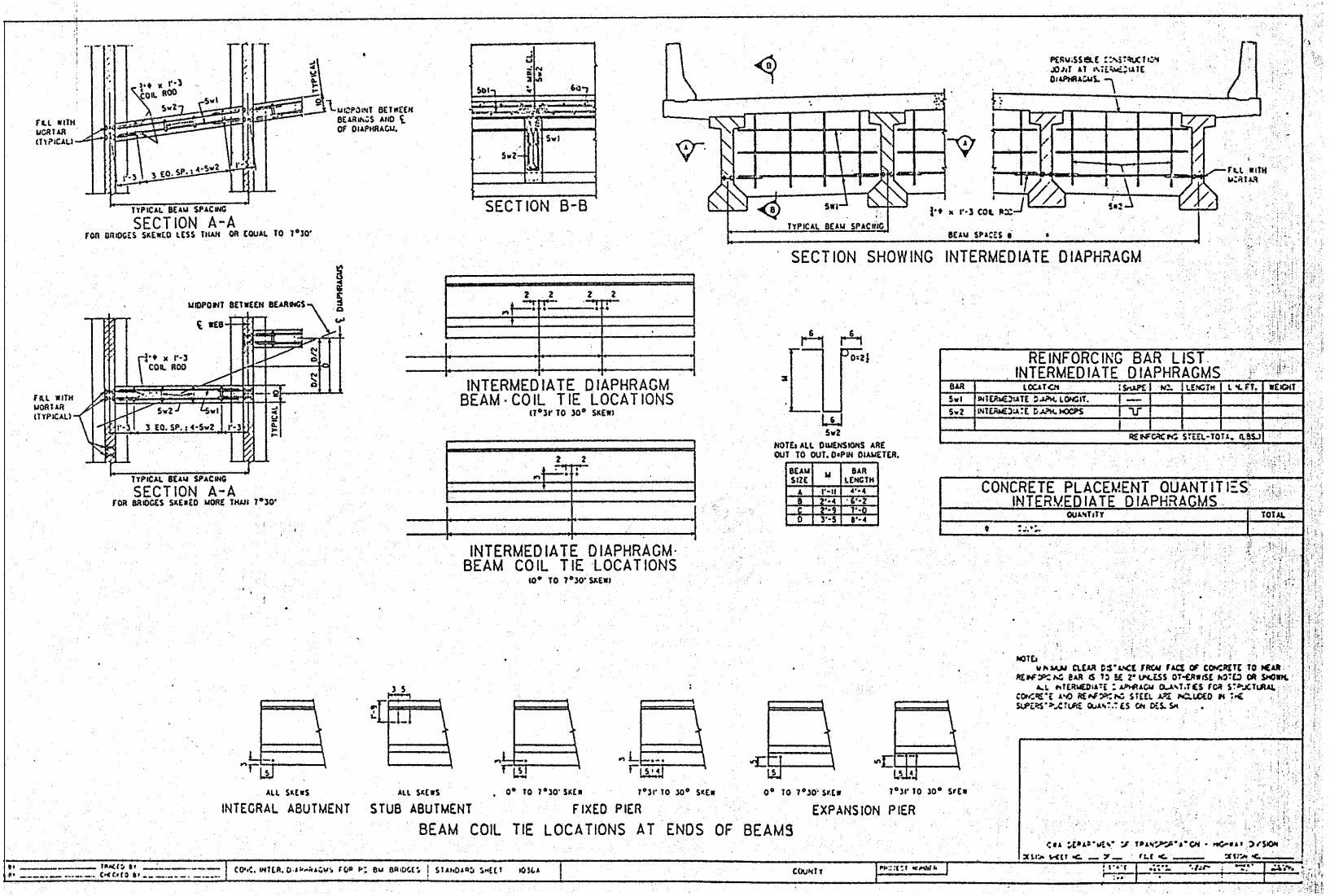

Figure 4.9. Iowa DOT reinforced concrete diaphragms (adapted from the Iowa DOT standard details)

at the same elevation and at a spacing of 4 in. on center. This spacing provided for a 3-in. clearance between each rod and its adjacent diaphragm edge. The 15-in. long, coil rods extended from both sides of the 7-in. thick, girder web.

For the finite-element model of the prototype, non-skewed, 97-ft long, bridge span, four, RC, intermediate diaphragms were positioned at the mid-span between the five, PC girders. Solid elements were used in modeling the diaphragms. Three layers of elements were positioned across the 10-in., diaphragm thickness. The thickness of each layer was selected so that the two, 3/4 - in. diameter, steel-coil rods occurred at the vertical faces of the inner layer of elements. Therefore, the thickness of the two, outer, element layers was 3 in., while that for the interior, element layer was 4 in. The concrete material properties for the diaphragms were the same as those for the deck.

Since monolithic concrete construction does not exist between the RC diaphragms and the PC bridge girders, common element nodes were not used at the boundaries between the diaphragms and the girders. Two set of nodes were used at these member surfaces. The first set of nodes was for a bridge girder and the second set of nodes was for the RC diaphragm. This modeling technique permits a separation to occur between the girders and the diaphragms. An identical modeling approach was applied at the interface between the deck and the diaphragms, even though these members are connected by the U-stirrups. To prevent the nodes at the interface between the diaphragms and the girders and between the diaphragms and the bridge deck from overlapping, sliding surface-to-surface contact elements were inserted along the common boundaries of these bridge components. Since a diaphragm has more axial stiffness than the transverse-bending stiffness of the PC girders, a diaphragm element was selected as the

target element, while a girder element was selected as the contact element. The coefficient of friction between these concrete-bridge elements was set equal to 0.6.

The steel-coil rods that provided a direct connection between the diaphragms and the girders were modeled as three-dimensional, truss links. Figure 4.10 shows that the coil rods passed through a girder web without being connected to any of the nodes for the web. Each node of a link element was connected to a node on the edge of the diaphragm in contact with the side of a girder. This modeling technique allowed a pulling force to be transferred from the pulled diaphragm on one side of a girder to the diaphragms on the other side of the girder through the coil rod without a direct connection to the girder that was located between the two diaphragms (see Fig. 4.10a). This behavior was based on the fact that a contact surface does not transfer tension across two surfaces which are in contact.

A similar modeling technique, shown in Fig. 4.10b, was used to idealize the connection between an exterior girder and its adjacent diaphragm. To model this connection, a steel plate that was not present in the prototype bridge needed to be attached to the exterior side of an exterior girder at the location where the coil rods were inserted through the girder's web. As shown in Fig. 4.10b, the plate, which was modeled by six, three-dimensional, solid elements, was positioned so that two, interior nodes for the plate match the two, corresponding nodes on the diaphragm edge that was in contact with the girder. The dimensions for these plates were 10-in. wide by 8.125-in. high by 1-in. thick. To prevent the plate nodes from overlapping the girder nodes, a contact surface was used at the common boundary between these parts. The contact surface was a sticking surface to prevent a change in the location of the coil rods when the bridge was loaded. One end of a coil-rod member was attached to the diaphragm edge that was in

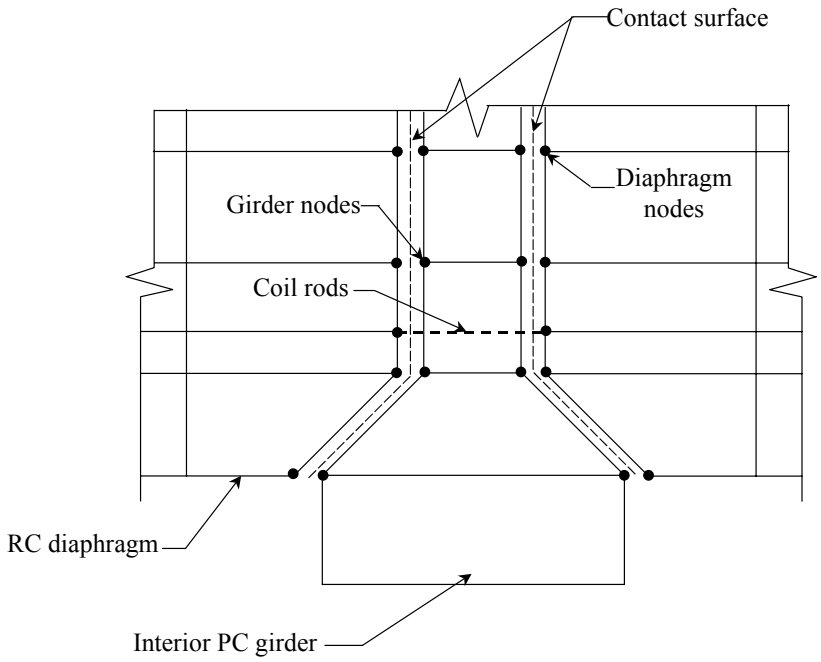

a. Interior girder connection

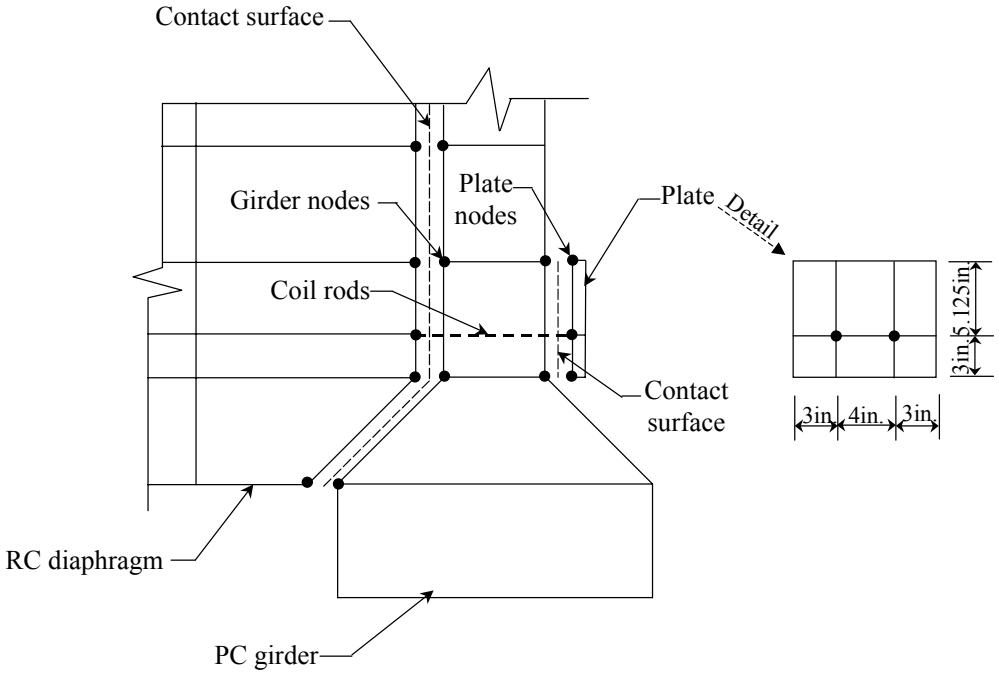

b. Exterior girder connection

Figure 4.10. Connection between the RC diaphragms and the PC girders

contact with the exterior girder, and the other end of a coil rod was attached to the steel plate surface that was in contact with the girder.

4.3.2.2. Steel X-braced with horizontal strut intermediate diaphragm

Figure 4.11 shows the geometric configuration of the steel, X-braced with horizontal strut, diaphragm currently used by the Iowa DOT, and how it is attached to the PC bridge girders. As shown in the figure, the diaphragm consists of two, angle-shaped, cross braces and a horizontal strut that has its bottom flange almost flush with the bottom of the girders. Each member of the X-brace is an L 6 x 4 x 5/16. The horizontal strut is a built-up-shape member that is formed by bolting together a WT6 x 17.5 and a W14 x 34 along their lengths. Two rows of ¾-in. diameter, high-strength bolts that are spaced at 6-in. on center connect the flange of the WT shape and the top flange of the W-shape.

As shown in Fig. 4.11, the X-brace and the horizontal strut are fastened to the PC girders using a bent-steel plate, which is formed into a 9 in. by 6 in. by ½ in. angle shape. The bent plate has a length of 2 ft – 5 in., and it is attached to the web of the girders. The 6-in. wide, angle leg of a cross-brace member is connected to the 9-in.-wide leg of the bent plate with four, 3/4–in. diameter, high-strength bolts. As shown in the figure the only connection between the horizontal strut and the bent plate is through the web of the WT-shape at the ends of the members. These end connections are made with four, 3/4–in., diameter, high-strength bolts. The bent plate is fastened to the web of a PC girder with three, 3/4–in. diameter, high-strength bolts that are positioned along the height of the 7-in. thick, girder web. For an interior girder, these bolts connected together the 6-in. legs of the bent plates on each side of the girder web. For an exterior girder, these bolts connect together a 3/8-in. thick by 6-in. wide by 2 ft – 5 in. long, steel

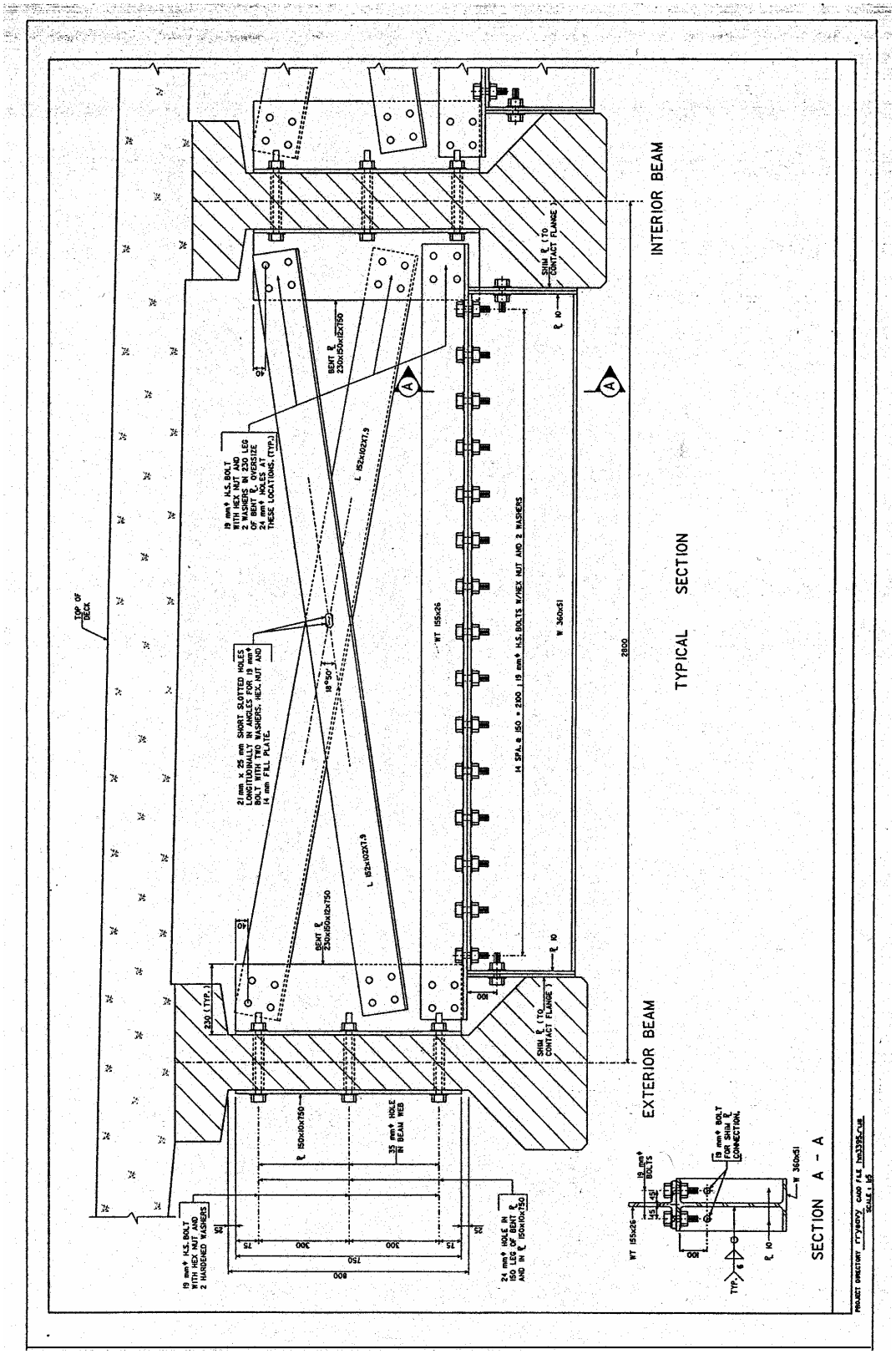

Figure 4.11. Iowa DOT X-Braced with horizontal strut diaphragm (adapted from the Iowa DOT standards)

plate on the exterior side of the girder web and the bent plate on the interior side of the girder web. To provide a bearing surface between the ends of the W-shaped, horizontal strut and the bottom flange of a girder, a shim plate is bolted with two, ¾-in.-diameter bolts to a 3/8-in. thick, steel-end plate, which is welded at each end of the W-shape. As noticed from Fig. 4.11, only a portion of the shim plate was in contact with the girder bottom flange.

All of the steel plates were modeled using shell elements, and the bolts were modeled using three-dimensional, truss elements. These bolts were connected only to the steel plates on each side of a girder web. This idealization for the bolts provided the only load-transfer mechanism when tensile forces are induced between the intermediate diaphragms. To prevent an overlap of the nodes for the steel plates and those for the girder web, surface-to-surface, contact elements were used on the surfaces between the plates and the girder web. To prevent movement of the high-strength bolts in a vertical plane, a sticky-surface characteristic was specified for these contact elements. Since the contact surfaces separated two different materials, the harder surface, which for this application is the steel plate, was modeled as the target surface, and the softer surface, which for this application is the RC girder, was modeled as the contact surface.

Figure 4.12 shows a sketch for the model developed for each cross-brace member of an intermediate diaphragm. Three-dimensional, beam elements rather than link-type elements were used to model these members. Beam elements allow the joint between a brace and a bent plate to be modeled as a semi-rigid joint. Nodes c and d, which are shown in Fig. 4.12, were used at the end of each cross-brace member. The 3-in. distance between the two nodes was the spacing between the high-strength bolts. Since a cross-brace member was an L 6 x 4 x 5/16, a 1.17-in.

eccentricity existed between the centerline of a bracing member and outstanding leg of a bent plate.

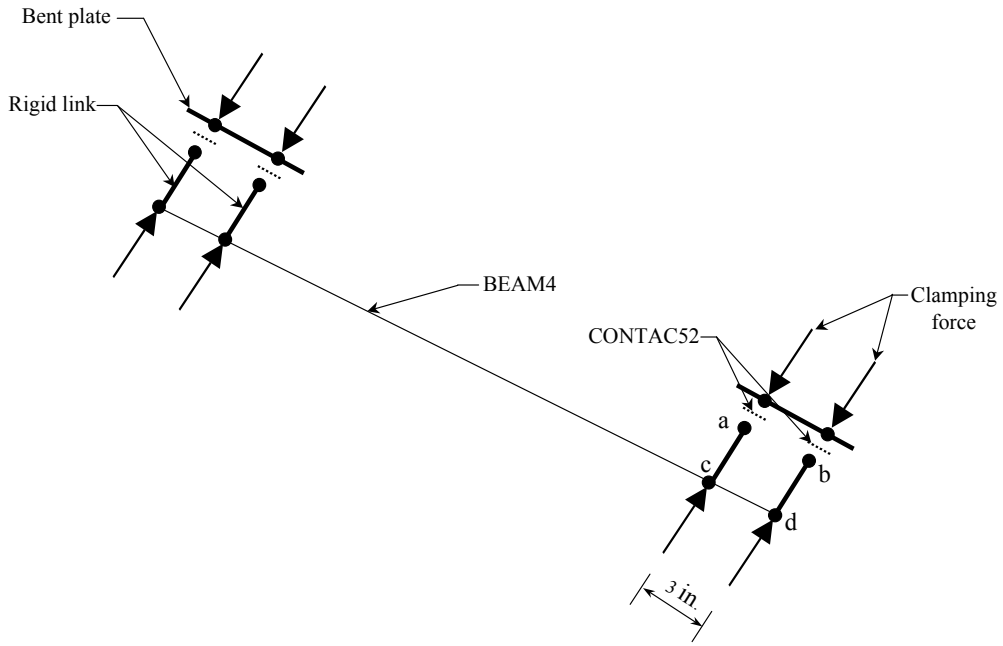

Figure 4.12. Finite element model of a cross bracing member (View looking along the member length)

To allow for a frictional force to develop between a diagonal member and a bent plate, common nodes were not used for these two parts. Nodes a and b, which are shown in Fig. 4.12, were on the surface of a bent plate, and they were in alignment with the Nodes c and d at the end of a bracing member. Nodes a and c and Nodes b and d were connected by a short, rigid-beam element. Node-to-node, contact elements were used to connect these rigid elements to the bent plate. This type of a contact element has only three, translation, degrees-of-freedom; therefore, bending moments can not be transferred through the element. To transfer any in- plane or out-

of-plane bending moments, the two-paired nodes (Nodes a and c, and Nodes b and d) will permit the development of a force couple.

The contact elements in this connection permits sliding and separation between a cross-brace member and its supporting bent plate. The formation of a gap between these two parts was restrained by the application of two, 56-kip, clamping forces at each of these connections. The total magnitude of the two clamping forces was set equal to the minimum bolt-tension that develops in four, ¾-in. diameter, A325, high-strength bolts. The resistive sliding force for a contact element was based on the clamping forces and a coefficient of friction equal to 0.33 for steel-on-steel bearing with a clean, mill-scale, surface condition.

As previously mentioned in the description of the diaphragm, geometrical configurations, an end plate was welded at each end of the W-shape that formed part of the horizontal strut. A shim plate was connected to an end plate using two, 3/4-in., diameter bolts. In the finite-element model, the shim plate and the end plate were modeled as one plate with a 3/8-in. thickness. Since this end plate will be effective only when a compressive force exists between the horizontal strut and the adjacent, bottom flange of a girder, sliding-surface-to-surface, contact elements were used to model the common surface between the end plate and the girder flange. These contact-surface elements prevent overlapping of the adjacent surfaces, and they allowed an end plate to separate from a girder flange when a horizontal strut is pulled away from that flange.

For the horizontal strut, sliding, surface-to-surface, contact elements were used to model the contact area between the bent plate and the web of the WT-shape. These elements allowed relative horizontal and vertical slippage to occur between the horizontal strut and its supporting bent plate. Clamping forces that are induced by the fully-tensioned, high-strength bolts at these

connections was modeled using the same techniques that were used for the cross-brace member for an intermediate diaphragm. A coefficient of friction equal to 0.33 was used for a clean-mill-scale, steel-surface condition.

4.3.2.3. Steel K-braced with horizontal strut intermediate diaphragm

The third type of intermediate diaphragm considered in this work has a steel, K-brace with a horizontal strut, as shown in Fig. 4.13. The diaphragm was formed from the same steel parts that were used for the steel, X-braced with horizontal strut intermediate diaphragm. As shown in the figure, the only difference between this K-braced diaphragm and the X-braced diaphragm involved the diagonal members. One leg of a diagonal member for the K-brace was bolted to the bent plate using four, 3/4-in. diameter, high-strength bolts. The other end of the member was bolted to a gusset plate that was welded to one side of the web for the WT-shape portion of the horizontal strut. The dimensions for the gusset plate are a function of the spacing between the PC girders and the girder depth. For the diaphragm studied, a ½ - in. thick by 7 3/4-in. wide by 18-in. long, gusset plate was modeled with shell elements. To provide symmetry for the K-brace, the gusset plate was positioned at the mid-length of the horizontal strut. The connection between the end of a diagonal member and the gusset plate was the same as that used at the other end of the member. Essentially, the finite-element idealization that was used for the X-braced diaphragm was also used for this diaphragm.

4.3.3. Load cases

Lateral-impact loads were applied to the bottom flanges of bridge PC girders to simulate an over-height vehicle collision as the vehicle travels underneath a bridge. There are several factors that influence the characteristics of this type of an impact load, e.g., the mass of the truck,

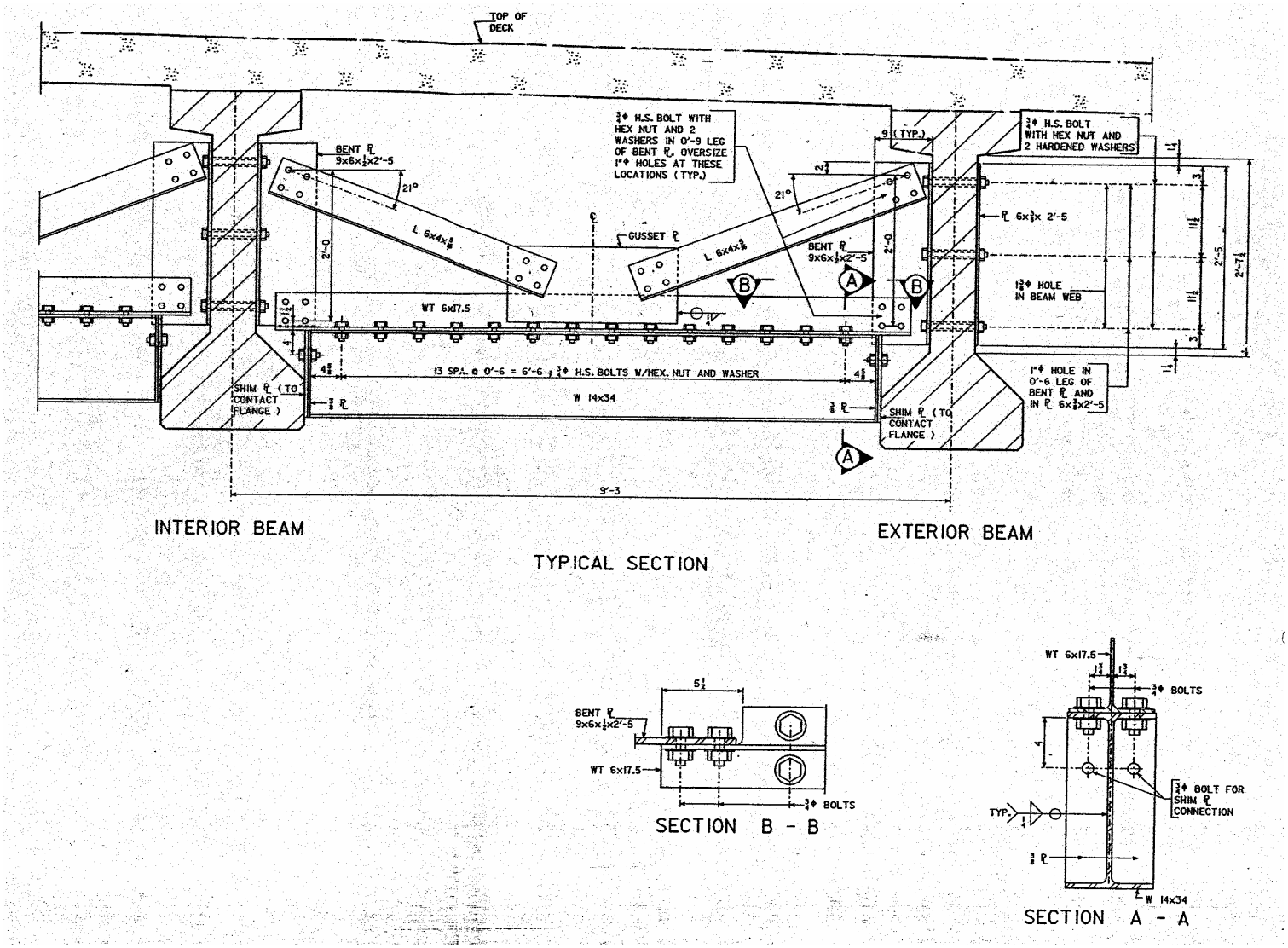

Figure 4.13. Iowa DOT K-Braced with horizontal strut diaphragm (adapted from the Iowa DOT standards)

the speed of the truck, the geometric configuration and the rigidity of the object that strikes the bridge. However, the mass and speed of the truck are two factors that have a significant effect on the magnitudes and duration for the impact load. The development of mathematical models to represent different load-history behavioral relationships for vehicle-impact force was beyond the scope of this research.

Since the main objective of this research was to conduct a comparative study that evaluates the effectiveness of different types of intermediate diaphragms in minimizing structural damage to a bridge superstructure when a lateral-impact force was applied to the bottom flange of PC bridge girders, a precise forcing function for an impact load did not need to be defined. Therefore, a constant-magnitude, impact load was selected to be applied over a short-time period for all bridge models. The impact load was applied at one of five locations, as shown in Fig. 4.14. Load positions 1 and 2 were at the intermediate-diaphragm location that was at the mid-span for Beams BM1 or BM5, respectively. Load positions 3 and 4 were 16-ft away from the intermediate-diaphragm location. As the analytical studies progressed, the researchers decided to apply the lateral load at a Load position 5, which was 4 feet away from the intermediate-diaphragm location. This fifth-load location was considered to investigate the efficiency of diaphragms on reducing the girders damage when the load was applied close to, but not, at the intermediate-diaphragm location.

One scenario that may occur when an over-height vehicle or vehicle load strikes a bridge on the bottom flange of girder is as follows: First, the over-height object would impact the first exterior girder (Beam BM1). Then, because the vehicle would not suddenly stop, but continue moving, the object being transported could displace downward, as the vehicle-suspension system reacts to the impact, which would allow the object to pass beneath Beam BM1. As the vehicle-

suspension system rebounds, the object could displace upwards and cause additional impacts of the object with some or all of the other bridge girders at either their bottom flange or somewhere

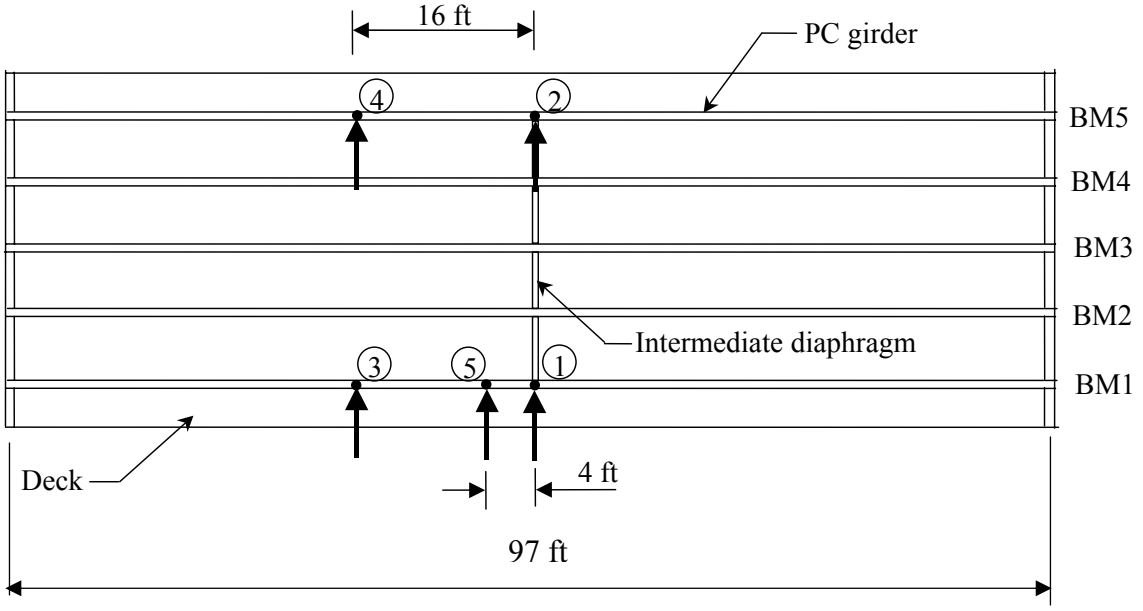

Figure 4.14. Load locations

on their web. Multiple-girder impacts were not included in this study because the reduction in the impact-force magnitude resulting from a reduction in the speed of the vehicle after the first impact is unknown. In this work, a single, impact load was applied on Beam BM1 or on Beam BM5 (see Fig. 4.14), since these loading conditions will induce the most severe, bridge response. When an over-height-object strikes Beam BM1, the bottom flange of this girder will laterally displace towards the first-interior girder (Beam BM2). That movement will induce a compression force in the intermediate diaphragm between these two girders. When an over-height-object strikes Beam BM5, the bottom flange of this girder will laterally displace away from the bridge and induce a tensile force at the interface between that girder and its adjacent intermediate diaphragm.

The maximum magnitude of an impact load was selected such that the maximum, principal-tensile strain that is induced in the impacted girder would not appreciably exceed the

modulus of rupture of concrete for the girder. Two, load magnitudes were selected. A 120-kip load was used when the load that was applied on a PC girder at an intermediate diaphragm location. A 60-kip load was used when the load was applied on a PC girder at a point not at an intermediate-diaphragm location. To establish a reasonable, load-duration time, a literature search was conducted, which revealed that the collision times were in the range of 0.05 to 0.15 sec. (Zaouk et al., 1996; Nalepa, 1990; Jiamaw and James, 1994; and Hohnason and Baughn, 1992) A 0.1-sec., load-duration time was selected for all impact loads used in this study. Figure 4.15 shows the dynamic-load histories for the two, different, lateral loads. These loads were applied to the analytical model of a bridge span as a pressure loading over an area on the bottom flange of a PC girder. This type of load application was selected over a concentrated load that would act at a single node, to minimize high-stress concentration at the location of the load.

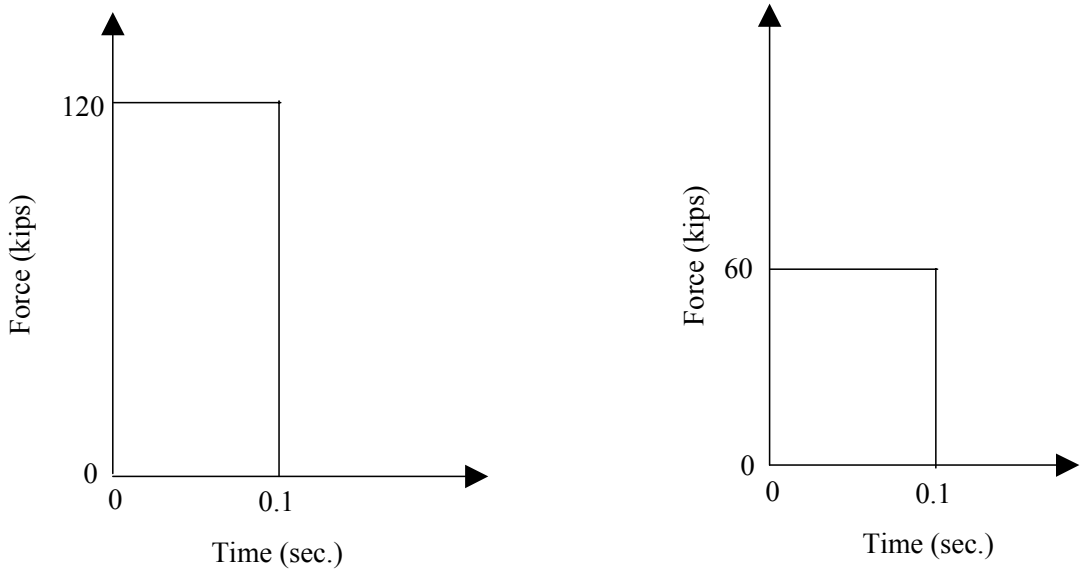

a) At the diaphragm location **b) Not at the diaphragm location**

Figure 4.15. Force versus time relations used in simulating lateral-impact load

4.4. Finite element model of the skewed bridge

A skewed bridge was analyzed to study the effect of the bridge-skew angle on the response and behavior of a bridge superstructure with different types of intermediate diaphragms. A 30-deg., skew angle was selected for the prototype bridge. This section describes the finite-element models that were developed for the skewed bridge and the loading cases that were considered in this theoretical study. Figure 4.16 shows a schematic, plan view of the skewed bridge and the location of the intermediate diaphragms.

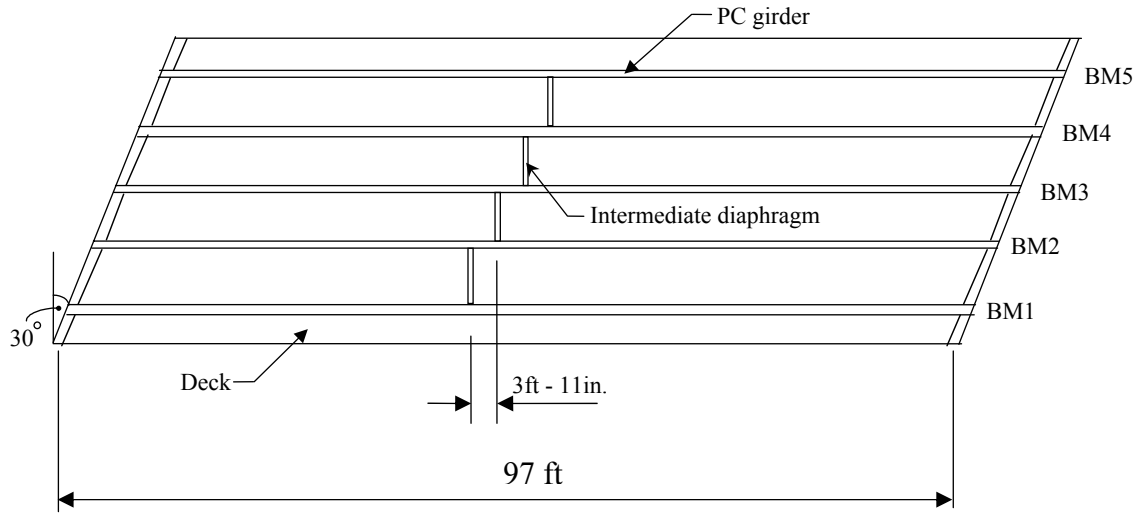

Figure 4.16. Arrangement of the intermediate diaphragms in the skewed bridge

4.4.1. Model description

Only the impacted, internal span was modeled for the analysis. The reason for modeling only one span rather than the complete-bridge structure was discussed in Section 4.3.1.2. Except for the direction of the horizontal-spring element that modeled the horizontal, in-plane, stiffness of a pier, the boundary conditions at the ends of the modeled, interior span for the skewed bridge were similar to those used in the analyses of the modeled, interior span for the non-skewed bridge. For the non-skewed-bridge model, these spring elements were aligned in a direction that

was perpendicular to the longitudinal direction of the bridge. For the skewed-bridge model, the piers were oriented parallel to the road passing underneath the bridge; therefore, a 60-deg. angle exists between the longitudinal direction of the piers and the longitudinal direction of the bridge. As a result, these horizontal-spring elements that were located at each end of the analytical model were aligned parallel to the pier diaphragms. The guidelines established in modeling the intermediate diaphragms for the non-skewed bridge were also used to model the different types of intermediate diaphragms for the skewed bridge.

4.4.2. Intermediate diaphragms

The 30-deg., skew angle and the 6 ft-9 in. girder spacing caused the intermediate diaphragms to be offset from each other by 3 ft-11 in., as shown in Fig. 4.17. The modeling techniques discussed in Section 4.3.2.1 and shown in Fig. 4.10 were also applied to model the connection of the RC, intermediate diaphragms with the bridge girders for the skewed bridge. However, since the intermediate diaphragms were not in alignment for the 30-deg., skewed bridge, the method that was used to make the connection between a diaphragm and an exterior girder for the non-skewed bridge was used to connect the intermediate diaphragms with all of the girders in the skewed bridge. The offset diaphragms for the skewed bridge also affected the connections of the X-braced and K-braced, intermediate diaphragms with the interior, PC girders. The modeling techniques discussed in Sections 4.3.2.2 and 4.3.2.3 for the connection between an X-braced and K-braced, respectively, intermediate diaphragm and an exterior girder for the non-skewed bridge was applied for all of the connections for the intermediate diaphragm to the PC girders in the skewed bridge.

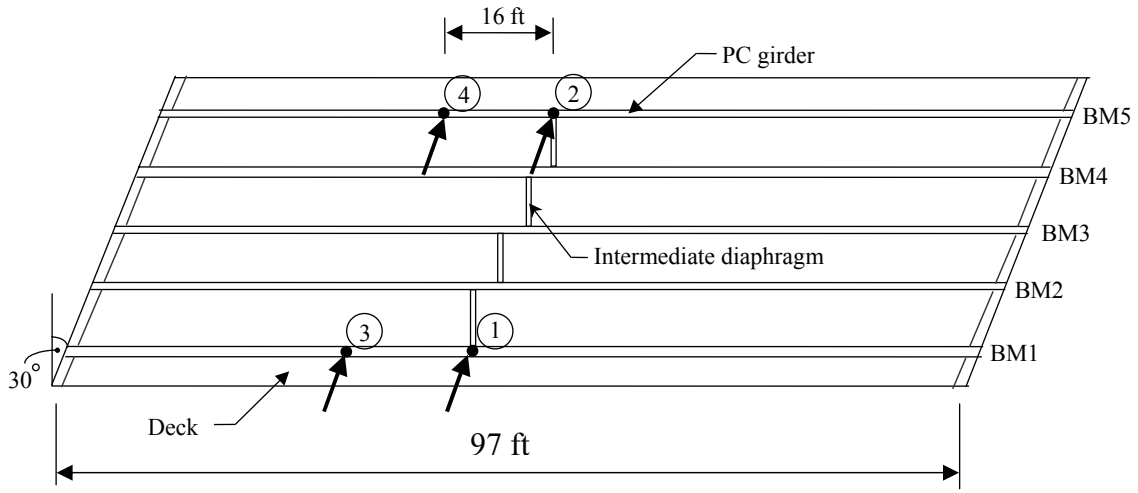

Figure 4.17. Load locations of the skewed bridge model

4.4.3. Load cases

The loads that were applied to the skewed-bridge model were static loads rather than dynamic loads. The decision of conducting a static-load analysis instead of a dynamic-load analysis for the skewed bridge was taken after evaluating a dynamic-load factor (DLF) for each of the intermediate-diaphragm studies for the non-skewed-bridge models. The DLF is a ratio of the response magnitudes for a given parameter, such as the maximum, principal-tension strain in a girder that is evaluated for dynamic and static loads. As expected, the principal strains and deflections for dynamic loading were higher than those for static loading. The range in the DLF for the maximum, principal-tensile strains in the impacted, PC girder was between 1.15 and 1.20. Essentially, the value for the DLF was almost the same for all of the intermediate-diaphragm types that were investigated. The consistency in the magnitude of the DLF for the different intermediate-diaphragm types was assumed to be applicable for a skewed bridge.

The lateral-load locations for the skewed-bridge model are shown in Fig. 4.17. The load was applied to the bottom flange of either Beam BM1 or Beam BM5 and in a direction that was parallel to the direction of the roadway passing underneath the bridge. For the 30-deg.-skewed-

bridge model, the line-of-action for the load was orientated at a 60-deg. angle, which was measured from the longitudinal axis of the bridge. The load was resolved into components that were perpendicular and parallel to the longitudinal axis of the bridge. The load was applied as a pressure with the same magnitudes as that which were used for the non-skewed, bridge models.

5. ANALYSIS RESULTS

5.1. Introduction

In this chapter the predicted, principal-tension strains and horizontal displacements that were induced by the lateral-impact loads are presented for the non-skewed-bridge and skewed-bridge, finite-element models. Since this research focused on minimizing potential damage to PC girders when a bridge is hit by an over-height vehicle or vehicle load, the ISU researchers concentrated the analysis on the response of the PC girders to the lateral-impact loads. The results of the four-span and one-span, finite-element models described in Chapter 4, as well as the results for the three, diaphragm types are summarized in separate sections of this chapter. In addition, comparisons are made between the different types of intermediate diaphragms for their effect on the structural behavior of the PC girders.

5.2. Four-span and one-span finite element models

In this study, the 120-kip, lateral-impact load with duration time of 0.1 sec. was applied at the mid-span of Beam BM1. The principal-tensile strain at the top fibers of the web for the impacted girder of the four-span model and the one-span model are presented in Fig. 5.1. This web location is where the highest, principal-tensile strains were induced in Beam BM1. The figure shows similar behavior over time for the two, finite-element models with about a 15-percent, maximum difference in the strain magnitudes.

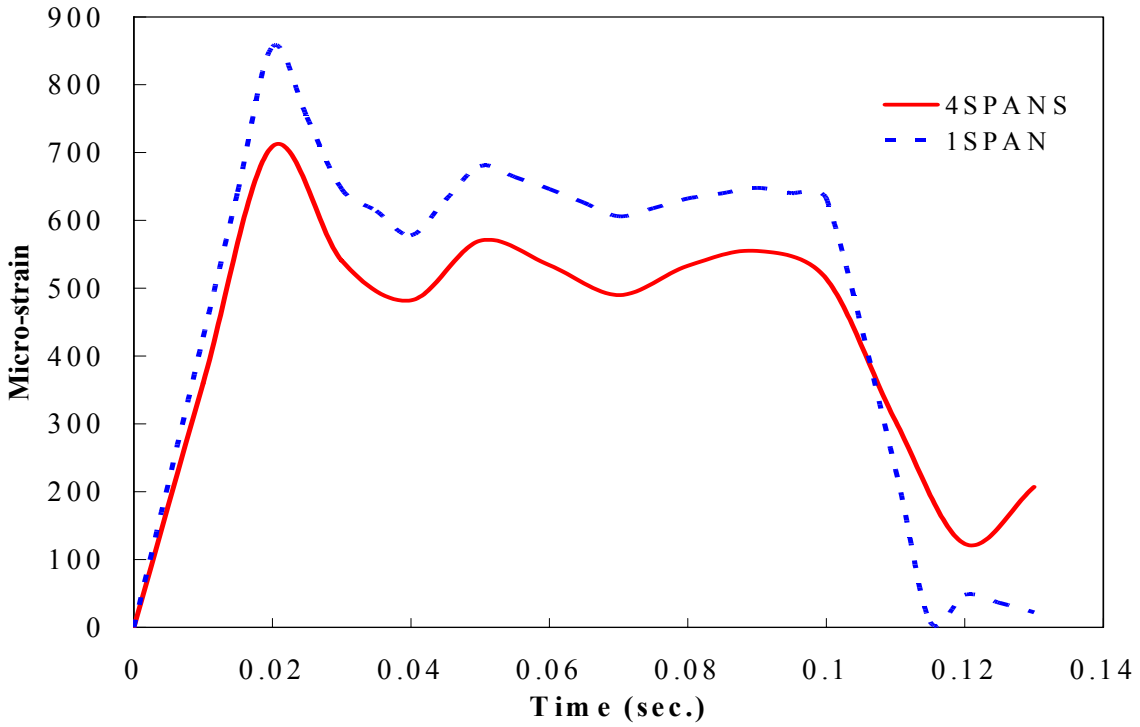

Figure 5.1. Maximum principal-tensile strain versus time for the four-span and one-span models without diaphragms (load and strains at the mid-span of Beam BM1)

The horizontal displacement results obtained from the analysis of the two different models are presented in Fig. 5.2. These displacements were calculated at the bottom flange of the impacted girder and at the location of the lateral load. Figure 5.2 illustrates the close agreement in the displacements that were predicted by the four-span and one-span finite-element models. Because of the similarity in the strain and displacement results that are presented in Figs. 5.1 and 5.2, the ISU researchers decided to conduct the rest of the research utilizing one-span, finite-element models.

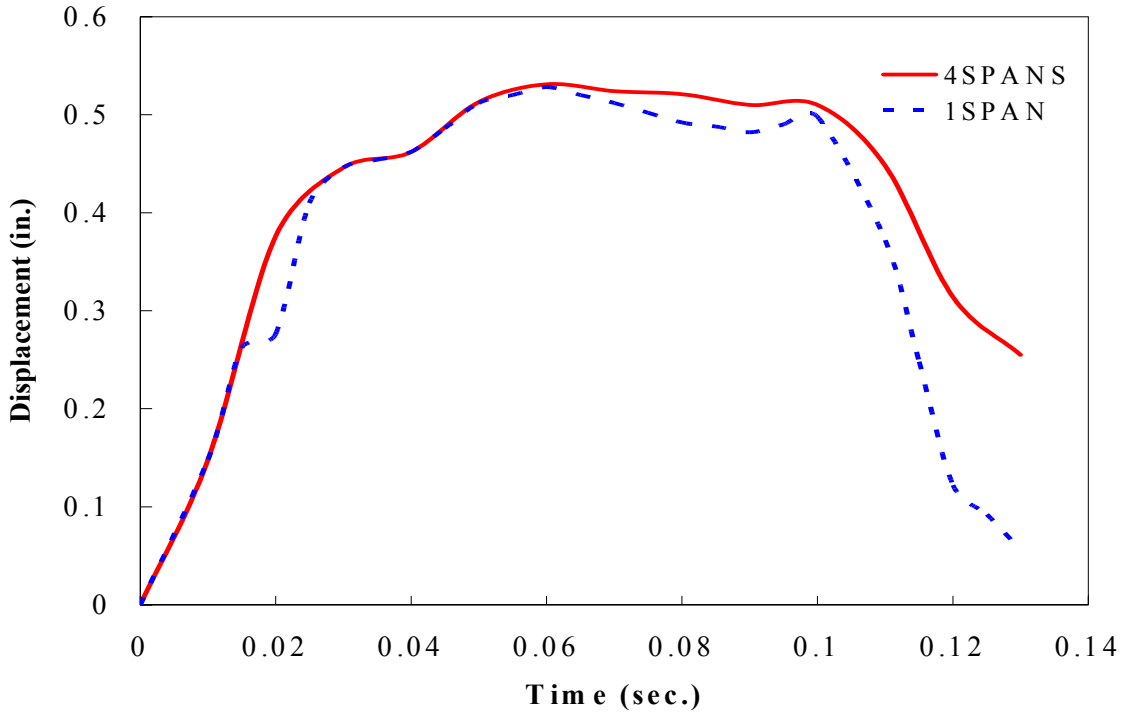

Figure 5.2. Horizontal displacement versus time for the four-span and one-span models (load and displacement at the mid-span of Beam BM1)

5.3. Non-skewed bridge model

This section presents the maximum, principal-tensile strains and horizontal displacements for the PC girders of the non-skewed, bridge models for each type of intermediate diaphragm. The lateral load that was applied for the analyses and the applied-load locations were presented in Section 4.4.3. Section 5.3.4 presents the maximum, principal-tensile strains in an impacted, exterior girder for a non-skewed bridge when the lateral-impact load was applied at 4 ft away from the mid-span.

5.3.1 Strains

To qualitatively evaluate the amount of potential damage that might occur in a PC girder after a bridge superstructure is hit by an over-height-vehicle load, the ISU researchers decided to

use the induced, principal-tensile strains in the girder as a measurement for potential-damage assessment. Strains rather than stresses give a more accurate representation of structural response. Except for localized damage at the point of impact, large tensile strains rather than large compressive strains will provide an indication as to where most of the damage will occur in a girder. All of the principal-tensile strains that are presented in this chapter are the maximum values that occurred in each girder. The maximum, principal-tensile strain occurred at the same location for the three types of intermediate diaphragms that were investigated in this research when the impact load was at mid-span, which was the location of the intermediate diaphragms. The maximum strain was in the bottom flange of the impacted girder at the mid-span cross section. This maximum-strain location was the same for the girders that were not directly impacted, when the load was applied at 16 ft away from the mid-span of the impacted girder.

When the lateral load was applied at a location that was not at an intermediate diaphragm, the maximum, principal-tensile strains that were induced in the impacted girder occurred at the cross section of the girder where the load was applied. Although the load was applied directly to the girder bottom flange, the maximum strains were at the top of the girder web because of the flexibility of the web for the girder in the plane of the cross section for the girder. This flexibility was restrained at the mid-span cross section for the girder by the intermediate diaphragm that was in contact with the web of this girder. The absence of this lateral restraint at a location away from the intermediate diaphragm allowed the top of the web to experience a high bending moment that acted in the plane of the cross section for the girder. When diaphragms were not present in the bridge, the maximum, principal-tensile strains always occurred at the cross section where the load was applied and in the top fibers of the girder web.

5.3.1.1. Reinforced concrete intermediate diaphragms

Figure 5.3 shows the maximum, principal-tensile strains in the five, PC girders when RC, intermediate diaphragms are present and the 120-kip, impact load was located at the mid-span of Beam BM1. The response of the girders was recorded for 0.03 seconds after the load has been removed. The figure shows a significant difference in the strains between the loaded girder (Beam BM1) and the other PC girders. As shown in the figure, the maximum, principal-tensile strains that were induced in each girder reached their peak value at sequential times.

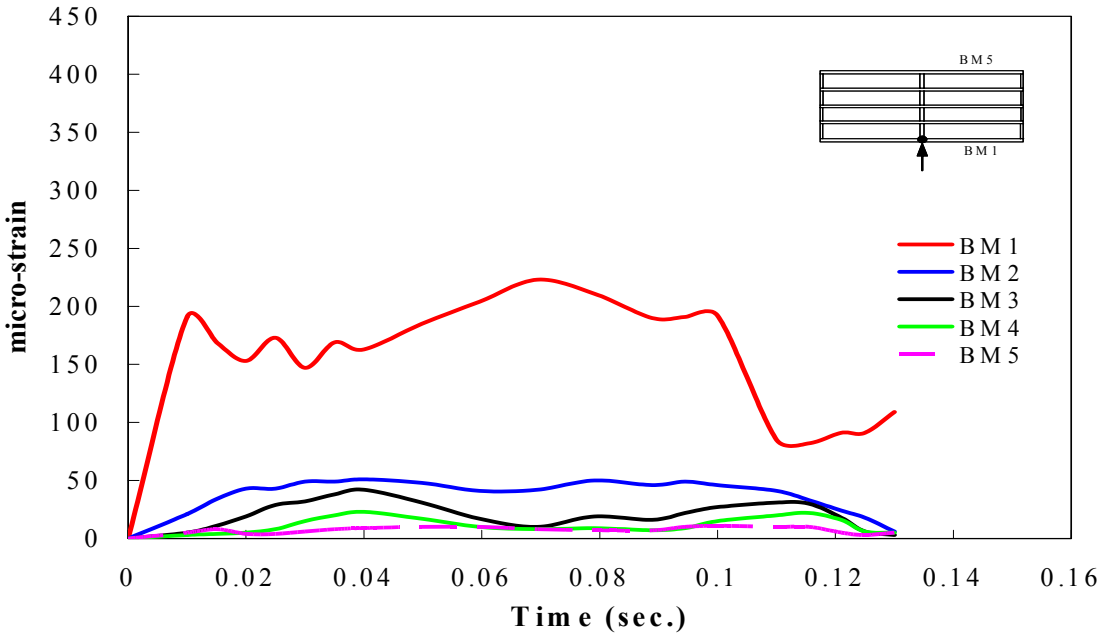

Figure 5.3. Maximum principal-tensile strain versus time for the RC diaphragms (no load offset on Beam BM1)

This time-delay effect was expected since a time lapse is necessary for a portion of the impact load to be transferred from the impacted girder (Beam BM1) to the next girders in order of their position with respect to Beam BM1. Figure 5.3 shows that the maximum, principal-tensile strain induced in Beam BM1 was equal to 223 micro-strains and that this strain occurred at 0.069 sec. after the initiation of the impact load. After the load was removed at 0.1 sec., this

strain in Beam BM1 initially decreased quite rapidly and then gradually increased again in response to the dynamic characteristics for the bridge. As one would expect, the strains in the girders that were closer to the impact location on Beam BM1 were higher than that for those girders that were further away from the impacted girder. But, what was not anticipated by the ISU researchers was the significant difference in the maximum, principal-tensile strains between Beams BM1 and BM2 when the impact load occurred at the diaphragm location.

Figure 5.4 shows the distribution of the maximum, principal-tensile strain along a portion of the length of the impacted girder at a time of 0.069 sec. after the 120-kip, impact load was applied to Beam BM1. The impact location corresponds with the zero distance on the abscissa scale for the graph. As shown in the figure, only one half of the beam length was considered in the study because of the symmetry of the model and loading.

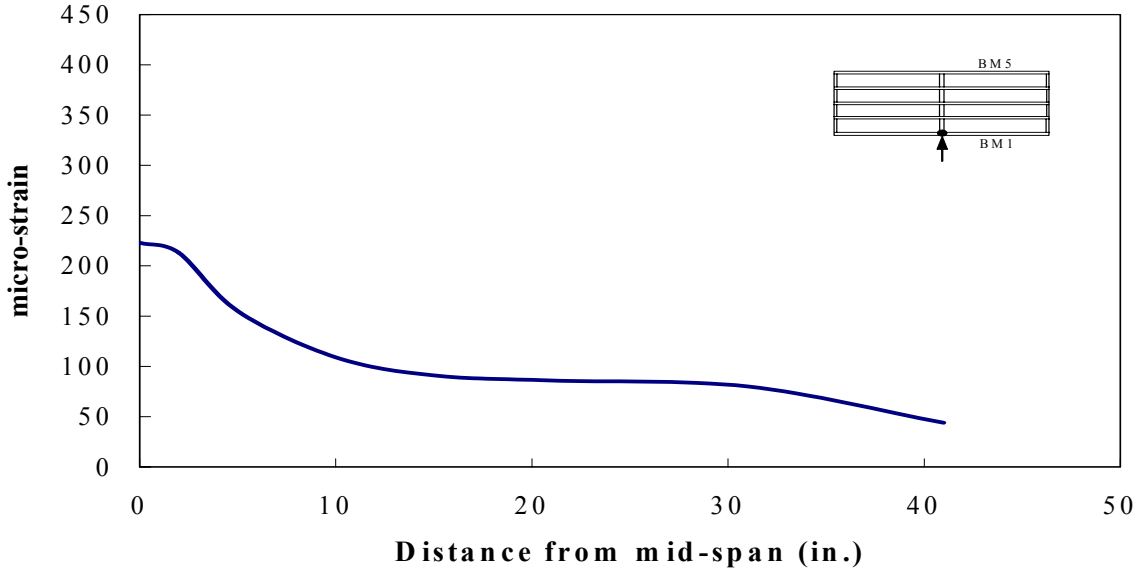

Figure 5.4. Maximum principal-tensile strain distribution along a portion of Beam BM1 for the RC diaphragms (no load offset on Beam BM1)

A maximum, principal-tensile strain of 223 micro-strains was predicted at the mid-span for the impacted girder. This strain rapidly diminished for girder cross sections that were slightly removed from the impact location. At a distance of 10 in. away from the mid-span for the girder, this strain was equal to about 50 percent of its maximum value. The strain continued to gradually decrease to about 20 percent of its maximum value at a distance of 40 in. away from the mid-span.

Figure 5.5 presents the maximum, principal-tensile strains that were predicted for the five, PC girders with the RC, intermediate diaphragm, when the 120-kip, impact load was applied at the mid-span of Beam BM5. This load was applied on the inside face of the bottom flange for this girder.

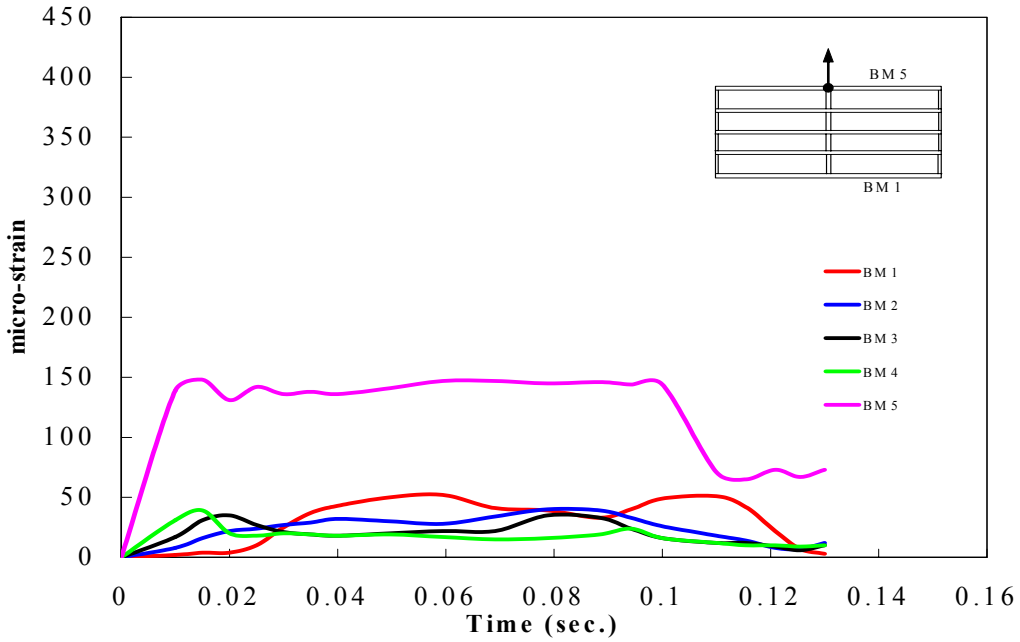

Figure 5.5. Maximum principal-tensile strain versus time for the RC diaphragms (no load offset on Beam BM5)

The loaded girder (Beam BM5) experienced the highest strain of 148 micro-strains at 0.015 sec. after the impact load was applied to this girder. Again, the strains in the impacted girder were significantly higher than the strains in the other girders. A comparison between the maximum-strain for Beam BM5 and that predicted for Beam BM1 (see Fig. 5.3), when the load impacted that girder, revealed that the geometrical conditions, which were associated with Fig 5.3, produced higher strains in the impacted girder than that for the geometrical conditions, which were associated with Fig. 5.5. This difference in the behavior between the two, load cases was caused by the geometry of the connection between each of the exterior, PC girders and the adjacent intermediate diaphragm. When Beam BM1 was loaded on the exterior face of the bottom flange, the impact load induced a compressive force between this loaded girder and its adjacent diaphragm. A force was transferred between the girder and the diaphragm by bearing along a portion of the depth of the diaphragm. The force in the coil rods that connected these members was almost equal to zero. On the other hand, when the load was applied on the interior face of the bottom flange for Beam BM5, the bottom flange for this girder was pulled away from the adjacent diaphragm. Only the coil rods provided a connection between the loaded girder and its adjacent diaphragm. As a result, a large tensile force was induced in the two, coil rods to resist the separation of this girder and this diaphragm. The force in the coil rods induced strains in the bottom flange of the loaded girder that were of opposite sense to the strains that were induced in the bottom flange of the loaded girder by the applied impact load. The same type of strains were induced when Beam BM1 was the impacted girder and the adjacent diaphragm induced a resisting pressure against the inside face of Beam BM1. Since the location of the coil rods were close to the bottom flange for Beam BM5, the strains induced in Beam BM5 by the resistance that was provided by the coil rods was higher than the strains that were induced in

Beam BM1 by the resistance that was provided by the bearing of the diaphragm that was adjacent to Beam BM1. The net effect of the load-transfer mechanisms that existed when Beam BM1 or Beam BM5 were the impacted girder caused smaller, induced, resultant strains in Beam BM5, when that beam was the impacted girder, than those strains in Beam BM1, when that beam was the impacted girder.

Figure 5.5 shows that the maximum, principal-tensile strains in the four, non-impacted, PC girders (Beams BM1 through BM4) were almost equal to each other. After about 0.05 sec. had elapsed since the load impact began, Beam BM1 started to experience higher, principal-tensile strains than those strains for the other unloaded beams. This behavior was induced by the load-transfer mechanisms between the girders and the diaphragms. When Beam BM5 was loaded, a tension force was induced in all of the coil rods that connected the diaphragms to the girders. These coil-rod tension forces caused all the intermediate diaphragms to displace towards Beam BM5. This diaphragm movement induced a contact pressure from the diaphragm on the side of a PC girder that faced Beam BM1, since the coil rods were not attached to the girders. For Beam BM1, there was not a diaphragm on the free side of the girder and only a small plate was used at the coil-rod location. Thus, the force transferred to Beam BM1 through the coil rods was a concentrated load rather than a distributed pressure. Since Beam BM1 was the farthest girder from the point of the applied load, the largest time delay occurred for this girder to reach its maximum, principal-tensile strain.

Figure 5.6 shows the distribution of the maximum, principal-tensile strains along a portion of the length for Beam BM5 at a time of 0.015 sec. after the 120-kip, impact load was applied to this girder. The largest strain of 148 micro-strains occurred at the mid-span of Beam BM5. Due to the symmetry of the bridge about its mid-span, the distribution of the strains is

only shown for one half of the beam length. The figure shows that the strains gradually decreased for the girder cross sections that were farther away from the point of impact until the strain was equal to about 15 percent of its maximum value at a distance of 20 in. from the mid-span. The strain distribution shown in Fig. 5.6 is quite similar to that shown in Fig. 5.4.

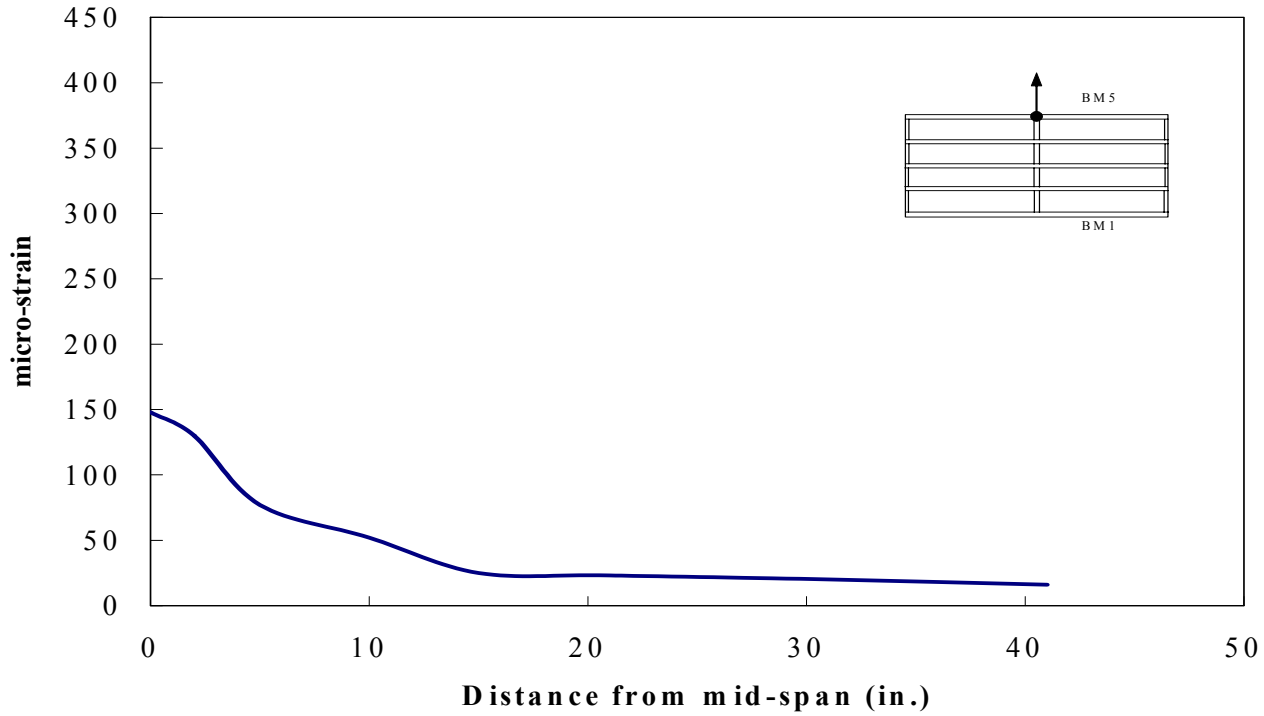

Figure 5.6. Maximum principal-tensile strain distribution along a portion of Beam BM5 for the RC diaphragms (no load offset on Beam BM5)

The slight difference in the distribution of the principal-tensile strains that are shown in Figs. 5.4 and 5.6 was attributed to the difference in the load-transfer mechanism that was associated with an impact load being applied to Beams BM1 or BM5.

Figure 5.7 presents the maximum, principal-tensile strains that were induced in the five, PC girders with the RC, intermediate diaphragms, when the 60-kip, impact load was applied at 16 ft away from the mid-span of Beam BM1. As shown in the figure, Beam BM1 was the girder

which was most affected by the applied load. This load-resistance behavior amongst the five girders was expected, since the impact load was applied away from the diaphragm location. A time delay was observed in the response of the unloaded girders because of the time required for a portion of the impact load to be transferred from the impacted girder through the diaphragms to the rest of the girders. As noticed from the figure, the strain response for the five girders is characterized by more vibration amplitude and even larger magnitudes than those shown in Fig. 5.3, when the 120-kip, impact load was applied at the mid-span of Beam BM1, which matched the location for a diaphragm. These behavioral differences were expected for the different load point with respect to the diaphragm location. For the geometric conditions that were associated with Fig. 5.7, the maximum, principal-tensile strain in Beam BM1 was 323 micro-strains, and it was predicted to occur 0.02 sec. after applying the 60-kip, impact load.

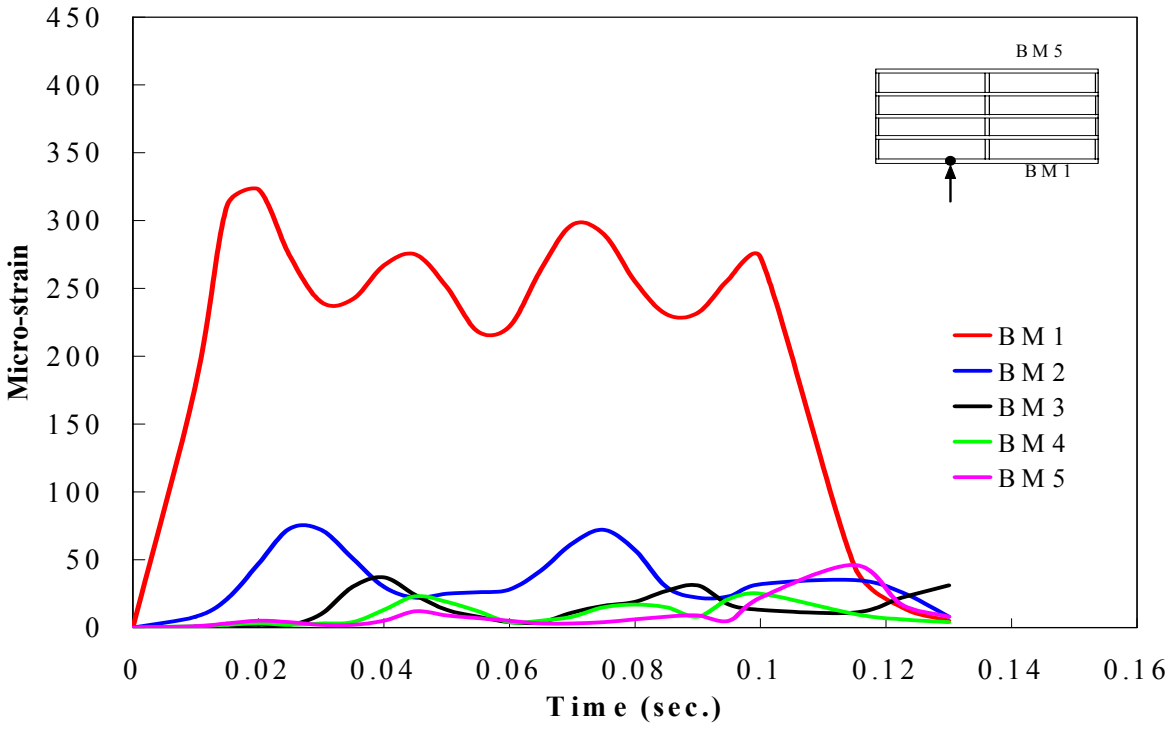

Figure 5.7. Maximum principal-tensile strain versus time for the RC diaphragms (16-ft load offset on Beam BM1)

For each of the four, non-impacted girders, the maximum, principal-tensile strain was in the bottom flange for each girder at the intermediate-diaphragm location and not at the point of application of the impact load. With regards to the girders that were not directly impacted, the first-interior girder (Beam BM2) was the most affected unloaded girder. The maximum strain induced in Beam BM2 was about 20 percent of that induced in the impacted girder. The rest of the unloaded girders (Beams BM3, BM4, and BM5) almost experienced the same behavior. The maximum, principal-tensile strains in these girders were significantly smaller than that in Beam BM2.

Figure 5.8 shows the maximum, principal-tensile strains in the five, PC girders with RC, intermediate diaphragm, when the 60-kip, impact-load was applied at 16 ft away from the mid-span of Beam BM5. The behavior shown in the figure is similar to that shown in Fig. 5.7, when the 60-kip, impact load was applied to Beam BM1. After about 0.02 sec. of applying the load,

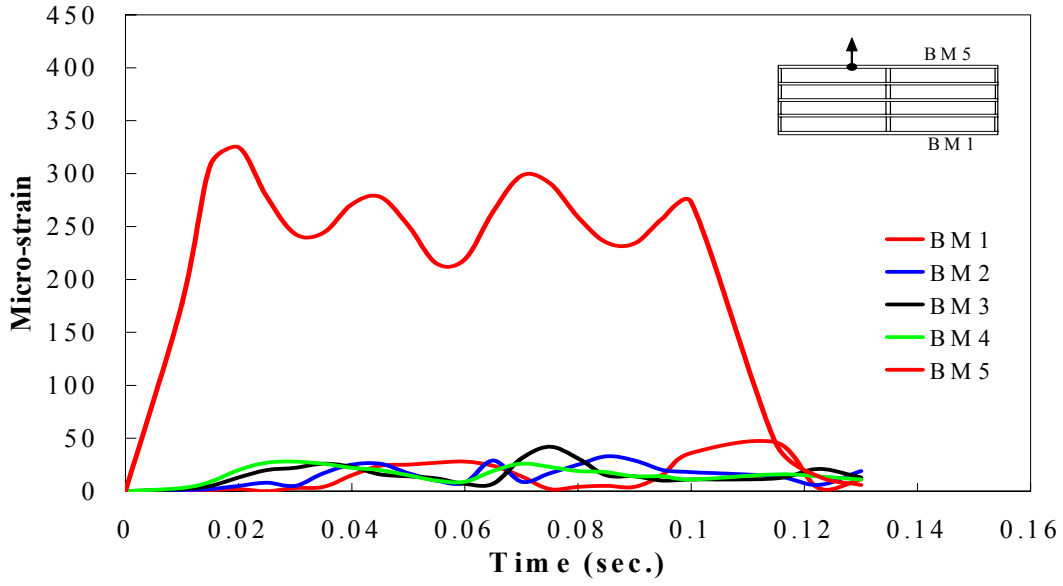

Figure 5.8. Maximum principal-tensile strain versus time for the RC diaphragms (16-ft load offset on Beam BM5)

the principal-tensile strain in Beam BM5 reached a maximum value of 325 micro-strains. The maximum, principal-tensile strains in each of the other girders were almost the same, and these strains were relatively small compared to those strains for Beam BM5.

5.3.1.2. Steel X-braced with horizontal strut intermediate diaphragms

Figure 5.9 shows the maximum, principal-tensile strains in the five, PC girders with the steel X-braced and horizontal strut, intermediate diaphragm. The 120-kip, impact load was applied at the mid-span of Beam BM1. As shown in the figure, Beam BM1 experienced the largest, principal-tensile strain. This strain was equal to 341 micro-strains, and it was induced 0.09 sec. after applying the load. The principal-tensile strains in Beam BM1 significantly decreased after the removal of the load at a time of 0.10 sec. The largest principal-tensile strain that was induced in Beams BM2 and BM3 was 159 and 84 micro-strains, respectively. These strains in Beams BM4 and BM5 were relatively small, which indicated that most of the lateral load was resisted by the first three girders, when the load was applied at the diaphragm location.

Figure 5.10 presents the distribution of the maximum, principal-tensile-strains along a portion of the length for Beam BM1 at a time of 0.9 sec. after the 120-kip, impact load was applied to this girder. Because of the symmetry of the model with the load applied at mid-span, only the distribution of these strains along a portion of one-half of the length of Beam BM1 is shown. The maximum strain of 341 micro-strains was induced in the bottom flange of this girder and at the mid-span of the girder. The strain gradually decreased in a cross section of a girder, as the distance increased between that cross section and the mid-span. At 40 in. from the mid-span, the maximum, principal-tensile strain was equal to about 38 percent of its maximum value at the mid-span.

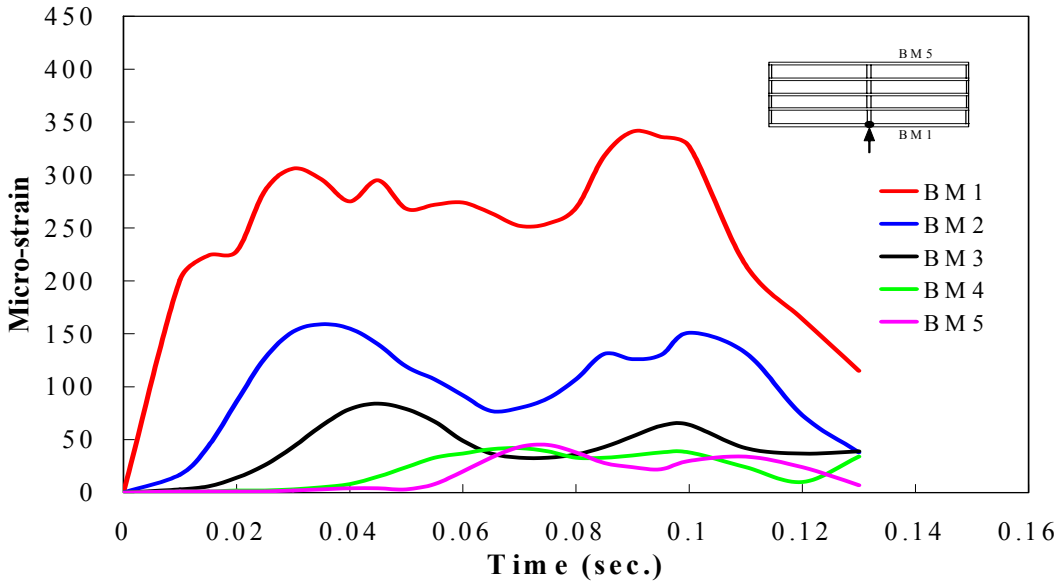

Figure 5.9. Maximum principal-tensile strain versus time for the X-braced diaphragms (no load offset on Beam BM1)

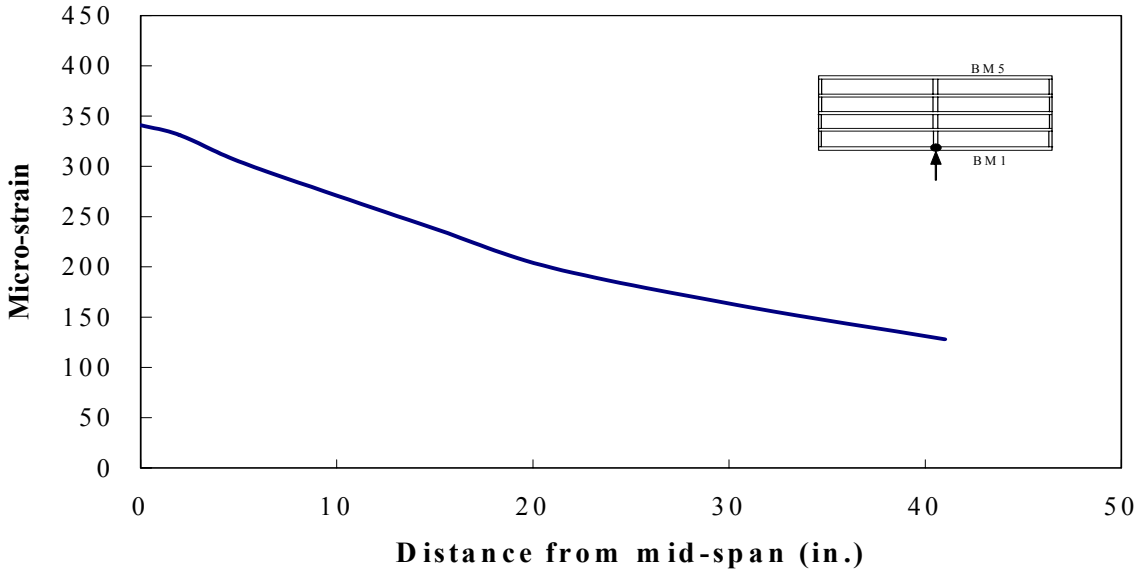

Figure 5.10. Maximum principal-tensile strain distribution along a portion of Beam BM1 for the X-braced diaphragms (no load offset on Beam BM1)

Figure 5.11 shows the maximum, principal-tensile strains in the five, PC girders with the X-braced and horizontal strut, intermediate diaphragm, when the 120-kip, impact load was applied at the mid-span of Beam BM5. This beam experienced slightly higher strains than the adjacent girder (Beam BM4). The maximum, principal-tensile strains in Beam BM5 were 264 micro-strains at a time of 0.03 sec., while that strain in Beam BM4 was 224 micro-strains at a time of 0.04 sec. The 15-percent difference between the maximum strains for Beams BM5 and BM4 was considered to be small compared to the 74-percent difference between those strains in those same girders (see Fig. 5.5) and for the same loading conditions when the RC, intermediate diaphragms were used. The ISU researchers attributed this difference in the strain magnitudes for these girders that have the RC, intermediate diaphragms or the steel, X-braced, intermediate diaphragms to be caused by the geometrical configuration for each diaphragm type and the connection detail between each diaphragm type and the PC girders. Since the maximum strains were induced at the bottom flange of each girder, the X-braced diaphragm was more likely to produce more strain in the bottom flange of the girder adjacent to the impacted girder because of the existence of the horizontal strut. As discussed in Section 4.3.2.2, this horizontal strut was in contact with the bottom flanges of adjacent girders, since steel-shim plates were used between the girders and the diaphragms. This connection allowed the horizontal strut to separate from the bottom flange of a PC girder, when the diaphragm was pulled away from the flange, or to press on the flange, when the diaphragm was pushed towards the flange. When the impact load was applied on the inner face of the bottom flange and at the mid-span of Beam BM5, a gap formed at each end of the horizontal strut that was located between Beams BM4 and BM5. These gaps were between the shim plates and the bottom flanges of the adjacent girders. Therefore, this horizontal strut did not transfer any force to the bottom flange of BM4. Horizontal forces were

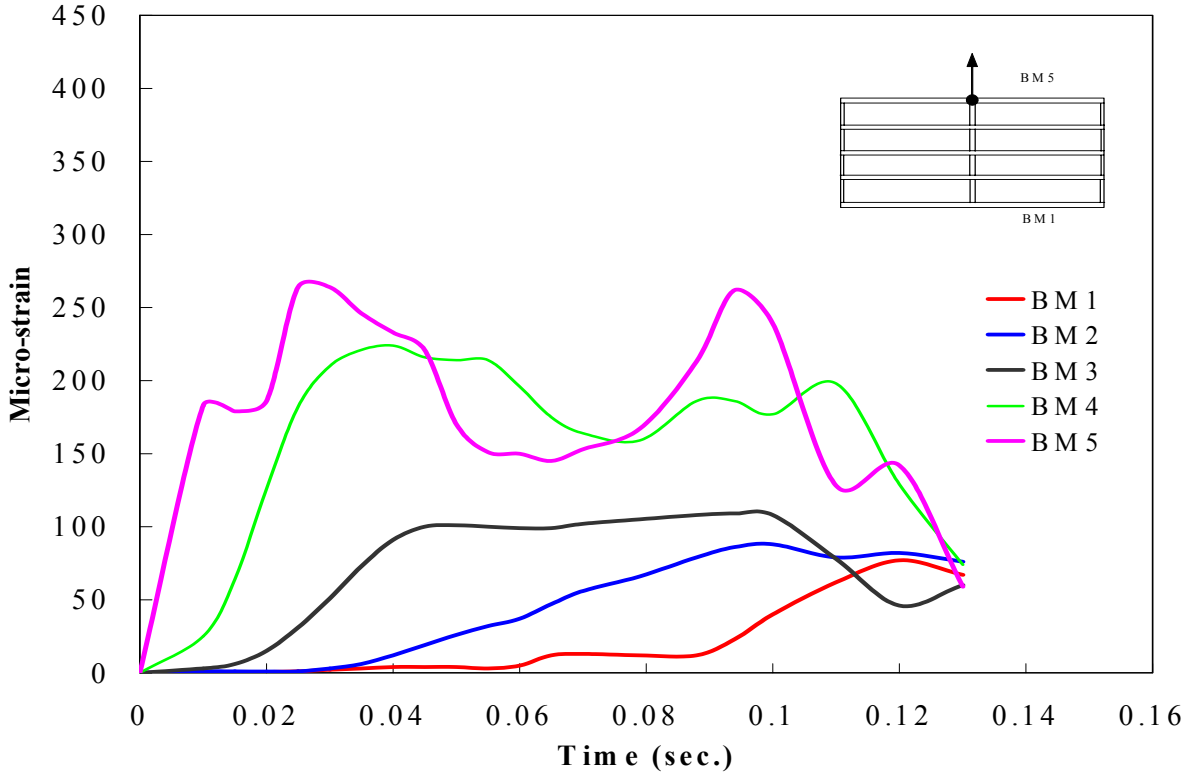

Figure 5.11. Maximum principal-strain versus time for the X-braced diaphragms (no load offset on Beam BM5)

transferred from Beam BM5 to Beam BM4 by the three bolts that connected this diaphragm to the web of Beam BM4, as shown in Fig. 4.11. The induced, tension forces in these bolts pulled the diaphragm that was located between Beams BM4 and BM3 towards Beam BM4 and thereby induced a contact pressure to develop between the horizontal strut for this second diaphragm and the bottom flange of Beam BM4. This contact pressure induced additional strains in the bottom flange of Beam B4. This type of behavior did not occur to the same degree with the RC, intermediate diaphragms because these diaphragms did not extend down to the bottom of the PC girders, as shown in Fig. 4.9.

Figure 5.12 presents the distribution of the maximum, principal-tensile strain along a portion of the length for Beam BM5 at a time of 0.03 sec. after the 120-kip impact load was

applied to this girder. Again, because of the symmetry of the bridge and with the load applied at the mid-span, only the strain distribution along one half of a portion of the girder length is shown in the figure. The maximum, principal-tensile strain for Beam BM5 was 264 micro-strains. Figure 5.12 shows that this maximum strain occurred near the intermediate diaphragm location, but not directly at the mid-span for the beam because of the slightly unsymmetrical connection between the X-braced diaphragm and the bridge girder. As one would expect, the strain gradually decreased in Beam BM5, as the distance increased between the girder cross section where the strain is evaluated and the diaphragm location.

The maximum, principal-tensile strains in the five, PC girders with the X-braced and horizontal strut, intermediate diaphragm, when the 60-kip, impact load was applied at 16 ft away from the mid-span of Beam BM1, are shown in Fig. 5.13. As shown in the figure, Beam BM1 resisted most of the impact load and the unloaded girders experienced minimal strains. The maximum, principal-tensile strain in Beam BM1 was 327 micro-strains at a time of 0.02 sec., while the average of the maximum, principal-tensile strain in the other four girders was about 40 micro-strains.

Figure 5.14 shows the maximum, principal-tensile strains in the five, PC girders with the X-braced and horizontal strut, intermediate diaphragm, when the 60-kip, impact load was applied at 16 ft away from the mid-span of Beam BM5. The strain versus time behavior for each of the girders is essentially identical to those behaviors that are shown in Fig. 5.7 for the RC, intermediate diaphragms. Beam BM5 resisted the majority of the impact load. The maximum, principal-tensile strains in Beam BM5 were about 330 micro-strains at a time of 0.02 sec after the load was applied to Beam BM5. For the other girders, the average, maximum, principal-tensile strain was about 45 micro-strains.

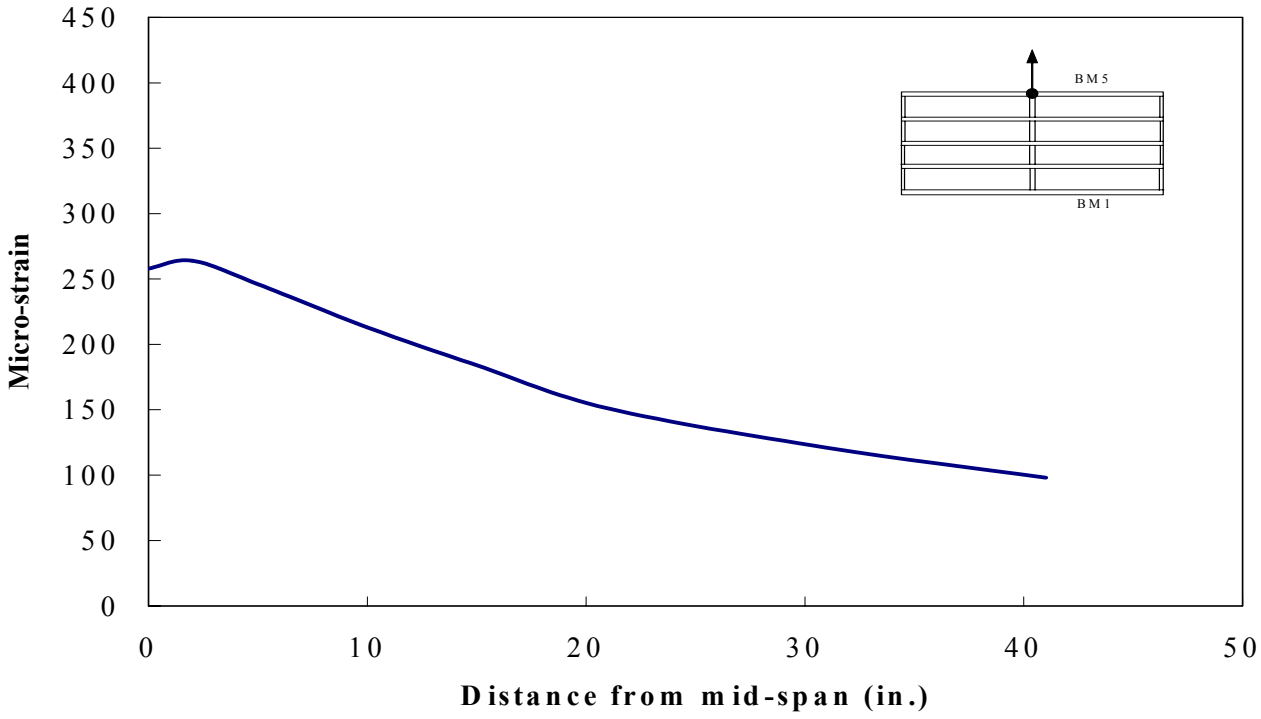

Figure 5.12. Maximum principal-tensile strain distribution along a portion of BM5 for the X-braced diaphragms (no load offset on Beam BM5)

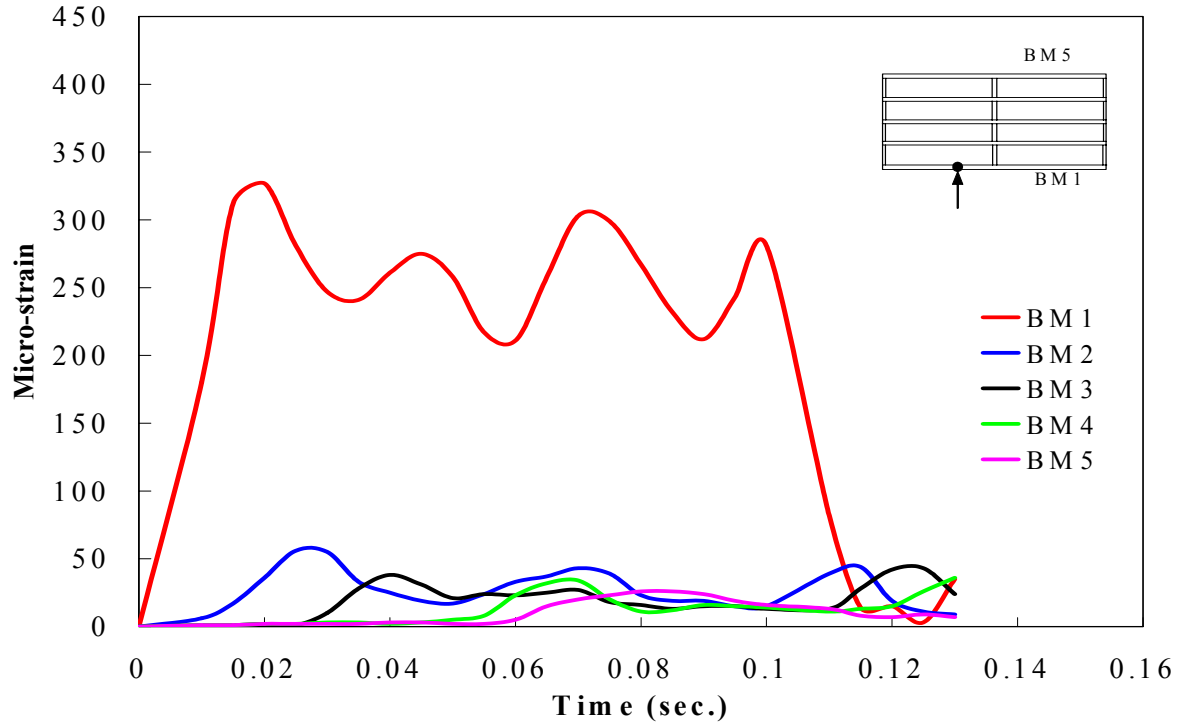

Figure 5.13. Maximum principal-tensile strain versus time for the X-braced diaphragms (16-ft offset load on Beam BM1)

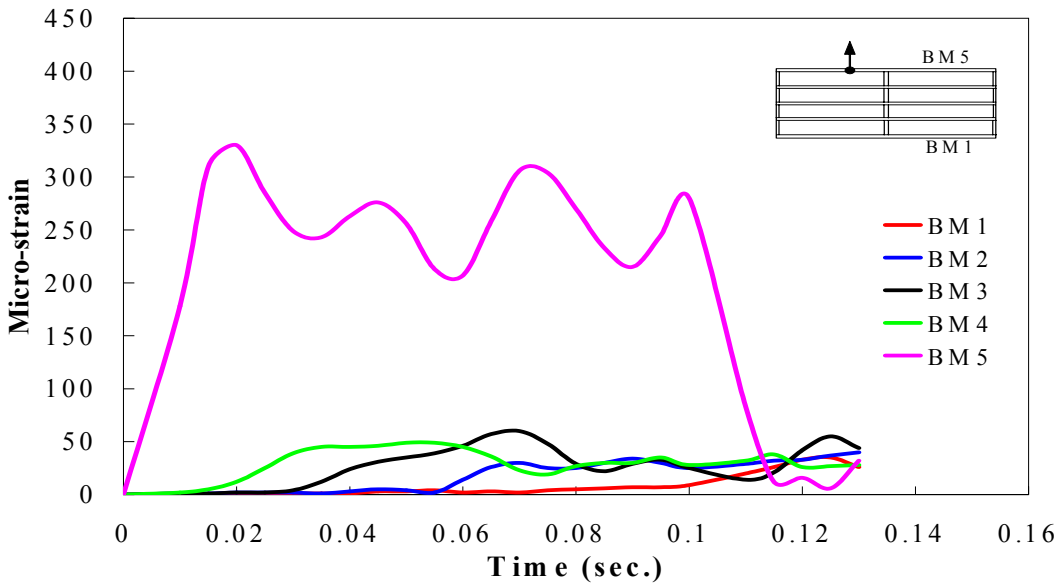

Figure 5.14. Maximum principal-tensile strain versus time for the X-braced diaphragms (16-ft offset load on Beam BM1)

5.3.1.3. Steel K-braced with horizontal strut intermediate diaphragms

Figure 5.15 shows the maximum, principal-tensile strains of the five, PC girders with the K-braced and horizontal strut, intermediate diaphragm, when the 120-kip impact load was applied at the mid-span of BM1. A comparison of this figure with Fig. 5.9, where the X-braced diaphragm was studied for the same loading, revealed very similar behavior of the bridge with either type of steel diaphragm. Despite this agreement in the overall-strain behavior, a slight difference occurred in the maximum magnitude of the principal-tensile strains. A more detailed comparison of the maximum, principal-tensile strain for the two types of structural-steel diaphragms and for the RC diaphragm is discussed in Section 5.3.3. The highest strain that was induced in Beams BM1, BM2, and BM3 was 317 micro-strains at a time of 0.09 sec., 111 micro-strains at a time of 0.11 sec., and 63 micro-strains at a time of 0.05 sec., respectively.

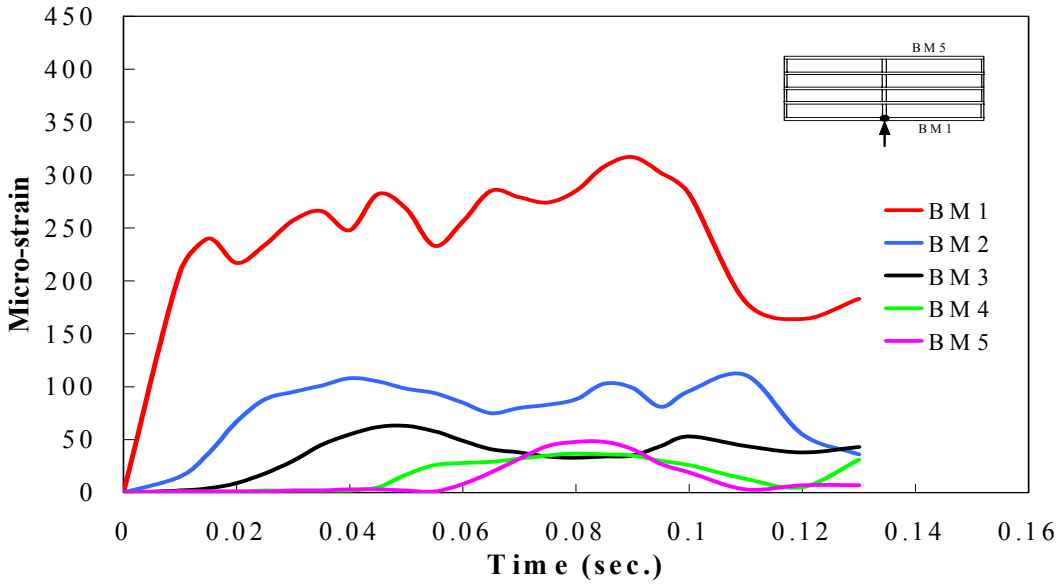

Figure 5.15. Maximum principal-tensile strain versus time for the K-braced diaphragms (no load offset on Beam BM1)

Figure 5.16 shows the distribution of the maximum, principal-tensile strain along a portion of the length for Beam BM1 with the K-braced and horizontal strut, intermediate diaphragms at a time of 0.09 sec. The loading that is associated with this figure was the same as that discussed for Fig. 5.15. The maximum strain was 317 micro-strains, and this strain occurred at the mid-span of the girder. The strains gradually decreased in the girder cross sections that were further from the load location. At a distance of 40 in. from the impact-load location, the maximum, principal-tensile strain in this girder was about 37 percent of its maximum value at the mid-span of the girder. This strain distribution was almost identical with that shown in Fig. 5.10 for the X-braced with horizontal strut diaphragms.

Figure 5.17 presents the maximum, principal-tensile strains in the five, PC girders with the K-braced and horizontal strut, intermediate diaphragms, when the 120-kip, impact load applied at the mid-span of Beam BM5. A comparison of this figure with Fig. 5.11, revealed similarities in the strain-versus-time behavior for the five girders. For the K-braced diaphragm,

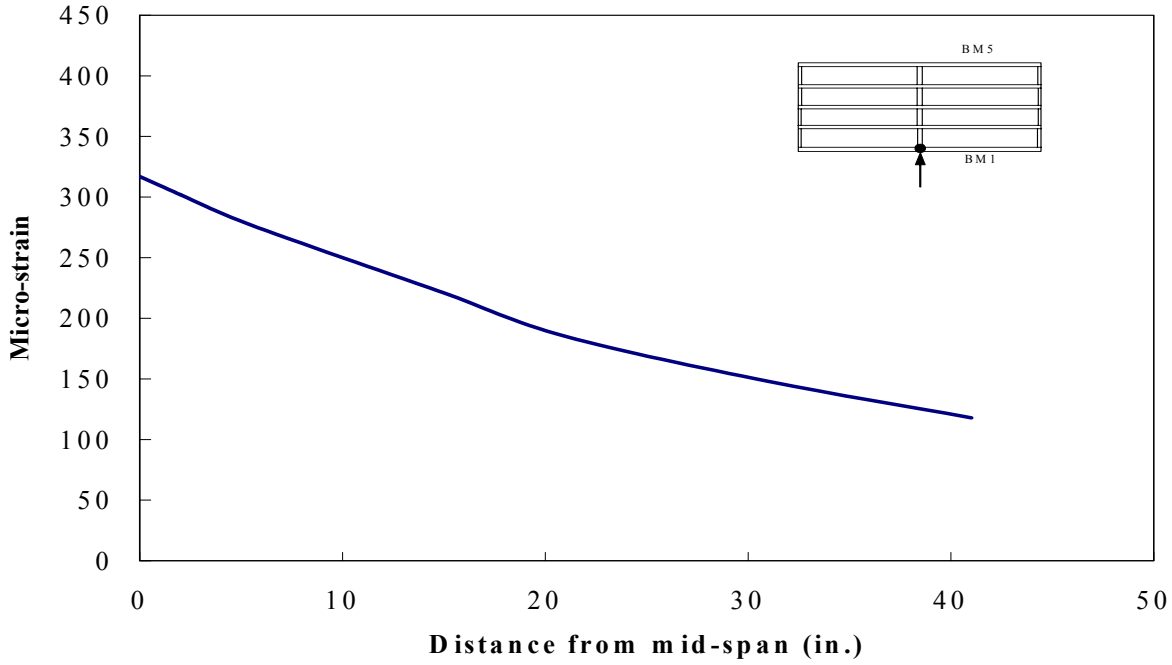

Figure 5.16. Maximum principal-tensile strain distribution along a portion of BM1 for the K-braced diaphragms (no load offset on Beam BM1)

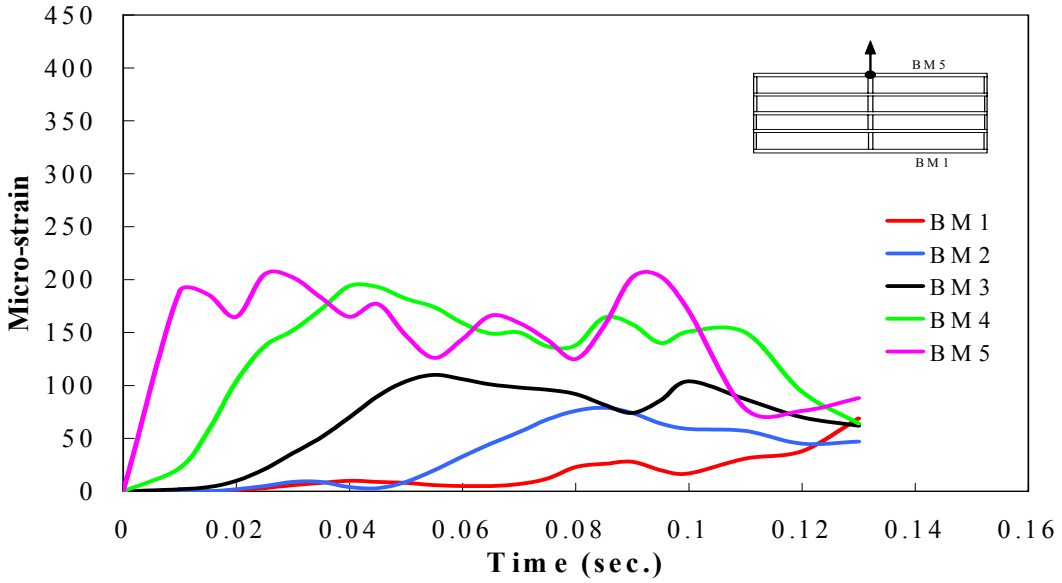

Figure 5.17. Maximum principal-tensile strain versus time for the K-braced diaphragms (no load offset on Beam BM5)

the largest, principal-tensile strain in Beam BM5 was 205 micro-strains, which occurred at 0.025 sec. after the load was applied to Beam BM5. Beam BM4, which was also highly affected by the impact load, experienced a maximum strain of 194 micro-strains at a time of 0.04 sec. The maximum, principal-tensile strain in Beam BM3 was about 50 percent of that strain in Beam B5.

Figure 5.18 shows the distribution of the maximum, principal-tensile strains along a portion of the length for Beam BM5 for the K-braced and horizontal strut, intermediate diaphragm at 0.025 sec. after the impact load was applied to this beam. This was the time when Beam BM5 experienced its largest principal-tensile strain. The loading that was associated with this figure was the same as that for Fig. 5.17. The overall, strain-versus-time behavior shown in this figure is essentially identical with that shown in Fig. 5.12 for the X-braced and horizontal strut, diaphragm. Just as for the X-braced diaphragm, the principal-tensile strains were a maximum at a location that was slightly offset from the intermediate diaphragm because of the

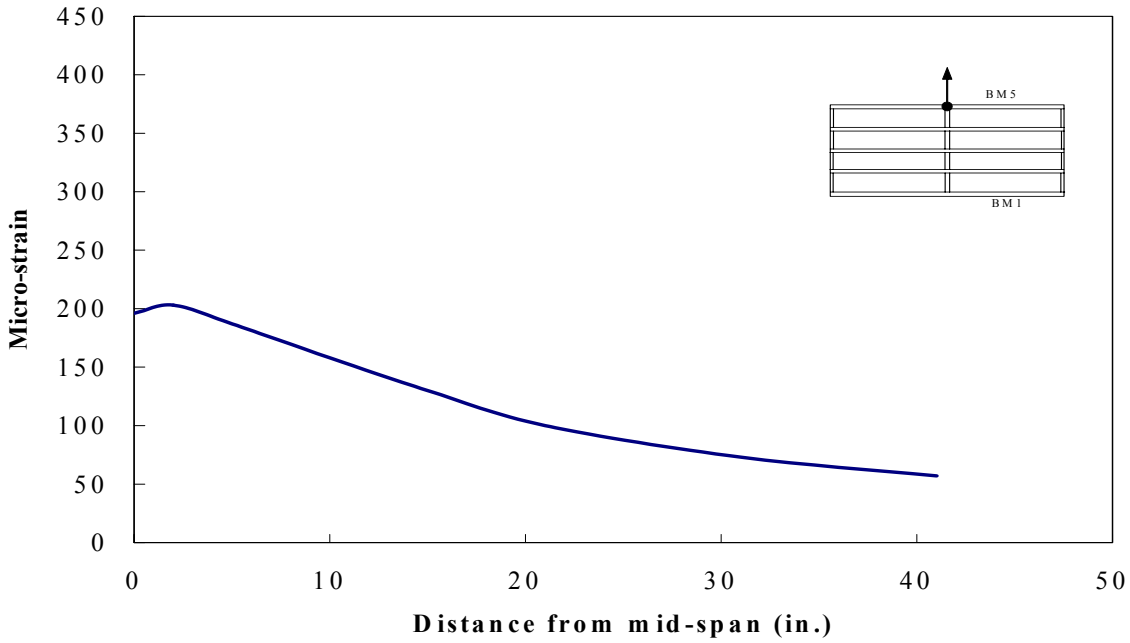

Figure 5.18. Maximum principal-tensile strain distribution along a portion of BM5 for the K-braced diaphragms (no load offset on Beam BM5)

slight asymmetry of the diaphragm-to-girder connections. The maximum, principal-tensile strain at 40 in. away from the impact load was equal to about 28 percent of its maximum value.

When the 60-kip, impact load was applied at 16 ft away from the mid-span of Beams BM1 and BM5, respectively, Figs. 5.19 and 5.20 show the maximum, principal-tensile strains for the five, PC girders with the K-braced and horizontal strut, intermediate diaphragm. A comparison of each of these figures with the corresponding Figs. 5.13 and 5.14 for the X-braced and horizontal strut, intermediate diaphragm revealed that almost identical strain-versus-time behavior occurred for the two types of steel diaphragms. Essentially the same, maximum, principal-tensile strains were induced in the impacted girder for both of these steel diaphragms. Based on these strain results, the K-braced and X-braced, intermediate diaphragms provided the impacted girder with essentially the same degree of impact-damage protection, when the impact load was applied at 16 ft away from the diaphragm location.

5.3.2. Displacements

This section presents the predicted, maximum, horizontal displacements of the impacted and non-impacted, PC girders that are subjected to different, lateral, impact loads. These displacement results are individually discussed for each type of intermediate diaphragm, and comparisons between the displacement results for each type of diaphragm are discussed in Section 5.3.3. For the three types of intermediate diaphragm and for the bridge without intermediate diaphragms, the maximum, horizontal displacement always occurred at the bottom of each of the five, PC girders. When the impact load was at the mid-span, the maximum, horizontal displacement occurred at the mid-span for each PC girder. When the impact load was

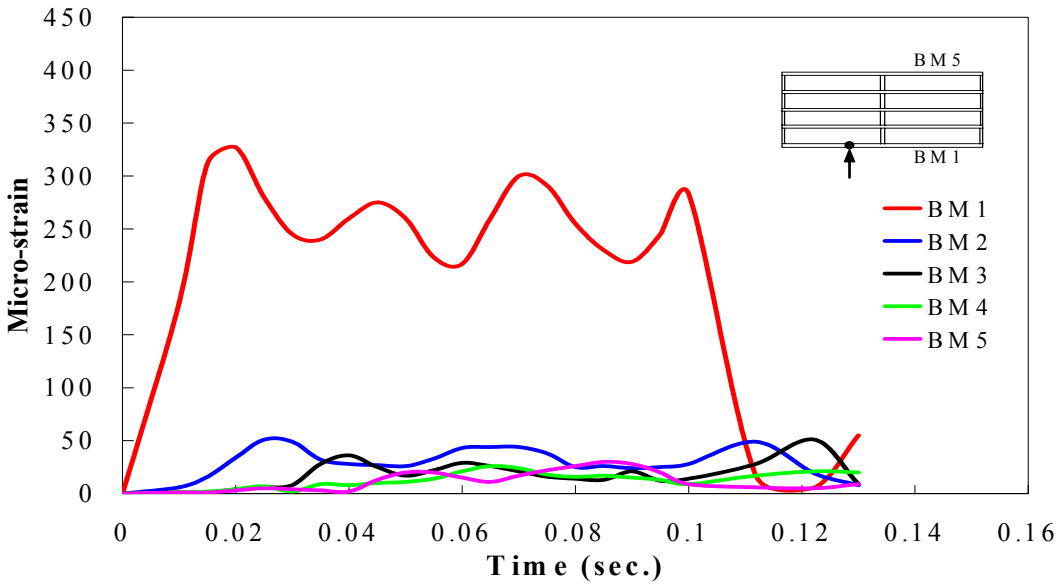

Figure 5.19. Maximum principal-tensile strain versus time for the K-braced diaphragms (16-ft load offset on Beam BM1)

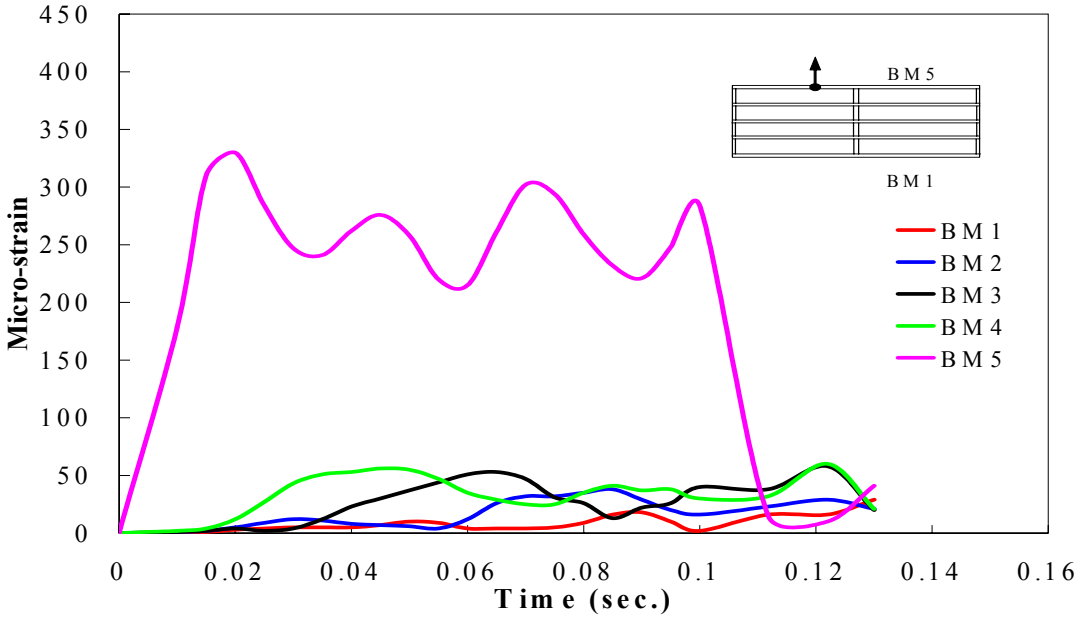

Figure 5.20. Maximum principal-tensile strain versus time for the K-braced diaphragms (16 ft load offset on beam BM5)

not applied at the mid-span, diaphragm location, the non-impacted girders had their maximum, horizontal displacement at the mid-span, and the impacted girder had its maximum, horizontal displacement at the location of the load.

Figures 5.21, 5.22 and 5.23 show the horizontal displacements of the five, PC girders with the RC, X-braced and horizontal strut, and K-braced and horizontal strut, intermediate diaphragms, respectively, with the impact load applied at the mid-span of Beam BM1. As shown in these figures, the horizontal displacement of each girder gradually increased during the 0.10-sec., time duration of the load. After the load was removed from the bridge at a time of 0.10 sec., the horizontal displacement for the impacted girder (Beam BM1) started to gradually decrease with time, while the horizontal displacements for the other girders continued to increase for a period of time. For the time period between 0.0 sec. and 0.10 sec., the horizontal displacements for Beam BM1 were the largest, and the magnitude of the horizontal displacements for the other beams were in consecutive order that depended on the location of each beam relative to Beam BM1.

As shown in Fig. 5.21, the maximum, horizontal displacement for Beam BM1 was 0.222 in., while that for Beam BM5 was 0.164 in., when RC, intermediate diaphragms were used in the bridge. The 25-percent difference between these two, girder displacements was relatively small due to the relatively large, axial rigidity of the RC diaphragms. Even though the relative horizontal displacements were small, a large difference occurred in the maximum, principal-tensile strains for these two girders (see Fig. 5.3). This difference between the strain and displacement behavior is because strains are a function of curvature, and they are not a function of displacement.

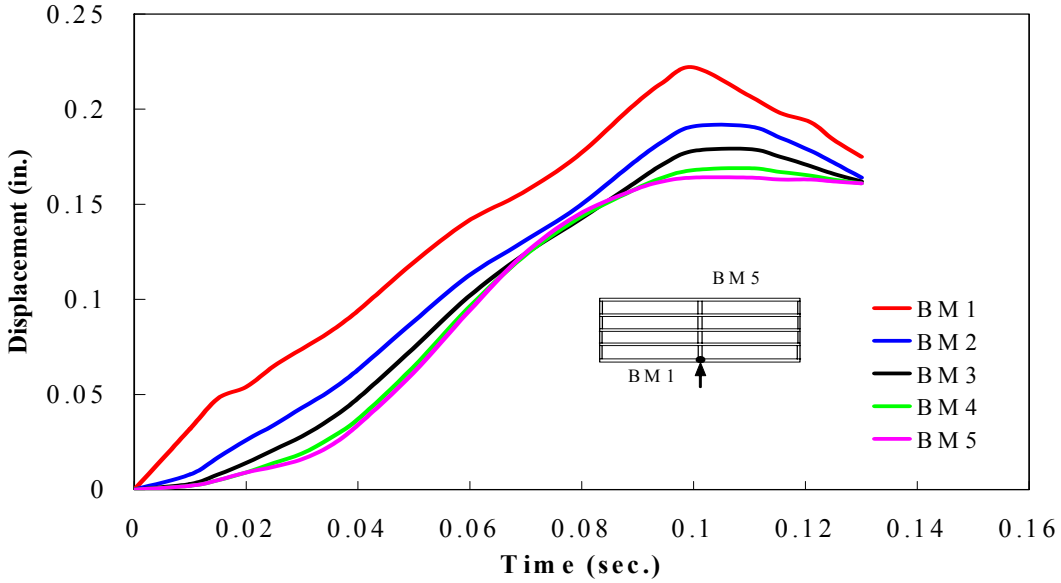

Figure 5.21. Horizontal displacement versus time for the RC diaphragms (no load offset on Beam BM1)

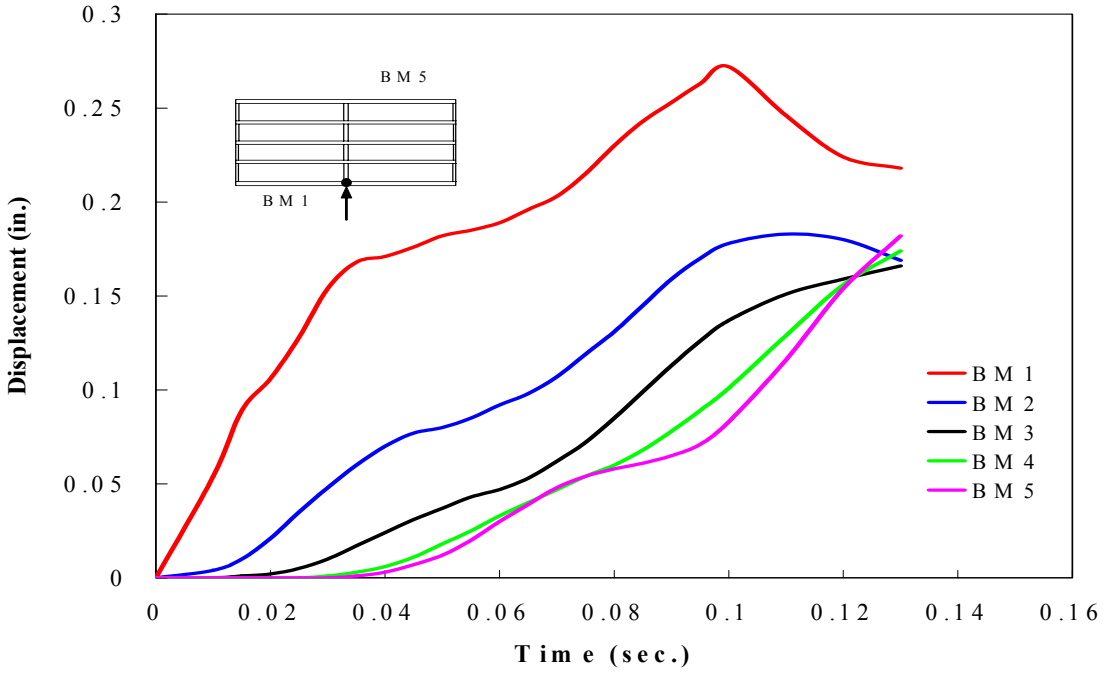

Figure 5.22. Horizontal displacement versus time for the X-braced diaphragms (no load offset on Beam BM1)

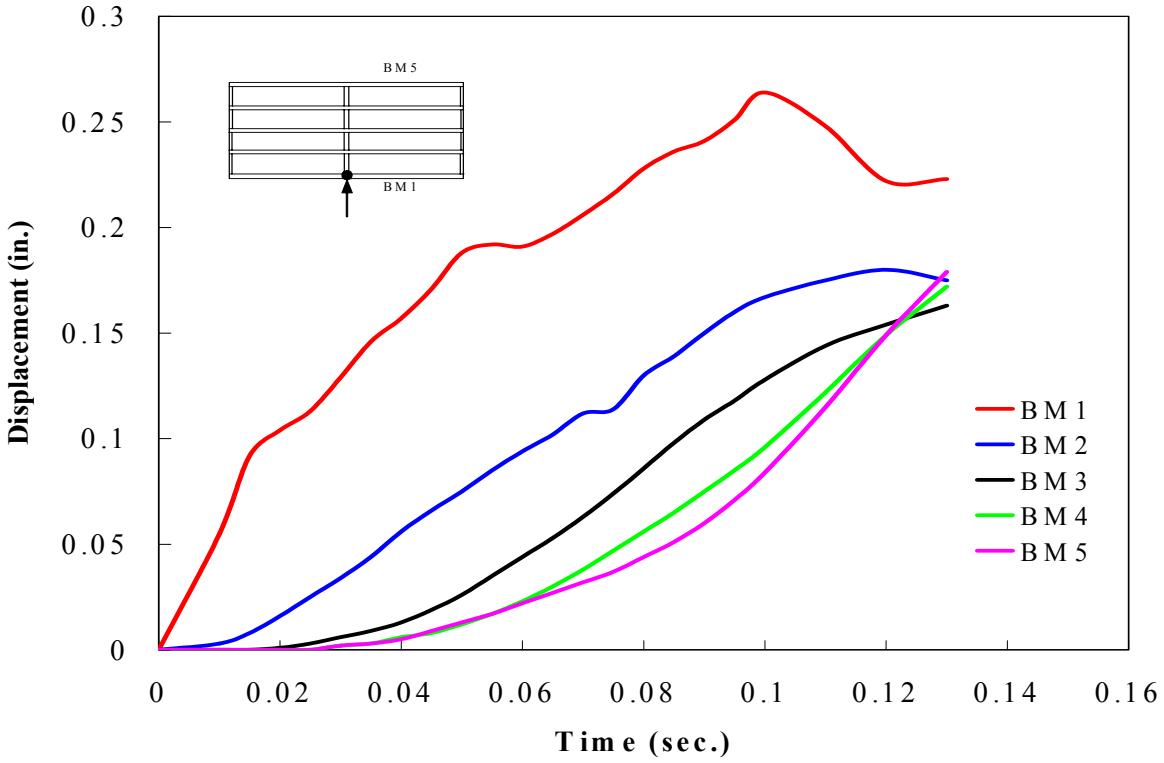

Figure 5.23. Horizontal displacement versus time for the K-braced diaphragms (no load offset on Beam BM1)

Figures 5.22 and 5.23 show a very similar displacement-versus-time behavior for the two types of steel, intermediate diaphragms. For the X-braced and horizontal strut, intermediate diaphragms and for the K-braced and horizontal strut, intermediate diaphragms, the maximum, horizontal displacement for Beam BM1 was 0.272 in. and 0.264 in., respectively. The relatively large difference in the horizontal displacements for the impacted girder and the other girders when the steel intermediate diaphragms were used indicates that the axial rigidity of these steel diaphragms was not as high as that for the RC diaphragm.

Figures 5.24, 5.25 and 5.26 present the maximum, horizontal displacements of the five, PC girders with the RC, X-braced and horizontal strut, and K-braced and horizontal strut, intermediate diaphragms, respectively, when the 120-kip, impact load was applied at the mid-

span of Beam BM5. A comparison of these displacement results for each type of diaphragm with those corresponding results that are shown in Figs. 5.21, 5.22, and 5.23 revealed essential identical displacement-versus-time behavior for each type of diaphragm. As shown in Figs. 5.24, 5.25 and 5.26, the largest, horizontal displacements for Beam BM5, when the RC, X-braced and K-braced, intermediate diaphragm were used in the bridge were 0.223, 0.270 and 0.265 in., respectively.

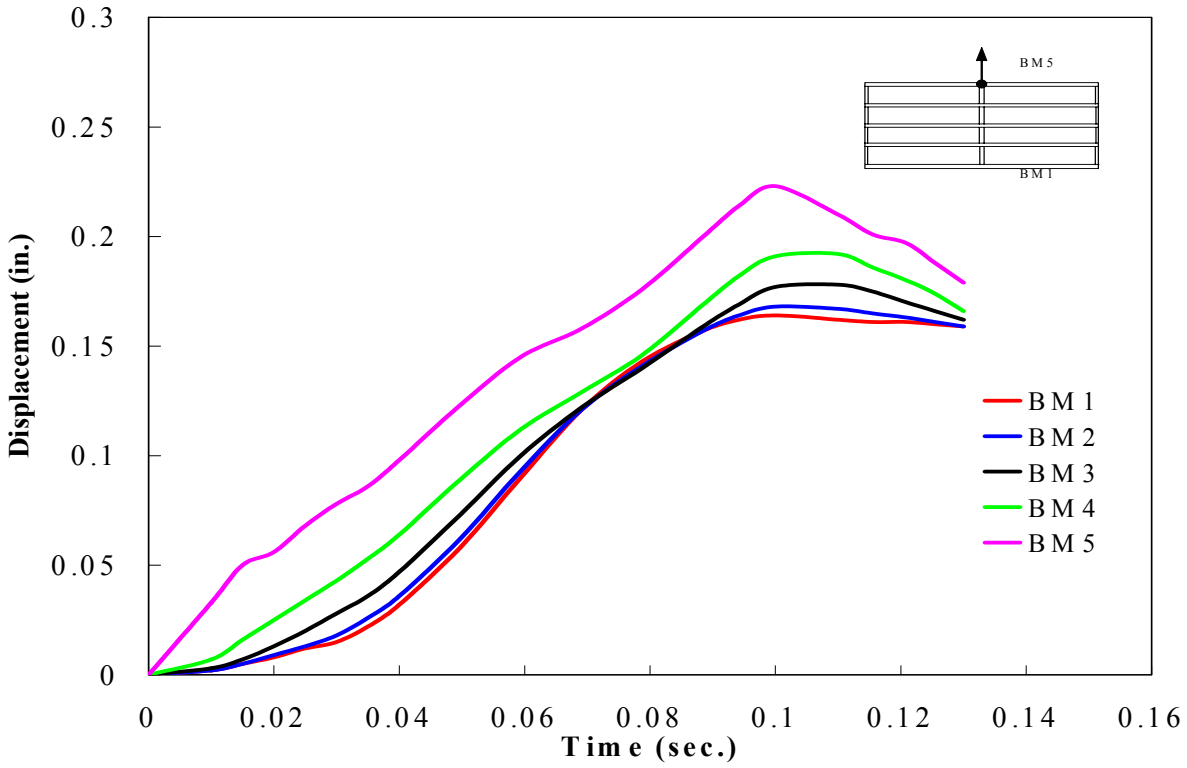

Figure 5.24. Horizontal displacement versus time for the RC diaphragms (no load offset on Beam BM5)

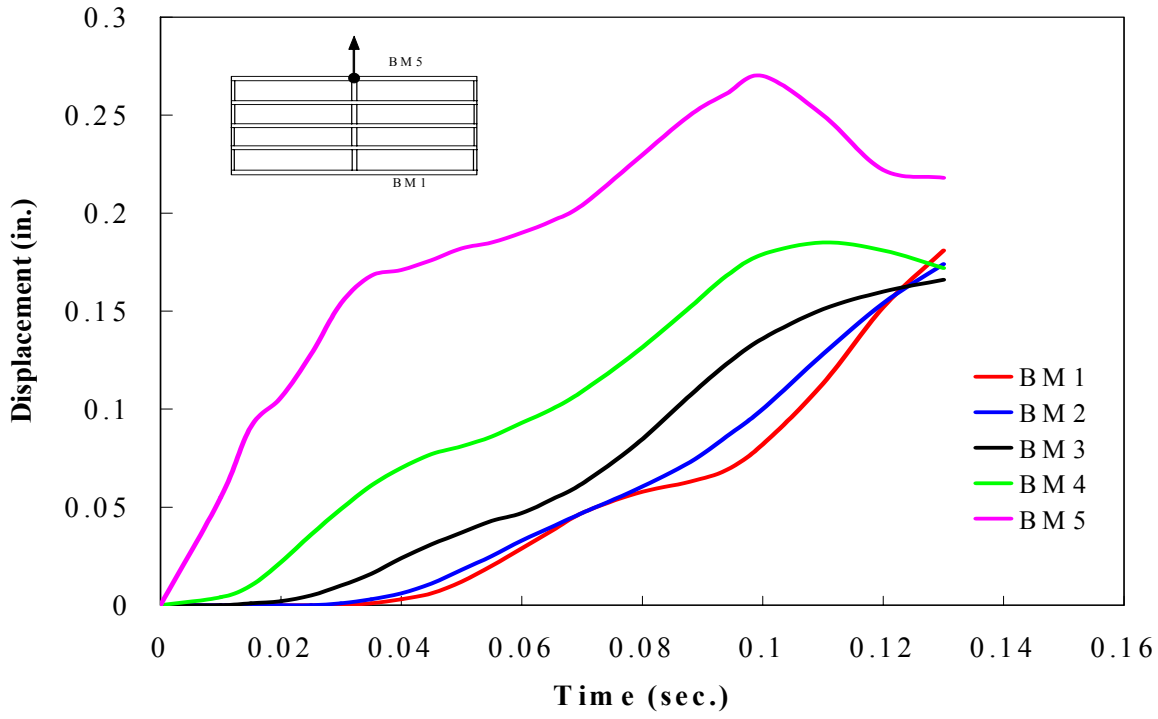

Figure 5.25. Horizontal displacement versus time for the X-braced diaphragms (no load offset on Beam BM5)

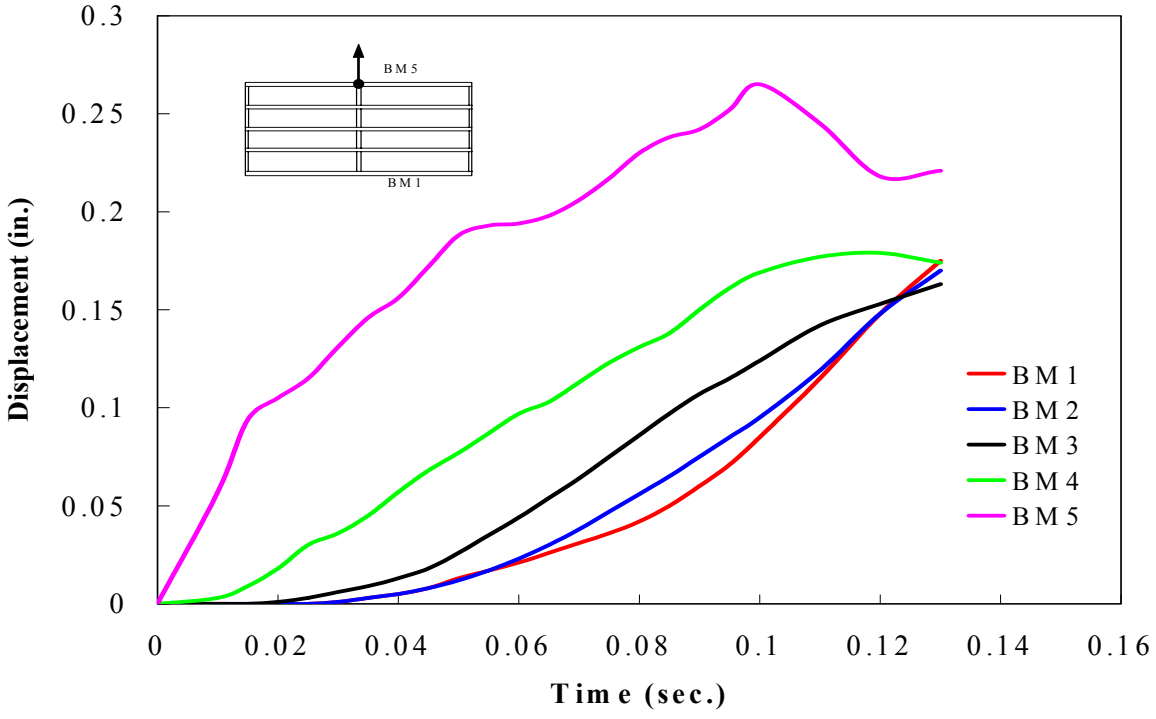

Figure 5.26. Horizontal displacement versus time for the K-braced diaphragms (no load offset on Beam BM5)

Figures 5.27, 5.28 and 5.29 present the maximum, horizontal displacements of the five, PC girders with the RC, X-braced and horizontal strut, and K-braced horizontal strut, intermediate diaphragms, respectively, when the 60-kip, impact load was applied at 16 ft away from the mid-span of Beam BM1. The displacement-versus-time behaviors and the horizontal, displacement magnitudes for the three types of diaphragms were very close to each other. The maximum, horizontal displacement for the impacted girder (Beam BM1), when the RC, X-braced, and K-braced, intermediate diaphragms were used in the bridge, was 0.227 in., 0.227 in., and 0.219 in., respectively. These maximum displacements all occurred at 0.075 sec. after the impact load was applied to Beam BM1. This almost identical, displacement-versus-time behavior for the different types of intermediate diaphragms indicates that the diaphragm material and configuration had a minor effect on the maximum, horizontal displacements that were

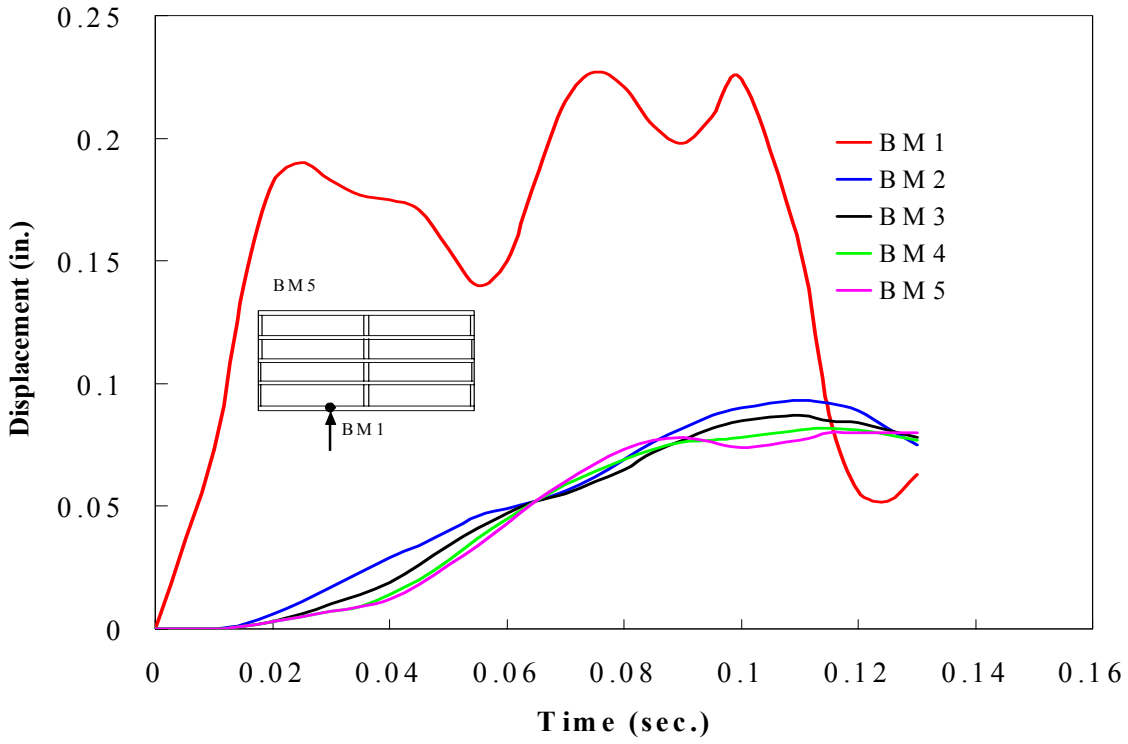

Figure 5.27. Horizontal displacement versus time for the RC diaphragms (16-ft load offset on Beam BM1)

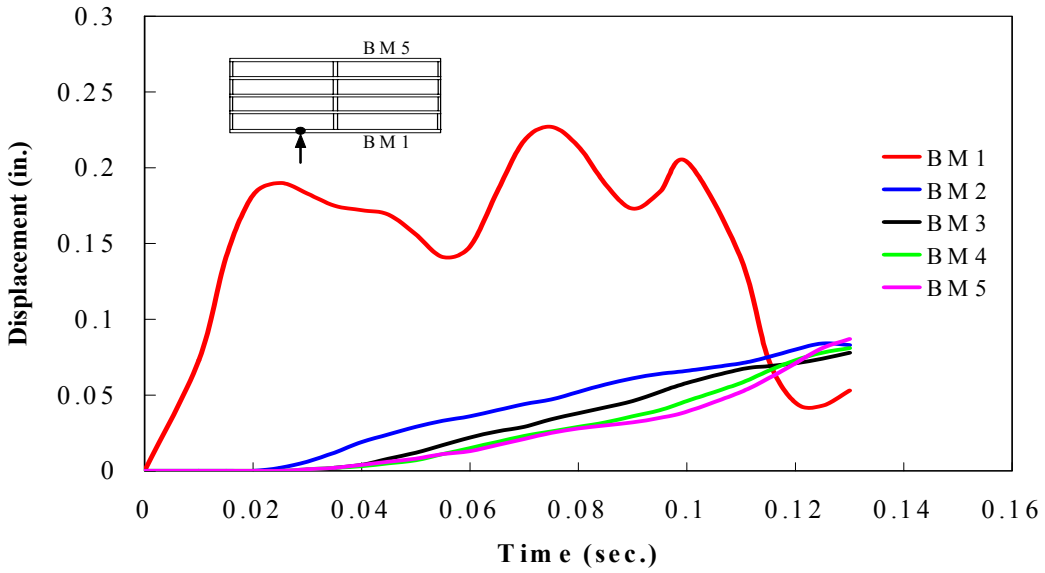

Figure 5.28. Horizontal displacement versus time for the X-braced diaphragms (16-ft load offset on Beam BM1)

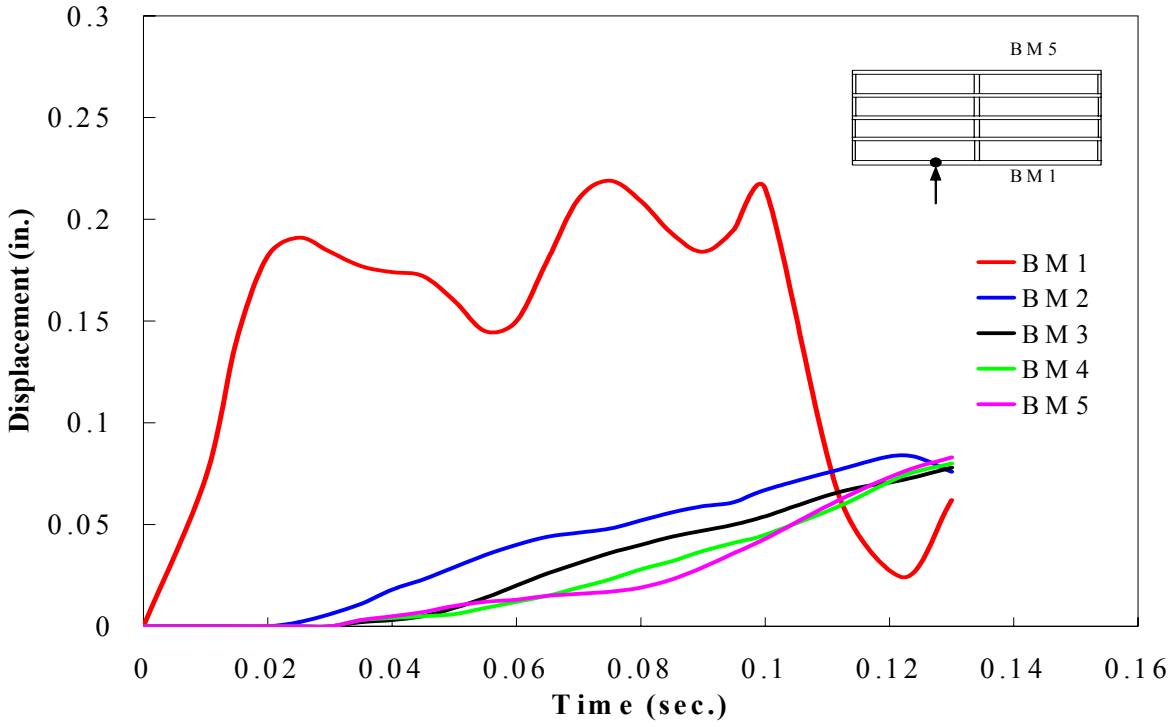

Figure 5.29. Horizontal displacement versus time for the K-braced diaphragms (16-ft load offset on Beam BM1)

induced in the girders, when the impact load was applied on Beam BM1 at a location that was not at an intermediate diaphragm.

Figures 5.30, 5.31 and 5.32 show the maximum, horizontal displacements of the five, PC girders with the RC, X-braced and horizontal strut, and K-braced and horizontal strut, intermediate diaphragms, respectively, when the 60-kip, impact load was applied at 16 ft away from the mid-span of Beam BM5. An agreement was observed in the displacement-versus-time behaviors and horizontal, displacement magnitudes between these figures and the corresponding figures (Figs. 5.27, 5.28 and 5.29), when this same impact load applied to Beam BM1. This agreement regarding the displacement of the girders supports the conclusion about the effectiveness of the diaphragm type with respect to the lateral stiffness of the bridge, when an impact load was applied to a girder at a point that was 16 ft away from the intermediate diaphragms.

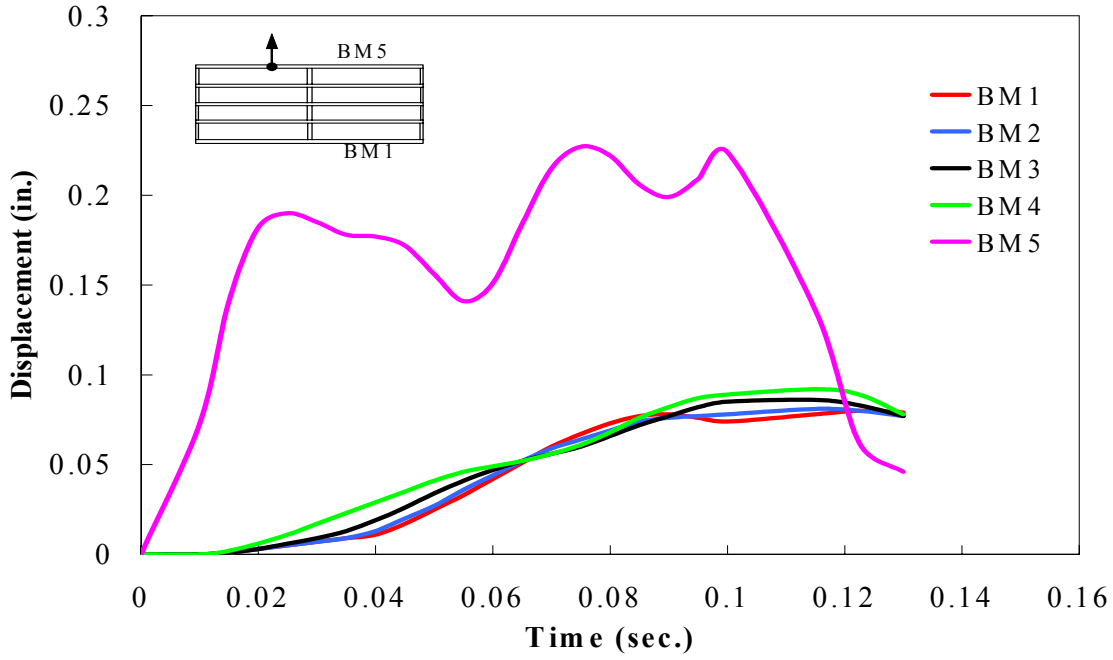

Figure 5.30. Horizontal displacement versus time for the RC diaphragms (16-ft load offset on Beam BM5)

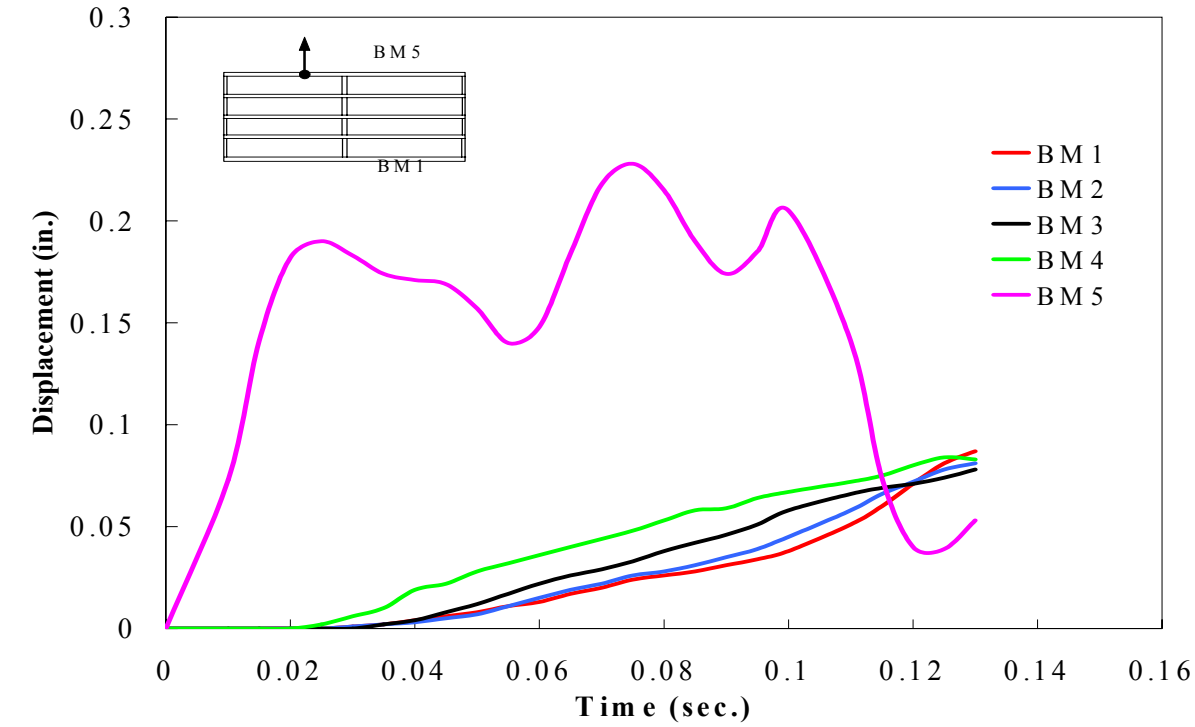

Figure 5.31. Horizontal displacement versus time for the X-braced diaphragms (16-ft load offset on Beam BM5)

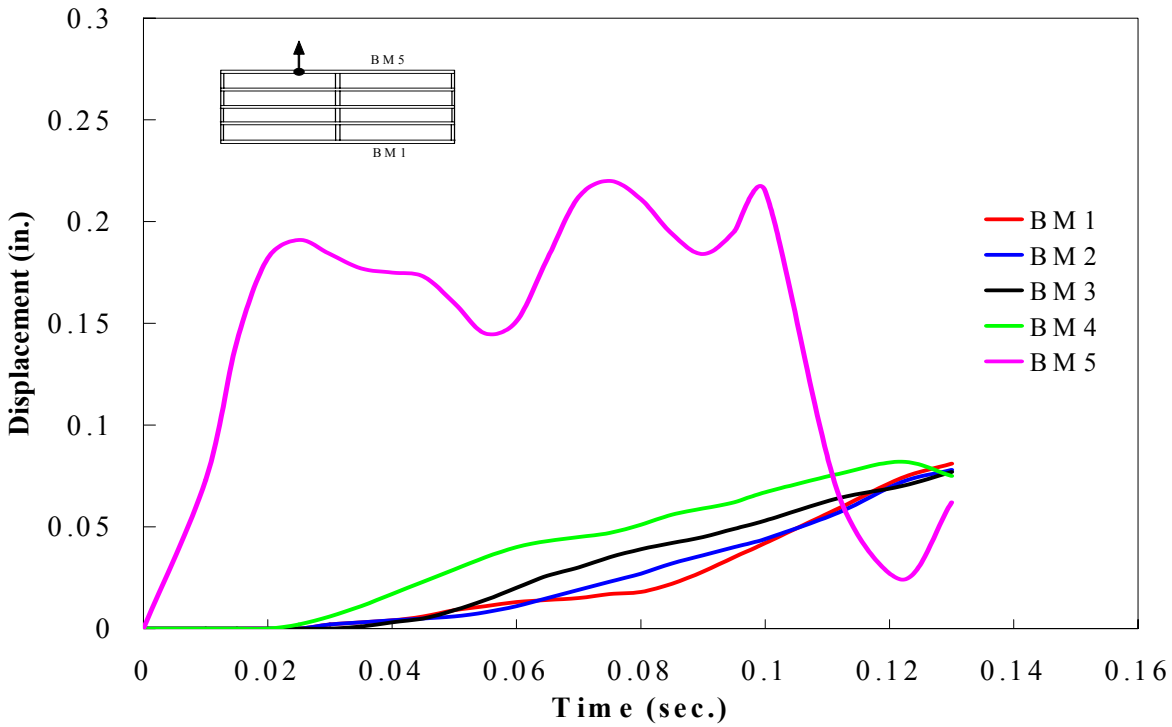

Figure 5.32. Horizontal displacement versus time for the K-braced diaphragms (16-ft load offset on Beam BM5)

5.3.3. Strain and displacement comparisons

In this section, comparisons are presented between the strain and displacement results for the PC girders with the three types of intermediate diaphragms and without any intermediate diaphragms. These comparisons will provide a basis to determine the effectiveness of intermediate diaphragms in reducing potential damage to the PC girders that might result from a lateral-impact load striking the bottom flange of one of the bridge girders. Since damage might also occur for the girder that is adjacent to the impacted girder, strain and displacement comparisons are made for both of these girders.

5.3.3.1. Strain comparisons

Figure 5.33 shows the maximum, principal-tensile strains in Beam BM1 with the RC, X-braced and horizontal strut, and K-braced and horizontal strut, intermediate diaphragms and without intermediate diaphragms, when the 120-kip, lateral-impact load with duration time of 0.10 sec. was applied at the mid-span of Beam BM1. The notation ND that is shown in the figure represents no intermediate diaphragms. As previously discussed in Section 5.3.1, the impacted girder (Beam BM1) was affected the most by the impact. This girder is expected to experience the most severe damage. Therefore, the strain results presented in this figure are only for the impacted girder. As shown in Fig. 5.33, the use of RC, intermediate diaphragms produced the smallest magnitudes for the maximum, principal-tensile strains in Beam B1, when compared to those strains that were associated with the other three, diaphragm conditions. When RC diaphragms were used, the maximum strain induced in Beam BM1 was about 26 percent of the maximum strain that was induced in this beam when intermediate diaphragms were omitted from the bridge. The strain-versus-time behavior and the magnitudes for the maximum, principal-tensile strains in Beam BM1 were very similar for the two types of steel diaphragms.

The largest strains that were induced in Beam BM1, when the K-braced and X-braced, intermediate diaphragms were used, was about 37 percent and 40 percent, respectively, of that strain which was induced in Beam BM1 when intermediate diaphragms were not present in the bridge. Although there was about 7-percent difference between the largest strains that were induced in Beam BM1 for the two types of steel diaphragms, this minor difference was considered insufficient to establish which one of the two, steel, intermediate diaphragms was the most effective in minimizing any potential damage to the impacted, PC girder, when the impact was at the diaphragm location.

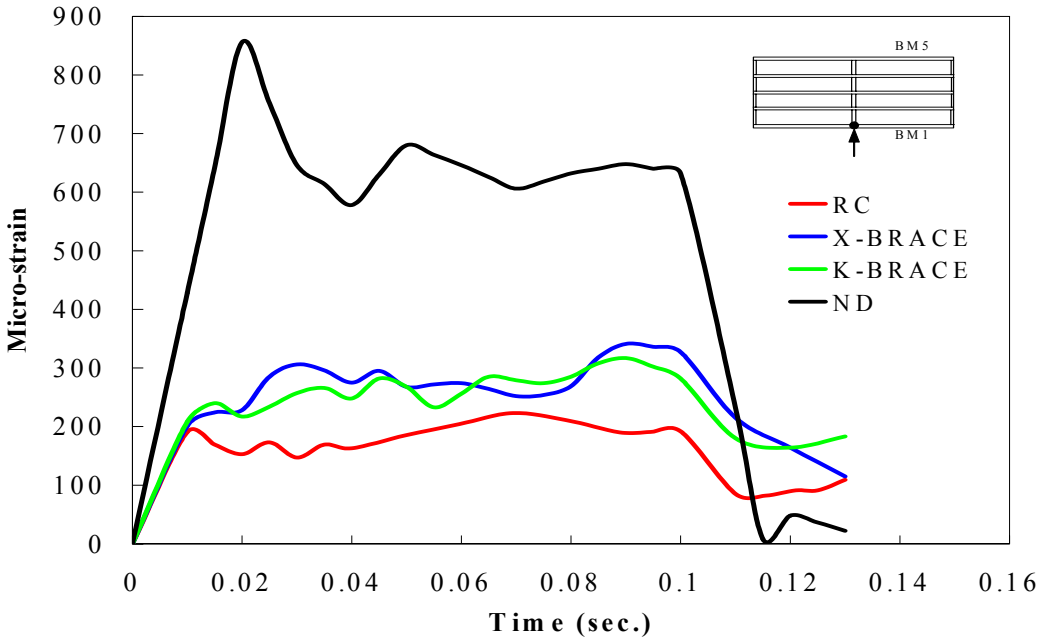

Figure 5.33. Maximum principal-tensile strain in Beam BM1 versus time for the diaphragm conditions (no load offset on Beam BM1)

Figure 5.34 shows the distribution of the maximum, principal-tensile strains along the length of Beam BM1 for the different types of intermediate diaphragms and for the bridge without intermediate diaphragms. The load associated with this figure was the same as that for

Fig. 5.33. Due to the symmetry of the model and loading, the strain distribution was presented for a portion of one half of the length for the impacted beam. Each of the strain distributions was established at the time when the principal-tensile strains at the mid-span, cross section for Beam BM1 was at its maximum magnitude. This time was not the same for the different diaphragm conditions. As shown in the figure, the absence of intermediate diaphragms in the bridge superstructure caused a longer portion of the impacted-beam length to be subjected to principal-strain magnitudes that were close to the maximum, principal-tension strain than that for the same bridge with intermediate diaphragms. When the 120-kip, impact load was applied to Beam BM1

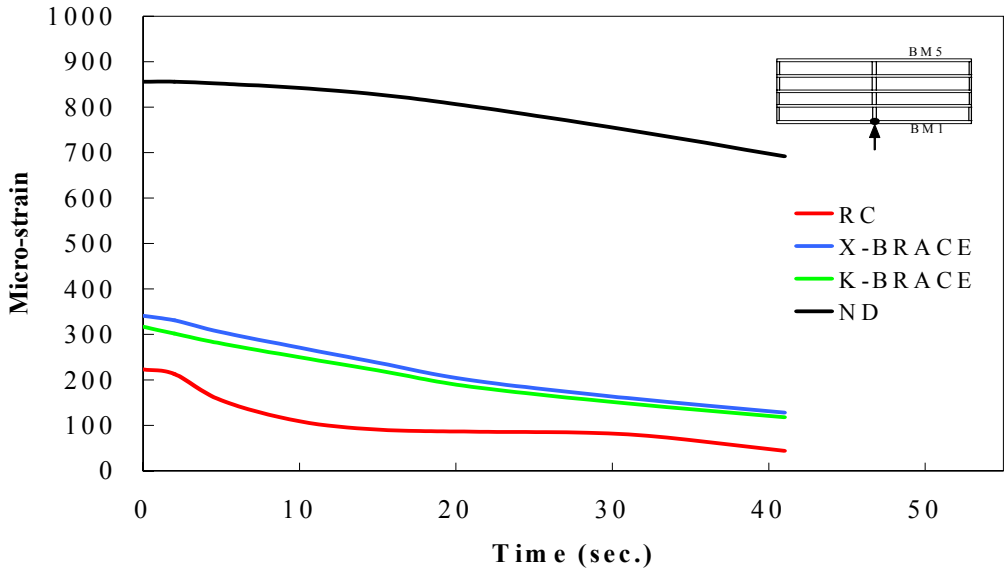

Figure 5.34. Maximum principal-tensile strain distribution along a portion of Beam BM1 for the diaphragm conditions (no load offset on Beam BM1)

at the mid-span diaphragm location, the use of RC, intermediate diaphragms caused the smallest, principal-tensile strains to be induced in Beam BM1 and the shortest length for the larger magnitudes for these strains, than that for the other diaphragm conditions. Both types of steel,

intermediate diaphragms had essentially the same effect on the magnitudes and distribution of the principal-tensile strains along the length of the impacted beam.

To establish a more complete indication of any potential damage that a bridge might sustain when a PC girder is struck by an object that is transported on a vehicle which travels under a bridge, the ISU researchers also evaluated the maximum, principal-tensile strains that are induced in the girder adjacent to the impacted girder. The purpose for this phase of the research was to determine whether intermediate diaphragms spread the impact force from the impacted girder to the other bridge girders. Figure 5.35 illustrates the maximum, principal-tensile strains that are induced in Beams BM1 and BM2 when each of the types of intermediate diaphragm are used and when intermediate diaphragms are not used in a bridge. The impact load that is associated with Fig. 5.35 is the same as that which is associated with Fig. 5.33. The strain results that are presented in the figure for the different diaphragms were in the extreme fiber of the bottom flanges of Beams BM1 and BM2 at the girder cross section where the load was applied. For the no diaphragm condition, the maximum, principal-tensile strains were at the top fibers of web element for each of these girders. For each intermediate-diaphragm condition, the maximum strains in Beams BM1 and BM2 were induced at different times after the impact load was applied to Beam BM1. These times were when the largest strains were induced in these two girders.

When intermediate diaphragms were not present, (the ND diaphragm type in Fig. 5.35) the impacted girder (Beam BM1) resisted the vast majority of the impact load, and the corresponding, principal-tensile strains were relatively large. The strains that were induced in the girder (Beam BM2) that was adjacent to Beam BM1 were relatively very small. As long as the over-height load would not strike any other girder, as the vehicle passed under the bridge,

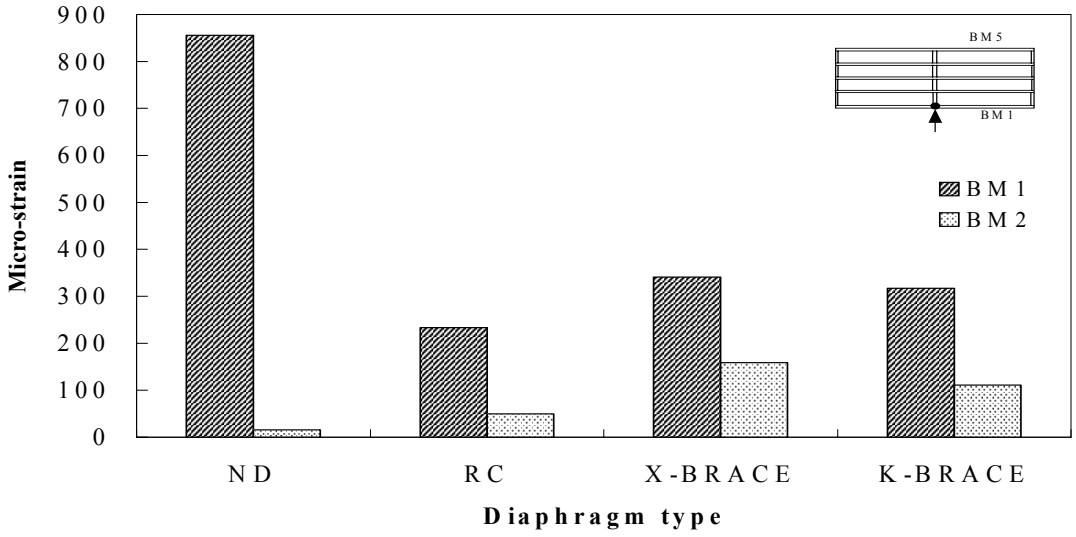

Figure 5.35. Maximum principal-tensile strains in Beams BM1 and BM2 for the diaphragm conditions in the non-skewed bridge (no load offset on Beam BM1)

only Beam BM1 would be possibly severely damaged by the impact. When intermediate diaphragms were added to the bridge, the magnitude of the maximum, principal-tensile strains that were induced in Beam BM1 significantly decreased from the strain levels that occurred when intermediate diaphragms were not present in the bridge. A significant decrease in these strains implies that a significant decrease for potential damage would occur for this girder. On the other hand, the diaphragms transferred a portion of the impact load from the impacted girder to the other girders in the bridge. As shown in Fig. 5.35, the portion of impact load that was transferred by the diaphragms to the other girders is affected by the type of intermediate diaphragm. For the two, steel, intermediate diaphragms, larger strains were induced in Beams BM1 and BM2 than that for the RC, intermediate diaphragms. This strain result was attributed to the geometry of the steel diaphragms and the existence of the horizontal struts. These struts caused a direct transfer of a portion of the applied load from the bottom flange of Beam BM1 to the bottom flange of Beam BM2. A comparison of the strain results for the two types of steel

diaphragms revealed that a 30-percent difference occurred for the maximum strains that are induced in Beam BM2. This strain difference was attributed to the alignment of the steel-bracing members in the K-braced and X-braced diaphragms. For the K-braced diaphragms, the diagonal-bracing members did not extend to the bottom flange of a PC girder, and for the X-braced diaphragms, the diagonal-bracing members extended to the bottom flange of a girder. As previously mentioned, the absence of a direct connection between the RC diaphragms and the bottom flanges of Beams BM1 and BM2 reduced the strains induced in Beam BM2 compared to those strains associated with the use of the steel diaphragms. The use of the RC, intermediate diaphragms induced a maximum, principal-tensile strain in Beam BM2 that was 55 percent less than that associated with the use of the K-braced, intermediate diaphragms.

A simplified, static-load study of the two types of steel, intermediate diaphragms was conducted to investigate their potential to spread impact damage to adjacent girders. The simplified models for the K-braced and X-braced, intermediate diaphragms were made by representing the diagonal members and horizontal struts with truss-type, finite elements. The bracing members and the horizontal struts were the only parts of the diaphragms that were modeled for the simplified analyses. A horizontal strut was modeled as two, separate members (WT6x17.5 and W14x34). Figure 5.36 shows the geometrical arrangement for these members and the axial forces that were induced in these members, when a 120-kip, static load was applied

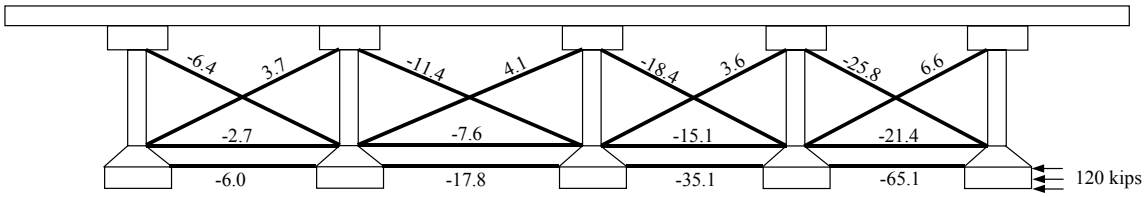

a. X-braced diaphragm

Figure 5.36. Forces in the X-braced and K-braced diaphragms for the simplified models

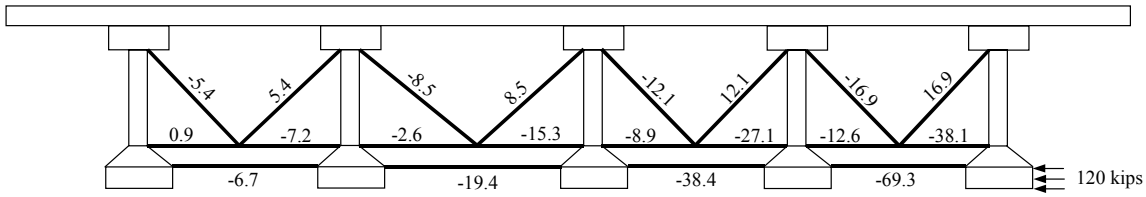

b. K-braced diaphragm

Figure 5.36. Continued

at the mid-span of Beam BM1. The negative sign for a member force indicates a compressive force.

To calculate the horizontal force that was transferred to each girder from an adjacent girder that was closer to Beam BM1, the horizontal components of the forces induced in the diaphragm members that were connected to that girder profile were added together. The forces that were transferred to Beam BM2, when the X-braced and K-braced diaphragms were used in the model, were approximately 104 kips and 94 kips, respectively, and for Beam BM3, these transferred forces were 64 kips and 56 kips, respectively. For Beams BM4 and BM5, these transferred forces were essentially the same, when either type of steel diaphragm was used. An 11-percent difference between the forces transferred to Beams BM2 and BM3 for the two types of steel diaphragms confirmed the conclusion that the X-braced diaphragms has the potential to cause slightly more damage to be spread to adjacent girders than that for the K-braced diaphragms.

Figure 5.37 shows the maximum, principal-tensile strains in the impacted girder (Beam BM5) for the four, intermediate-diaphragm conditions, when the 120-kip, impact load was applied at the mid-span of Beam BM5. During most of the 0.10-sec., load-duration time, the girder strains that were associated with RC, intermediate diaphragms were the smallest of these strains for the four, diaphragm conditions. The use of the RC diaphragms reduced the maximum,

principal-tensile strains in Beam BM5 by about 82 percent from those strains that were induced in this beam, when intermediate diaphragms were omitted from the bridge. The strain-versus-time behavior of the two, steel diaphragms was almost the same, but the use of the K-braced diaphragms produced smaller strains in Beam BM5 than those that were associated with the use of the X-braced diaphragms. The reduction in the maximum, principal-tensile strains for Beam BM5 from those strains that were associated with the no diaphragm condition that were produced by the use of K-braced and the X-braced diaphragms were about 75 percent and 69 percent, respectively. Although there was about 15-percent difference in the strain magnitudes that were related to the use of the two, steel diaphragms, the ISU researchers believe that this strain difference was not sufficient enough to select the K-braced diaphragms as being more efficient than the X-braced diaphragms in reducing the potential for impact damage to the bridge PC girders.

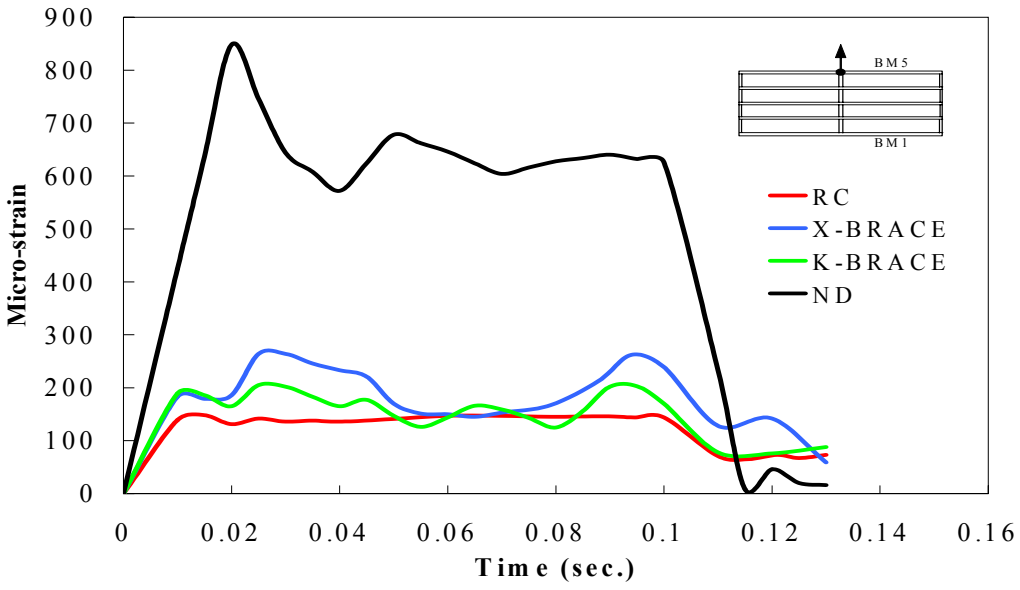

Figure 5.37. Maximum principal-tensile strain in BM5 versus time for diaphragm conditions (no load offset on Beam BM5)

Distributions of the maximum, principal-tensile strains along a portion of the length for the impacted girder (Beam BM5) for the four, diaphragm conditions, when the 120-kip, impact load was applied at the mid-span of Beam BM5, is presented in Fig. 5.38. The strain response of each of the diaphragm conditions was at the time when the largest, principal-tensile strains occurred at the mid-span cross section for Beam B5. This time was different for each of the diaphragm conditions. The strain-versus-time behaviors that are presented in this figure were almost identical with those that were discussed for Fig. 5.34, when Beam BM1 was the impacted girder.

Another damage-spread study was conducted to establish the extent to which a particular intermediate-diaphragm condition would contribute to damage that may be induced in the other PC girders, when an impact load was applied at the mid-span of Beam BM5. This study was similar to one that was discussed to explain the strain results shown in Fig. 8.35. Figure 5.39 shows the maximum, principal-tensile strains that were induced in the Beam BM5 and its adjacent girder (Beam BM4).

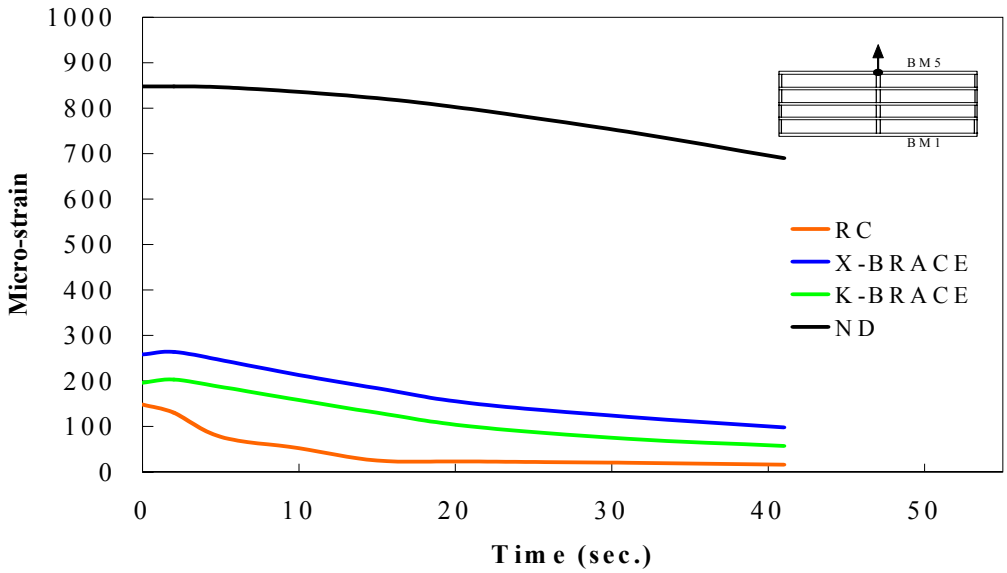

Figure 5.38. Maximum principal-tensile strain distribution along a portion of BM5 for the diaphragm conditions (no load offset on Beam BM5)

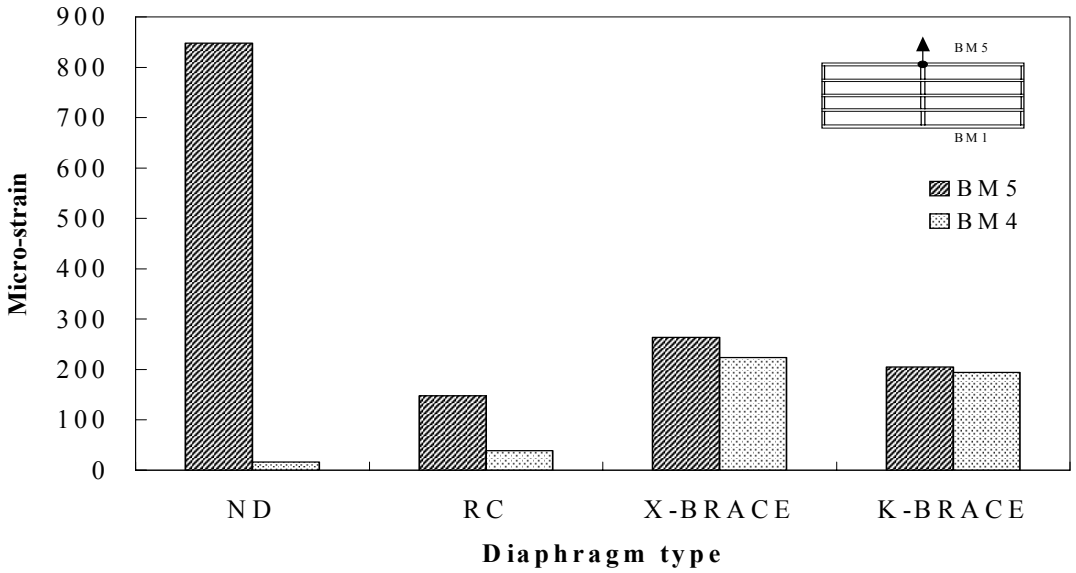

Figure 5.39. Maximum principal-tensile strains in Beams BM5 and BM4 for the diaphragm conditions in the non-skewed bridge (no load offset on Beam BM5)

As expected, the no diaphragm condition produced minor strains in Beam BM4. When compared to those strains that were associated with the no diaphragm condition, a significant decrease in the maximum, principal-tensile strains that were induced in the impacted beam occurred when intermediate diaphragms were installed in the bridge. About a 13-percent difference in the strains that were induced in Beam BM4 occurred between for the two types of steel diaphragms. This difference was probably caused by the geometric shape of the steel-bracing members for X-braced diaphragms, which transferred loads to the bottom flange of Beam BM4. For the K-braced diaphragms, the diagonal-bracing members were not connected to the bottom flange of the PC girders. The use of the RC diaphragm produced relatively small strains in Beam BM4 compared to those strains that were associated with the use of the steel diaphragms. About an 80-percent difference occurred for the maximum, principal-tensile strains that were induced in Beam BM4, when the RC diaphragms were used rather than the K-braced

diaphragms. This relatively large, percent difference in the strains was due to the existence of the horizontal strut in the two, steel diaphragms that was located at the bottom flanges of the PC girders.

Figures 5.40 and 5.41 show the maximum, principal-tensile strains that are induced in the impacted girder for the different diaphragm conditions, when the 60-kip, lateral-impact load with a 0.10-sec., duration time was applied at 16 ft away from the mid-span of Beams BM1 and BM5,

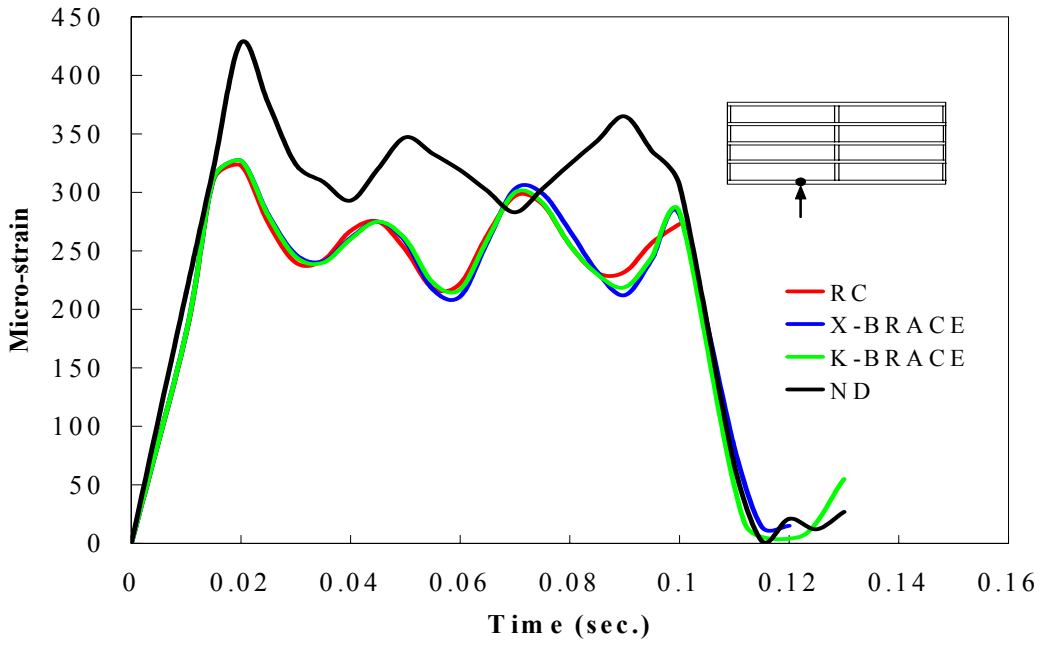

Figure 5.40. Maximum principal-tensile strain in Beam BM1 versus time for the diaphragm conditions (16-ft load offset on Beam BM1)

respectively. For all cases, the largest strains were at the top fibers of the web, where the web was connected to the top flange. The strain-versus-time behavior and the magnitude for these strains that are shown in these two figures are essentially identical. The three types of intermediate diaphragms had almost the same strain response. This strain behavior indicates that when an impact load is applied far enough away from the diaphragm location, any potential

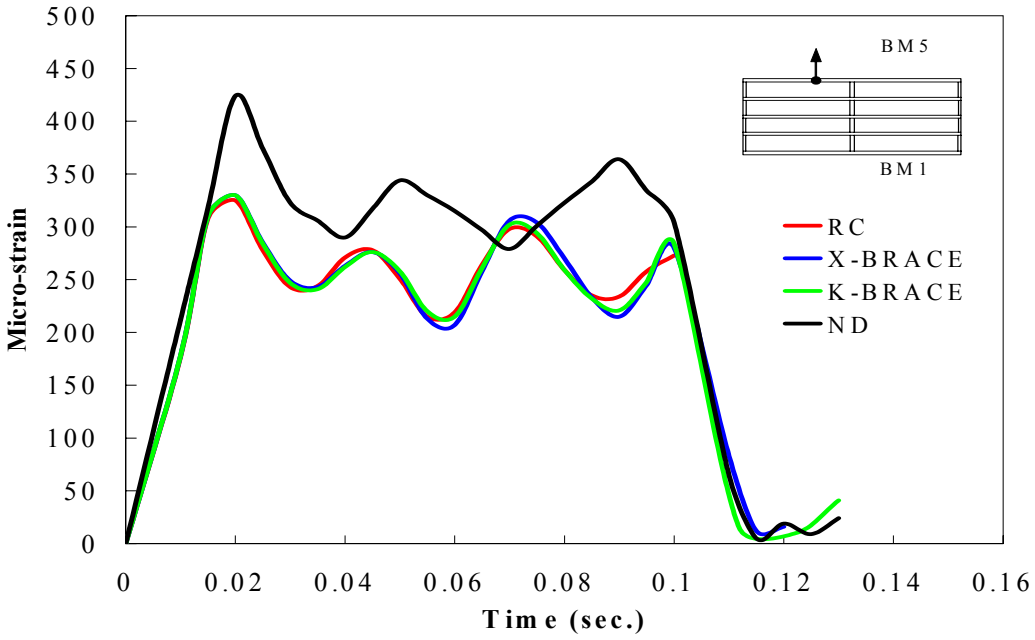

Figure 5.41. Maximum principal-tensile strain in Beam BM5 versus time for the diaphragm conditions (16-ft load offset on Beam BM5)

damage that would occur to a PC girder due to an over-height-vehicle impact does not depend on the type of intermediate diaphragms that were studied in this research. This conclusion does not weaken the previous conclusion regarding the effectiveness of intermediate diaphragms in reducing potential, impact damage, as can be observed from Figs. 5.40 and 5.41 by comparing the strain-versus-time behaviors that are associated with the diaphragm and no diaphragm conditions. As shown in these figures, the existence of any one of these three types of intermediate diaphragms reduced the maximum, principal-tensile strains in the impacted girder by about 25 percent compared to those strains that were associated with the no diaphragm condition. This type of a strain reduction is expected to increase, when the lateral load is applied closer to the intermediate diaphragms. A study involving impact loads that are applied closer to the intermediate diaphragms is discussed in Section 5.3.4.

5.3.3.2. Displacement comparisons

Figures 5.42 and 5.43 show the horizontal displacements at the bottom flange of the impacted girder, when the 120-kip, impact load was applied at the mid-span of Beams BM1 and BM5, respectively, for the four, intermediate-diaphragm conditions. The displacement-versus-time behavior and displacement magnitudes that are shown in these two figures are almost identical. The displacement results that are associated with the two, steel, intermediate diaphragms were basically the same. Both the K-braced and horizontal strut and the X-braced and horizontal strut, intermediate diaphragms produced about a 48-percent reduction in the maximum, horizontal displacement of the impacted girder compared to that for the same bridge without intermediate diaphragms. The use of the RC, intermediate diaphragms reduced the maximum, horizontal displacement of the impacted girder by about 58 percent compared to that displacement which was associated with the no diaphragm condition. These displacement results demonstrate that a RC, intermediate diaphragm is more axially rigid than either type of steel, intermediate diaphragm.

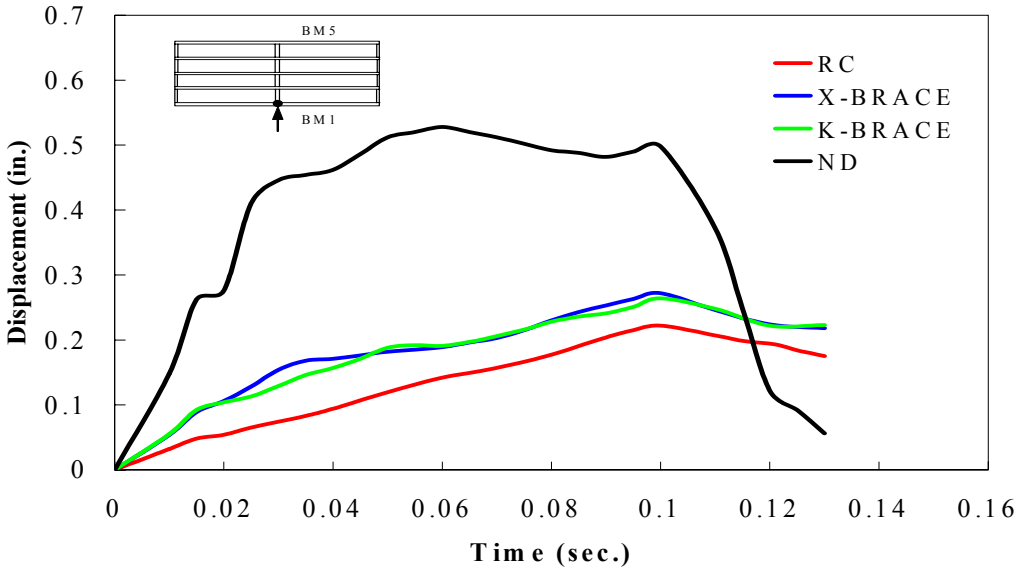

Figure 5.42. Horizontal displacement of Beam BM1 versus time for the diaphragm conditions (no load offset on Beam BM1)

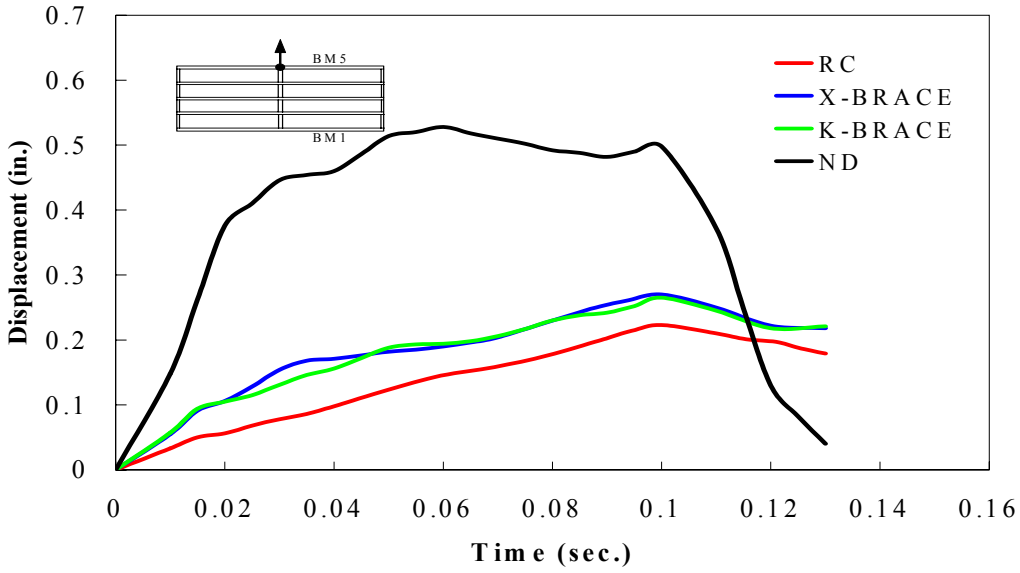

Figure 5.43. Horizontal displacement of Beam BM5 versus time for the diaphragm conditions (no load offset on Beam BM5)

The horizontal displacements at the bottom flange of the impacted girder, when the 60-kip, impact load was applied at a distance of 16 ft away from the mid-span of Beams BM1 and BM5 are presented in Figs. 5.44 and 5.45, respectively. A comparison of the displacement results that are shown in these two figures, revealed that the displacement-versus-time behavior and the displacement magnitudes for each intermediate-diaphragm condition are essentially the same. The horizontal displacements of the impacted girder that were associated with all three intermediate-diaphragm types were almost identical up to the maximum displacement that occurred about 0.75 sec. after the start of the impact load. About a 15-percent reduction the maximum, horizontal displacement of the loaded girder occurred because of the existence of any one of the three intermediate diaphragms, when compared with that displacement which occurred when the intermediate diaphragms were omitted from the same bridge. These displacement results confirmed that the existence of any one of the three types of intermediate diaphragms that were investigated in this research increased the lateral rigidity of the bottom flanges for the girders above that for the same bridge without intermediate diaphragms.

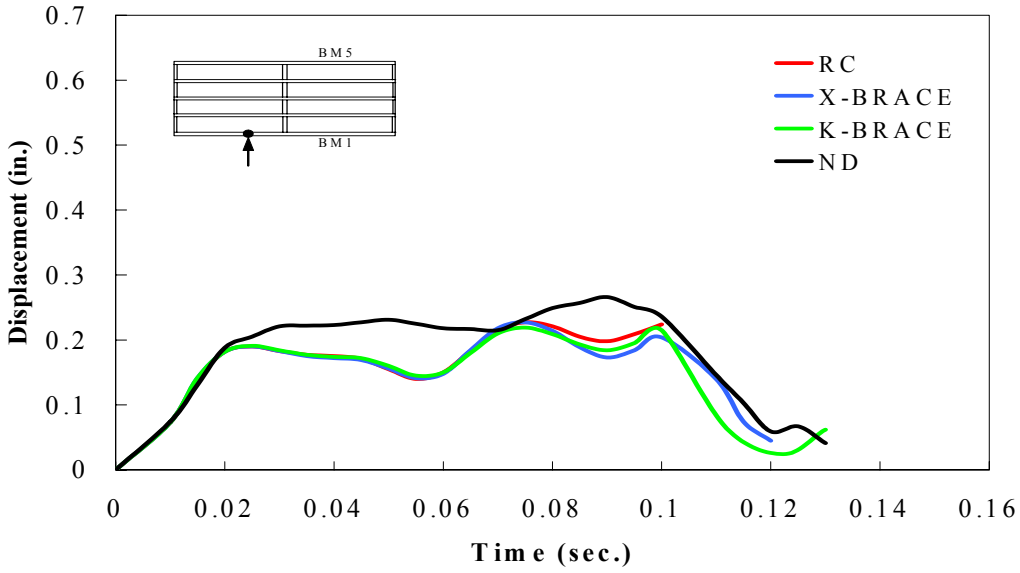

Figure 5.44. Horizontal displacement of Beam BM1 versus time for the diaphragm conditions (16-ft offset on Beam BM1)

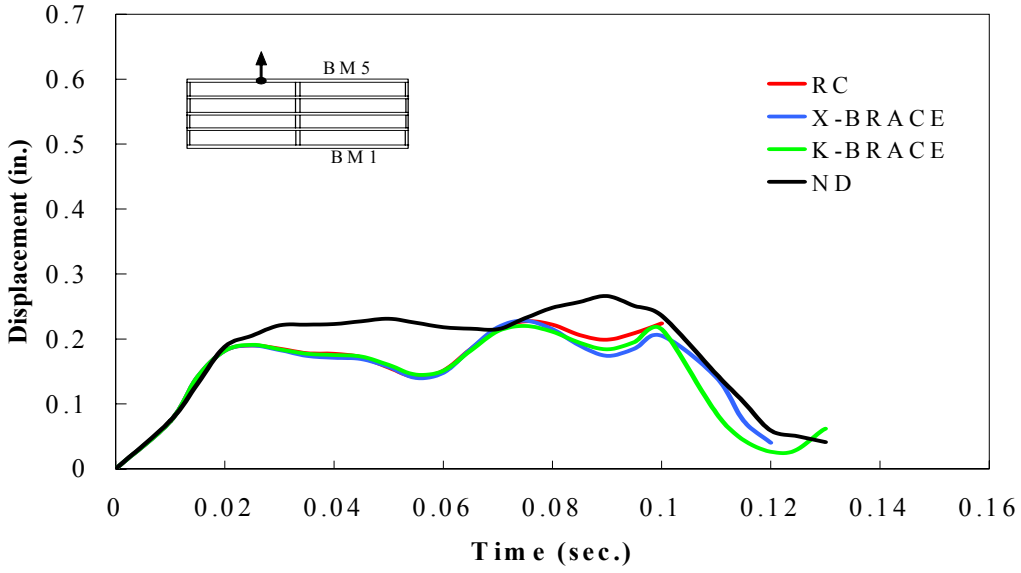

Figure 5.45. Horizontal displacement of Beam BM5 versus time for the diaphragm conditions (16-ft offset on Beam BM5)

5.3.4. Four foot load case

The effectiveness of intermediate diaphragms in reducing impact damage to PC-bridge girders depends on the location of the impact force relative to the location of the intermediate diaphragms. The previous investigations for impact loads that were applied to PC girders were performed when these loads were at the diaphragm location or at 16 ft away from the diaphragm location. As shown in Fig. 4.7, the point of impact for an over-height vehicle load that may hit the bottom flange of a PC girder is based on the width of the roadway passing underneath the bridge. All three types of intermediate diaphragms that were investigated in this research provided the PC girders with essentially the same degree of impact protection when the impact load was applied at a distance that was 16 ft away from the diaphragms. However, when the impact load was applied at the intermediate diaphragm location, different degrees of impact protection were provided by each diaphragm type.

To investigate the effect of load impacts that are close to but not at the intermediate-diaphragm location on the maximum, principal-tensile strains, which are induced in an impacted girder, a 4-ft offset for the impact load from the diaphragm location was selected for all four, intermediate-diaphragm conditions. The 60-kip, impact load shown in Fig. 4.23b was applied as a pressure, as shown in Fig. 4.24. Beam BM1 was considered as the impact girder in this study. The maximum, principal-tensile strain that were induced in this girder for the three types of intermediate diaphragms and for the same bridge without intermediate diaphragms is presented in Fig. 5.46. Due to the rotational restraint about the longitudinal axis for a PC girder that is provided by the intermediate diaphragms, the location for the maximum, principal-tensile strains in the loaded girder was not the same for the bridge with and without intermediate diaphragms.

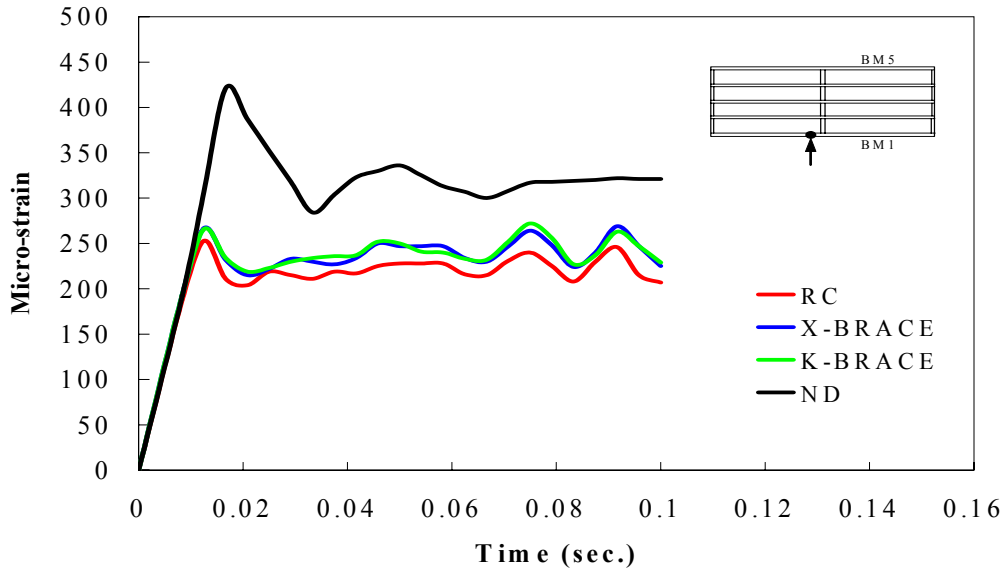

Figure 5.46. Maximum principal-tensile strain in Beam BM1 versus time for the diaphragm conditions (4-ft load offset on Beam BM1)

For the three types of intermediate diaphragms, the largest strains were in the bottom flange of the loaded girder and at the girder cross section where the impact load was applied. For the no diaphragm condition, the largest strains occurred in the top fibers of the web for this girder and at the girder cross section where the impact load was applied. As shown in Fig. 5.46, the strain-versus-time behaviors and the strain magnitudes that were associated with the three types of intermediate diaphragms were still very close to each other. Again, the strain results for the bridge with either type of steel, intermediate diaphragm were almost the same. The use of either type of steel diaphragm reduced the maximum, principal-tensile strain that was induced in the impacted beam by about 36 percent compared to those strains that were associated with the bridge without intermediate diaphragms. The use of the RC, intermediate diaphragms produced about a 40-percent reduction in the maximum strains, induced in the impacted girder, when compared to those strains for the no diaphragm condition. These minor differences in the percent reduction in strain implied that the degree of impact protection for the impacted, PC

girder that is provided by each of the three types of intermediate diaphragm is essentially identical, when the impact load was applied at 4 ft from the diaphragm location.

5.4. Skewed bridge model

This section addresses the analytical results for the skewed-bridge, finite-element model shown in Fig. 4.16. Bridges with a significant-skew angle have a staggered arrangement for the intermediate diaphragms. The description of the finite-element model was presented in Section 4.3.1. Since variation in the magnitude of the dynamic-load factor (DLF) was small for all the intermediate diaphragm conditions that were investigated for the non-skewed-bridge model (see Section 4.4.3), the ISU researchers decided to conduct the investigations of the skewed-bridge models using a static analysis instead of a dynamic analysis. The magnitudes and locations for the lateral loads that were applied to the skewed-bridge model are discussed in Section 4.4.3.

Figure 5.47 shows the maximum, principal-tensile strains that were induced in the directly load girder (Beam BM1) for the four, intermediate-diaphragm conditions, when the 60-

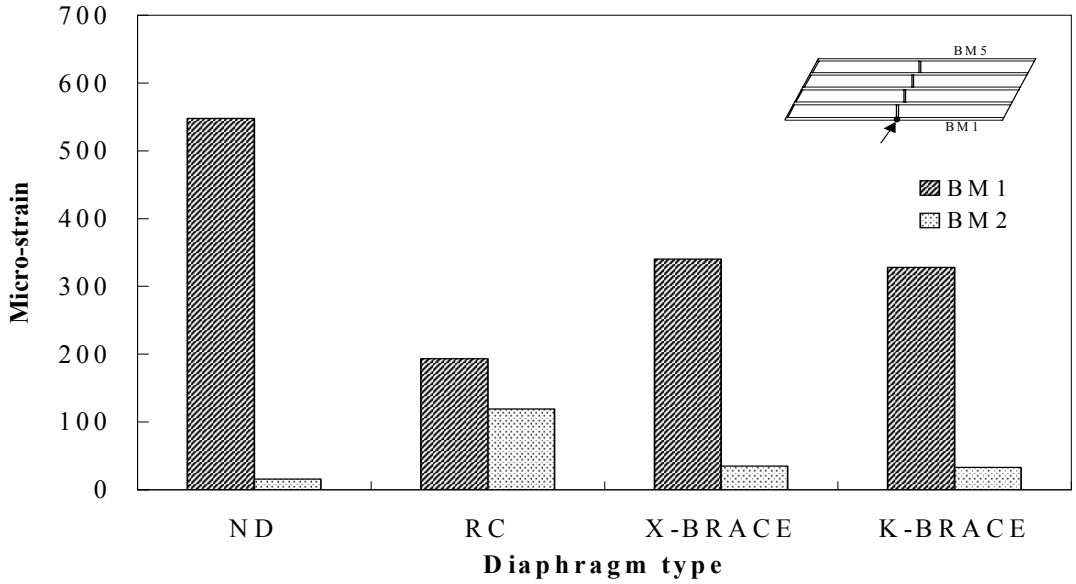

Figure 5.47. Maximum principal-tensile strains in Beams BM1 and BM2 for the diaphragm conditions in the skewed bridge (no load offset on Beam BM1)

kip, static load was applied to the bottom flange of Beam BM1 and at the mid-span, intermediate-diaphragm location. The strain data presented in this figure are for the directly loaded girder (Beam BM1) and the adjacent girder (Beam BM2). For the three types of intermediate diaphragms, the maximum strains in Beams BM1 and BM2 were in the bottom flange and at the girder cross section where the intermediate diaphragm was installed between these two girders. When intermediate diaphragms were omitted (the ND-diaphragm type shown in Fig. 5.47) from the bridge, the maximum strains were in the top fibers of the web and at the location of the applied load. Figure 5.47 shows that when intermediate diaphragms were omitted from the bridge, the 120-kip, inclined-plan-view, static load, which was applied to the mid-span of Beam BM1, induced a 548 micro-strains, maximum, principal-tensile strain in Beam BM1. For these same conditions, very small strains were induced in Beam BM2.

The use of intermediate diaphragms in the bridge reduced these strains in the directly loaded beam (Beam BM1) and caused the transfer of a portion of the statically applied load to the adjacent beams. The strain results that are shown in Fig. 5.47 for K-braced and horizontal strut and X-braced and horizontal strut, intermediate diaphragms are essentially the same. Therefore, the ISU researchers concluded that the two types of steel diaphragms provided basically the same amount of damage protection to the directly loaded girder (Beam BM1) and to the adjacent girder (Beam BM2). The use of the RC diaphragms and either type of steel diaphragm provided about a 65-percent reduction and about a 39-percent reduction, respectively, in the maximum, principal-tensile strains that were induced in Beam BM1, when compared to those strains that were associated with the no diaphragm condition. Although the RC diaphragms would provide more damage protection to the directly loaded girder (Beam BM1) than that which would be provided by the two types of steel diaphragms, the use of the RC

diaphragms induced more strains in the adjacent girder (Beam BM2) than that which was induced by either type of steel diaphragm. About a 70-percent increase occurred in the maximum, principal-tension strains that were induced in the Beam BM2 when the RC diaphragms rather than either type of steel diaphragm was used in the bridge. This induced-strain result for Beam BM2 contradicts a similar strain comparison that was made for the non-skewed bridge (see Fig. 5.35). The ISU researchers believe that this difference in the strains for the adjacent girder in skewed and non-skewed bridges was due to the staggered alignment of the intermediate diaphragms for the skewed bridge.

Figure 5.48 presents the maximum, principal-tensile strains in Beams BM4 and BM4 for the four, intermediate-diaphragm conditions, when the 120-kip, inclined-plan-view, static load was applied at the mid-span diaphragm location on Beam BM5. The location for the maximum

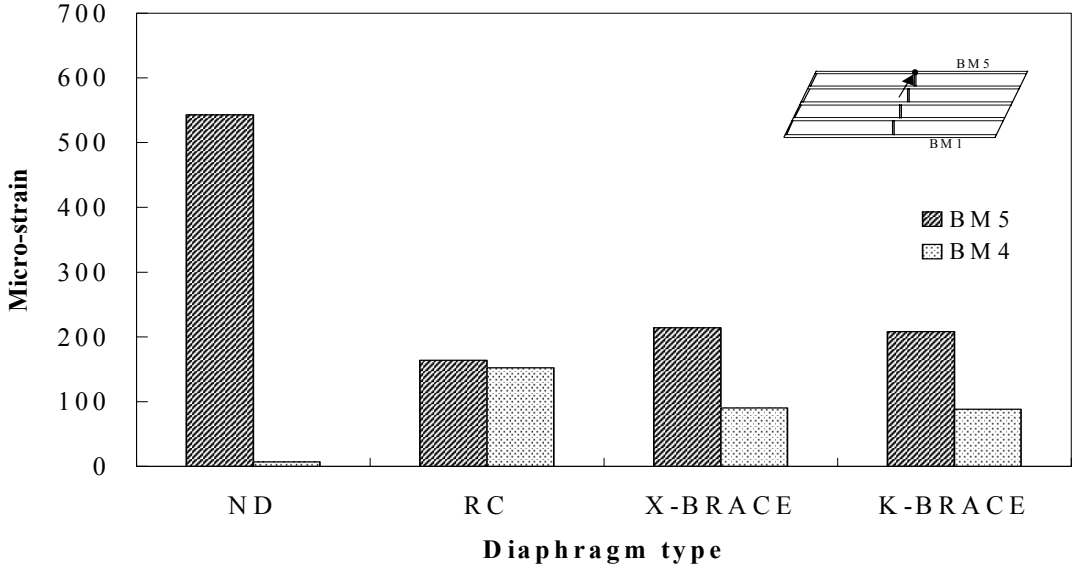

Figure 5.48. Maximum principal-tensile strains in Beams BM5 and BM4 for the diaphragm conditions in the skewed bridge (no offset load on Beam BM5)

strains in the directly loaded girder and in the adjacent girder was the same as that associated with Fig. 5.47. A comparison of Figs. 5.47 and 5.48 revealed a similar relationship for the strain magnitudes amongst the three types of intermediate diaphragms. Again, the K-braced and horizontal strut and X-braced and horizontal strut, intermediate diaphragms cause essentially the same maximum, principal-tensile strains to be induced in the directly loaded girder and adjacent girder. Based on the strain results that are shown in Fig. 5.48, the RC, intermediate diaphragm provided the directly loaded girder (Beam BM5) with a slightly better degree of damage protection than that provided by the two types of steel diaphragms. About a 70-percent reduction and a 60-percent reduction in the maximum strains in the directly loaded girder (Beam BM5) was caused by the use of the RC diaphragms and by the use of either type of steel diaphragm, respectively, when compared to those strains for the same bridge without intermediate diaphragms. Also based on the strain results that are shown in Fig. 5.48, the amount of potential damage to the adjacent girder that is caused by an impact load on Beam BM5 would be higher when the RC, intermediate diaphragms are used in the bridge than that when either the K-braced or X-braced, intermediate diaphragms are used in the bridge. This conclusion is the same one that was made when Beam BM1 was the directly loaded girder (see Fig. 5.47).

To study the behavior of the skewed-bridge when an over-height vehicle strikes an exterior girder at a location that was not at the intermediate diaphragms, two sets of structural analyses were performed for the modeled-bridge span with the four, intermediate-diaphragm conditions. In one set of analyses, Beam BM1 was the directly loaded girder, and in the other set of analyses, Beam BM5 was the directly loaded girder. A 60-kip, inclined-plan-view, static load was applied to these beams at a point that was 16 ft away from the intermediate diaphragms, as shown in Fig. 4.17.

Figure 5.49 shows the maximum, principal-tensile strains that were induced in the directly loaded girder (Beam BM1) when the load was applied at 16 ft away from the mid-span of Beam BM1. All of the strains shown in Fig. 5.49 were induced in the top fiber of the girder web and at the girder cross section where the load was applied to Beam BM1. The figure shows that the use of any one of the three types of intermediate diaphragms that were investigated in this research had essentially no effect on the maximum, principal-tensile strains that were induced in Beam BM1, when the lateral load was applied to a point that was at a substantial distance from the intermediate diaphragms in the skewed bridge. This conclusion was not true for the non-skewed bridge with a similar loading condition. Recall that for this lateral-load position on the non-skewed bridge, the type of intermediate diaphragm had an affect on the maximum, principal-tensile strains that were induced in Beam BM1. The difference in the geometrical arrangement of the intermediate diaphragms for the non-skewed and skewed bridges

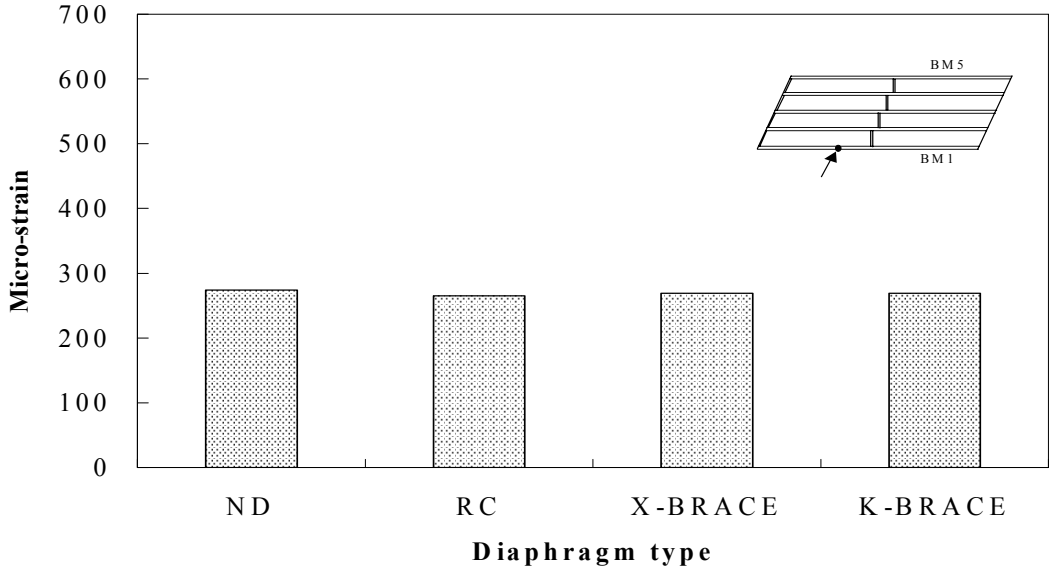

Figure 5.49. Maximum principal-tensile strains in Beam BM1 for the diaphragm conditions in the skewed bridge (16-ft offset load on Beam BM1)

caused this difference in the maximum, principal-tensile strains in the directly loaded girder for these bridge geometries.

5.5. Maximum principal-tensile strain locations

The finite-element models for the non-skewed and skewed, prototype, PC-girder bridges, which were subjected to a lateral load, predicted that the location of the maximum, principal-tensile strains is dependant on the impact location. When the impact was on the bottom flange of a PC girder at an intermediate diaphragm location, the maximum, principal-tensile strains were induced in the bottom flange of the impacted girder at the diaphragm location. When the impact was on the bottom flange of a PC girder at a significant distance away from an intermediate diaphragm location, the maximum, principal-tensile strains were induced in the upper portion of web just below the top flange of the impacted girder at the location of the impact. When the impact was on the bottom flange of a PC girder at a location that was adjacent to but not at an intermediate diaphragm location, the maximum principal-tensile strains were induced in the web just below the top flange of the impacted girder at the location of the impact and large principal-tensile strains were also induced in the bottom flange of the impacted girder at the diaphragm location. Figure 5.50 shows regions of a PC girder where close observations need to be made during field inspections of an impacted bridge to assess potential damage to the PC girder.

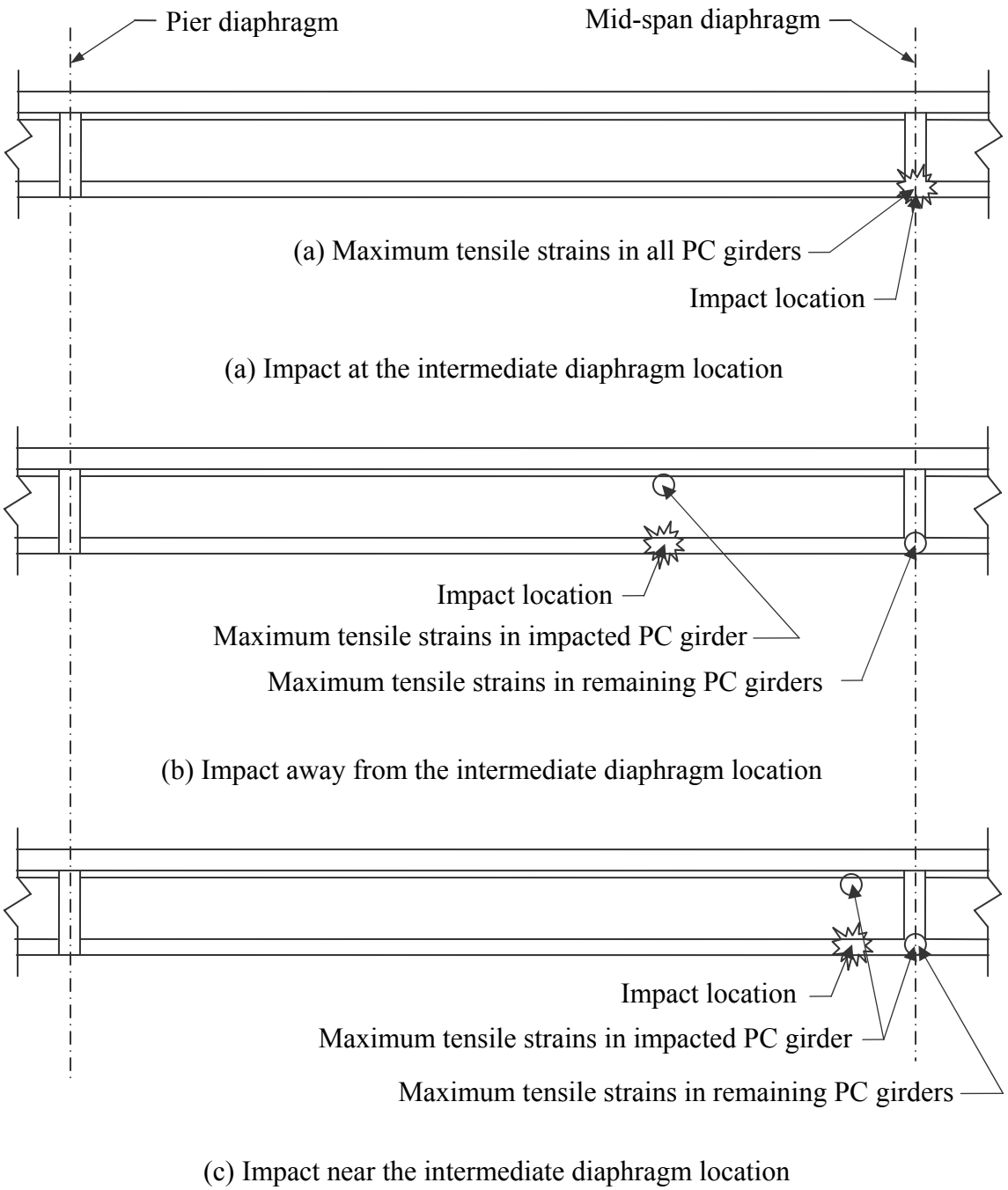

Figure 5.50. Locations for maximum principal-tensile strains

6. CLOSING REMARKS

6.1. Summary

This research analytically evaluated the maximum, principal-tensile strains in the PC girders and the maximum, horizontal displacements at the bottom flanges for the PC girders of a non-skewed bridge and a skewed bridge. These strains and displacements were induced by a lateral load, which was applied to the bottom flange of either exterior girder for the bridge. This load was either a single-magnitude, dynamic-load pulse or a static, concentrated load that was not intended to actually model the collision forces that occur when an over-height vehicle or vehicle load strikes a bridge girder. The hypothetical, dynamic load and the static load were used to establish a qualitative comparison of the maximum, principal-tensile strains and horizontal displacements for the bridge girders to determine the effectiveness of intermediate diaphragms in reducing the potential damage sustained to the PC girders when an exterior girder was subjected to a simulated, lateral-impact load. This research also investigated the possibility of substituting a steel, intermediate diaphragm, which has a practical configuration and connection details, as an alternative for the RC, intermediate diaphragms that are currently used by the Iowa DOT in PC-girder bridges. The steel, intermediate diaphragm needs to provide the bridge girders with essentially the same degree of impact-damage protection as that which is provided by the current RC diaphragm.

A literature search was conducted to review publications related to the use of intermediate diaphragms in resisting lateral loads. Several domestic and international data bases were used for this search. Most of the publications discussed diaphragm effectiveness in laterally distributing wheel loads. Only a few publications addressed the resistance of intermediate diaphragms to lateral loads. Different points of view regarding the lateral-load-

resistance effectiveness of diaphragms were documented in the literature. Some of the opinions and conclusions in these publications contradicted each other about whether intermediate diaphragms are useful or harmful in PC-girder bridges.

A survey was conducted of the departments of transportation in all fifty states to determine the types of intermediate diaphragms that are currently used by their design agencies and to establish the methods that are used to design these diaphragms. The survey included questions related to the types of intermediate diaphragms for PC-girder bridges when a bridge is crossing a highway, a navigable waterway, a railroad right-of-way, or a grade separation without traffic beneath the bridge.

Before a finite-element model for a PC-girder bridge with intermediate diaphragms can be used to predict member strains and displacements, calibration of a similar model that incorporates the specific details that will be used in the final models needs to be performed by comparing predicted responses with known measured values. This calibration was done using experimentally measured, girder strains and displacements from published test results. The purpose of this calibration study was to develop the type of finite elements and the appropriate mesh size that should be used in modeling PC-girder bridges. Several sizes of finite-element meshes and detail-modeling techniques were investigated to improve the accuracy of the predicted results.

Two, four-span, Iowa DOT, PC-girder bridges were used as prototype bridges for creating the finite-element models that were used in this research. One of these bridges was essentially a non-skewed bridge and the other one was a 30-deg., skewed bridge. Due to the complexity of the finite-element models and the large amount of computer time that was required to solve a complete-bridge model, only one of the two, interior spans was modeled for the final

analyses. The accuracy of using single-span models was verified by computing displacements and strains for the PC girders that were predicted by both the single-span and four-span models and then comparing these results. This single-span-model simplification was proven not to significantly affect the displacement results for the PC girders. The model simplification produced less than a 15-percent underestimation of the maximum, principal-tensile strains in the PC girders.

Three types of intermediate diaphragms that were located at the mid-span of the girders were considered in this study. These diaphragms were a RC diaphragm, an X-braced with horizontal strut, steel diaphragm, and a K-braced with horizontal strut, steel diaphragm. The three types of diaphragms are currently used by the Iowa DOT in PC-girder bridges.

In the study of the non-skewed bridge, the two, exterior girders were loaded by a lateral-impact load that was used to simulate the effect of an over-height vehicle or vehicle load striking the bottom flange of a PC girder when the vehicle passed beneath the bridge. In the study of the skewed bridge, a static rather than a dynamic load was used to simplify the analytical solution. This static-load-modeling simplification was determined not to significantly affect the displacement and strain results for the PC girders because the dynamic-load factor for the non-skewed, bridge model with the different intermediate-diaphragm conditions was between 1.15 and 1.20. A lateral load was applied at the mid-span, cross section for the impacted girder or at 16 ft from the mid-span. To study the diaphragm effectiveness in reducing the potential damage to the PC girders when the lateral load was close to the diaphragm location, the models were analyzed for an impact load on one of the exterior girders at four feet from the diaphragm location.

A qualitative prediction for the occurrence of damage to a PC girder that was caused by an impact load was based on the magnitude of the maximum, principal-tensile strains that were induced in each PC girder. To predict the effectiveness of a particular type of intermediate diaphragm in providing impact protection for a PC girder, these strains for the impacted girder were compared to those strains that were induced in that same girder, when intermediate diaphragms were omitted from the bridge span. The spread of damage to other girders was examined in similar ways. These strain results that were associated with the different types of intermediate diaphragm were compared to each other to determine the relative effectiveness of each diaphragm type in preventing damage to a PC girder.

6.2. Conclusions

The following conclusions were made from this study:

- Approximately 75 percent of the state departments of transportation returned the survey questionnaire. Almost 95 percent of the respondents use intermediate diaphragms in PC-girder bridges. Less than 40 percent of the respondents use structural-steel diaphragms in PC-girder bridges, and about 95 percent of them permit their use of cast-in-place, RC diaphragms, when a bridge crosses over a highway. Approximately 70 percent of the respondents documented that they do not use intermediate diaphragms to minimize the potential damage to the PC girders that would result from impact forces that are caused by an over-height vehicle or vehicle load passing beneath the bridge.
- The ANSYS, finite-element method has the capabilities to accurately model PC-girder bridges with complex connection details between the intermediate diaphragms and the girders, when lateral-impact loads are applied to the structure. During the calibration process for establishing the proper modeling details, predicted member strain and

displacement results were compared to those measured results from a previous research study (Abendroth, et al. 1991). An average, maximum, difference of 20 percent was observed in the strain and displacement results that were predicted by a finite-element model and those results that were measured during the previous testing of an experimental bridge. These differences could have resulted from the presence of concrete cracks in the bridge deck for that experimental bridge. Concrete cracks were not included in the idealization of the bridge structure for the finite-element analysis.

- Modeling only one of the spans instead of modeling all four spans of the bridge for the finite-element analysis, did not significantly affect the overall bridge responses for that single span. A comparison of the displacement and strain responses that were predicted by the two, analytical models revealed that the difference in the horizontal displacements of the girders were insignificant and the difference in the maximum, principal-tensile strains, which were induced in the impacted girder, was less than 15 percent.
- The dynamic-load factor (DLF) for the induced, maximum, principal-tensile strains in the PC girder that was subjected to the impact load was in the range of 1.15 to 1.20 for the three, intermediate diaphragms that were investigated in this research. This small range for the DLF indicated that the type of intermediate diaphragm had a minor effect on the dynamic characteristics of the PC girder bridge.
- Although the K-braced with horizontal strut, intermediate diaphragm may provide PC-bridge girders with a slightly better degree of impact-damage protection than that which may be provided by the X-braced with horizontal strut, intermediate diaphragm, the difference in performance between these two types of steel diaphragms was not sufficient to recommend using the K-braced diaphragm instead of the X-braced diaphragm.

- Both the X-braced with a horizontal strut and K-braced with a horizontal strut, intermediate diaphragms essentially provided the same degree of rigidity to a bridge structure. This conclusion was reached by observing essentially equal, horizontal displacements at the bottom flange of a directly loaded girder in bridges with these two types of diaphragms.
- The RC, intermediate diaphragms would provide the PC-bridge girders with a higher degree of impact-damage protection than that provided by the two types of steel diaphragms, when a lateral-impact load was applied directly at the diaphragm location.
- A comparison of the horizontal displacements of the PC girders in a bridge span with the RC, intermediate diaphragms and another, identical, bridge span with either the K-braced, or X-braced intermediate diaphragms, revealed that the RC diaphragm was more axially rigid than that for either type of steel diaphragm.
- The RC, intermediate diaphragm has a slightly greater capability of limiting extent of the potential damage along the length of the impacted girder than that for either the K-braced with horizontal strut or the X-braced with horizontal strut, intermediate diaphragms.
- For the non-skewed bridge, both the K-braced with horizontal strut and the X-braced with horizontal strut, intermediate diaphragms would permit more damage to occur in the PC girder that is adjacent to the impacted girder than that for the RC, intermediate diaphragms. Even though the RC, intermediate diaphragm had more axial rigidity than that for either of two, steel diaphragms, the RC diaphragm was less capable of spreading impact damage to the adjacent bridge girder because of this diaphragm's geometrical configuration and connections to the bridge girders.

- For the skewed bridge, both the K-braced with horizontal strut and the X-braced with horizontal strut, intermediate diaphragms provided more impact-damage protection to the girder that was adjacent to the impacted girder than that provided by the RC, intermediate diaphragms. This damage assessment, which was the reverse of that for the non-skewed bridge, was caused by the staggered arrangement of the diaphragms in the skewed bridge compared to the aligned arrangement of the diaphragms in the non-skewed bridge.
- The diaphragm type had a significant effect on the amount of impact-damage protection that was provided for the PC-bridge girders when the impact force was at the diaphragm location.
- The diaphragm type did not have any significant effect on the amount of impact-damage protection that was provided for the PC-bridge girders, when the impact force was applied at even a relatively small distance from the diaphragm location.
- When an over-height vehicle or vehicle load strikes a bridge girder at a point that is not at a diaphragm location, the existence of intermediate diaphragms would reduce the amount of damage to the PC-bridge girders.
- For most geometrical alignments for highway overpasses, an over-height vehicle or vehicle load that travels beneath a bridge would strike a bridge girder at a point that is not at a diaphragm location. Then, the RC, K-brace with horizontal strut, or the X-brace with horizontal strut, intermediate diaphragm could be used in a PC-girder bridge and essentially the same degree of impact-damage protection would be provided to the bridge girders by each of these types of intermediate diaphragms.

6.3. Recommendations for future work

The following recommendations for future work were made to provide a better understanding of the effects that impact loads have on PC-girder bridges.

- More experimental testing should be conducted to investigate the effect of the type of intermediate diaphragm when an impact load is applied to a PC girder at a point which is at or not at a diaphragm location.
- More advanced, finite-element analyses should be performed to more accurately predict girder strains and displacements that are caused by impact loads. In these analyses, concrete cracking and the prestressing forces in the PC girders should be incorporated into the finite-element models.
- A more expanded study should be conducted on the effect of the magnitude and duration time of an impact load on the overall response of PC-girder bridges.

REFERENCES

Abdullatif K. Zaouk, Nabih E. Bedewi, Cing-Dao Kan, and Dhafer Marzougui. (1996). "Validation of a non-linear finite element vehicle model using multiple impact data," AMD-vol. 218, *Crashworthiness and Occupant Protection in Transportation Systems, ASME,* pp. 91-106.

Abendroth, R. E., Klaiber, F. W., and Shafer, M. W. (1991). "Lateral load resistance of diaphragms in prestressed concrete girder bridges." *Iowa DOT Project HR-319*, ISU-ERI-Ames-92076, Highway Division of the Iowa Department of Transportation and the Highway Research Advisory Board.

American Association of State Highway and Transportation Officials (AASHTO), (1996). *Standard Specifications for Highway Bridges*, 16th Edition. Washington, DC.

American Institute of Steel Construction, Inc. (AISC), (2002). *LRFD Manual of Steel Construction, Load and Resistance Factor Design*, 3rd Edition.

Andrawes, B.O. (2001). "Lateral impact response for prestressed concrete girder bridges with intermediate diaphragms," M.S. thesis, Iowa State University, Ames, Iowa.

Cheung M. S., R. Jategaonkar, and L.G. Jaeger. (1986). "Effects of intermediate diaphragms in beam-slab bridges." *Canadian Journal of Civil Engineering*, vol. 13, No. 13, June, pp. 278-292.

De Salvo G. J., and J. A. Swanson. (1985). *ANSYS Engineering Analysis System User's Manual*, vols. 1-4, Houston, Penn.: Swanson Analysis System, Inc.

Doong, J. and Cheng, J. C. (1994). "Computer simulations for frontal impact." *Computers in Engineering*, vol. 2, 1994, ASME, pp. 597.

Johnson, W. R., Baughn, T. V., and Johnson, D.B. (1992). "Modeling and simulation of a low speed passenger car collision." *International Journal of Vehicle Design*, vol. 13, nos. 5/6, pp. 505-523.

Kostem, C. N., and DeCastro, E. S. (1977). "Effects of diaphragms on lateral load distribution in Beam-Slab bridges." *Transportation Research Record 903*, Transportation Research Board, pp. 6-9.

McCathy W., K. R. White, and J. Minor. (1979). "Interior diaphragms omitted on the Gallup East Interchange Bridge—Interstate 40." *Journal of Civil Engineering Design*, vol.1, No.1, pp. 95-112.

Nalepa, E. (1990). "Crash-worthiness simulation of the Opel Vectra using the explicit finite element method." *International Journal of Vehicle Design*, vol. 11, no. 2, pp. 160.

Omar, T. A., Eskandarian, A., and Bedewi, N. E. (1998). "Crash analysis of two vehicles in frontal impact using adaptive artificial neural networks." AMD-vol. 230/BED-vol. 41, *Crashworthiness, Occupant Protection and Biomechanics in Transportation Systems*-1998, ASME, pp. 115-129.

Shanafelt G. O., and Horn W. B. (1980). "Damage evaluation and repair methods for prestressed concrete bridge members." *NCHRP Report 226*, Nov., pp. 66.

Sengupta S., and J.E. Breen. (1973). "The effect of diaphragms in prestressed concrete girder and slab bridges." *Research Report 158-1 F, Project 3-5-71-158*, Center for Highway Research, The University of Texas at Austin, October.

Sithichaikasem S., and W. L. Gamble. (1972). "Effect of diaphragms in bridges with prestressed concrete I-section Girders." *Civil Engineering Studies No. 383*, University of Illinois, Urbana.

Wei, Benjamin C. F. (1959). "Load distribution of diaphragms in I-Beam bridges." *Journal of Structural Division*, proceedings of the American Society of Civil Engineers, vol. 85, No. ST 5, May.

Wong, A. Y. C., and W. L. Gamble. (1973). "Effects of diaphragms in continuous slab and girder highway bridges." *Civil Engineering Studies, Structural Research Series No. 391*, University of Illinois, Urbana.

APPENDIX A: DESIGN AGENCY QUESTIONNAIRE RESULTS

The number shown in ( ) represents the number of design agencies that have selected this answer. The notes between [ ] are the agencies comments on specific questions.

Part I. State or Agency and Policy on the Use of Intermediate Diaphragms

1. Is your state or agency currently specifying any type of intermediate diaphragms for PC bridges?

   (36) Yes

   (2) No ***(If you answered no, please skip to Question 5 in this part of the survey.)***

2. Does your state or agency use structural-steel, intermediate diaphragms in PC girder bridges?

   (14) Yes

   (22) No ***(If you answered no, please skip to Part II of the survey.)***

3. Why does your state or agency use structural-steel, intermediate diaphragms in PC girder bridges? ***(Please check all that apply.)***

   (3) State or agency requirement.
   (1) To facilitate the use of stay-in-place, precast panel or metal deck forms that are used in bridge decks.
   (6) Bridge contractors have not chosen to use a reinforced concrete diaphragm alternate.
   (10) Other reason (please specify) __[Its faster, easier and cheaper than cast-in-place concrete diaphragms]

   (Please skip to Part II of the survey.)

4. Has your state or agency ever specified intermediate diaphragms for PC bridges?

   (8) Yes

   (0) No

   (If you answered no, please stop here. Do not complete the rest of the survey. Please return the survey in the enclosed, postage-prepaid, self-addressed envelope.

5. When did your state or agency discontinue using intermediate diaphragms for PC bridges?

(0) Date is not known.

(4) Date is known.

When? _____

6. Why did your state or agency discontinue using intermediate diaphragms for PC bridges?

(0) Reason is not known.

(4) Reason is known.

Why? [Based on research results, which demonstrated that intermediate diaphragms do not affect live load distribution]

Note: Please answer the remaining questions in this survey with respect to the last time intermediate diaphragms were used in PC girder bridges.

Part II. Intermediate Diaphragm Construction Material

1. What type of intermediate diaphragm material is permitted by your state or agency when a PC girder bridge is above a **highway** where an over-height vehicle or load could impact against a girder bottom flange? ***(Please check all that apply.)***

(35) Cast-in-place RC concrete
(4) Precast concrete
(9) Rolled steel channel shape
(0) Welded steel channel shape
(2) Rolled steel I-shape
(0) Welded steel I-shape
(3) Steel truss
(5) Steel cross bracing
(4) Other [Bent plate steel diaphragms]

2. What type of intermediate diaphragm material is permitted by your state or agency when a PC girder bridge is above a **navigable waterway** where an over-height vessel or load could impact against a girder bottom flange? ***(Please check all that apply.)***

(32) Cast-in-place RC concrete
(4) Precast concrete
(7) Rolled steel channel shape
(0) Welded steel channel shape
(1) Rolled steel I-shape

(0) Welded steel I-shape
(3) Steel truss
(5) Steel cross bracing
(4) Other [Bent plate steel diaphragms]

3. What type of intermediate diaphragm material is permitted by your state or agency when a PC girder bridge is above a **railroad right-of-way** where an over-height load could impact against a girder bottom flange? ***(Please check all that apply.)***

(34) Cast-in-place RC concrete
(4) Precast concrete
(8) Rolled steel channel shape
(0) Welded steel channel shape
(2) Rolled steel I-shape
(0) Welded steel I-shape
(3) Steel truss
(5) Steel cross bracing
(4) Other [Bent plate steel diaphragms : no PC girder bridges over railroad]

4. What type of intermediate diaphragm material is permitted by your state or agency when a PC girder bridge is above a **grade separation that has no traffic (highway, water, or rail) of any type** below the girders? ***(Please check all that apply.)***

(33) Cast-in-place RC concrete
(4) Precast concrete
(8) Rolled steel channel shape
(0) Welded steel channel shape
(1) Welded steel channel shape
(0) Welded steel I-shape
(3) Steel truss
(5) Steel cross bracing
(4) Other [Bent plate steel diaphragms]

Part III. Design Criteria for Intermediate Diaphragms in PC Girder Bridges

1. Are intermediate diaphragms used for temporary lateral support of the PC girders during the construction of the bridge?

(32) Yes

(6) No

2. Are intermediate diaphragms used to minimize damage to the PC girders that would be caused by impacts from over-height traffic beneath the bridge?

   (12) Yes

   (26) No

3. Has your state or agency developed a structural-steel, intermediate diaphragm that can be used by bridge contractors as an alternate to a RC or PC, intermediate diaphragm in PC girder bridges which could have over-height traffic beneath the bridge?

   (9) Yes

   (29) No

4. Are **specific** criteria applied to establish the design of an intermediate diaphragm? (Note: This question only applies to the diaphragm itself and does not apply to the connections of the diaphragm to the PC girders and/or bridge deck.)

   (1) Yes *Note: A yes answer **would not** apply to a rule-or-thumb criteria.*

   (36) No *Note: A no answer **would** apply to a rule-of-thumb criteria.*

   Note: If you answered no to this question, please skip to Question 8 in this part of the survey

5. Does your state or agency use a static-lateral load to represent a lateral impact load, as a loading condition for the design of an intermediate diaphragm?

   (0) Yes

   (2) No

6. Does your state or agency use a dynamic-lateral load to represent a lateral impact load, as a loading condition for the design of an intermediate diaphragm?

   (0) Yes

   (2) No

7. What design criteria are applied to establish the size of an intermediate diaphragm?

   (1) No specific design criteria.

   (1) Specific design criteria (please specify) [Bridge cross section acts as a rigid body without deformation]

8. Are **specific** criteria applied to establish the design of the connections between an intermediate diaphragm and the PC girders and/or bridge deck?

(1) Yes *Note: A yes answer **would not** apply to a rule-or-thumb criteria.*

(37) No *Note: A no answer **would** apply to a rule-of-thumb criteria.*

Note: If you answered no to this question, please skip to Part IV of the survey.

9. Does your state or agency use a static-lateral load to represent a lateral impact load, as a loading condition for the design of the connections between an intermediate diaphragm and the PC girders and/or bridge deck?

(0) Yes

(2) No

10. Does your state or agency use a dynamic-lateral load to represent a lateral impact load, as a loading condition for the design of connections between an intermediate diaphragm and the PC girders and/or bridge deck?

(0) Yes

(2) No

11. What design criteria are applied to establish the connection between an intermediate diaphragm and the PC girders?

(0) No mechanical connection exists between an intermediate diaphragm and a PC girder.

(1) No specific design criteria.

(1) Specific design criteria (please specify) [Shear friction design]

12. What design criteria are applied to establish the connection between an intermediate diaphragm and the bridge deck?

(1) No mechanical connection exists between an intermediate diaphragm and the bridge deck..

(0) No specific design criteria.

(1) Design criteria (please specify) [Interface shear design]

Part IV. Impact Protection Performance of Intermediate Diaphragms

Complete the following table by placing a check mark in the appropriate cell to rate the overall performance of the listed intermediate diaphragm types in minimizing the damage to the PC girders caused by all incidences of lateral impacts from over-height vehicles or over-height loads striking a PC girder.

Note: If a particular intermediate diaphragm type listed is not used by your state or agency, leave that particular row in the table blank.

Intermediate Diaphragm Type	Intermediate Diaphragm Performance Rating Regarding Protection to PC Girders from Impacts Caused by Over-Height Vehicles or Over-Height Loads					
	Excellent	Good	Average	Fair	Poor	Comments
Cast-in-place RC concrete	(12)	(13)	(4)	(1)	(1)	
Precast concrete	(2)	(0)	(1)	(0)	(0)	
Rolled steel channel shape	(1)	(2)	(4)	(0)	(0)	
Welded steel channel shape	(0)	(0)	(0)	(0)	(0)	
Welded steel channel shape	(0)	(0)	(0)	(0)	(0)	
Welded steel I-shape	(0)	(0)	(0)	(0)	(0)	
Steel truss	(0)	(2)	(2)	(0)	(0)	
Steel cross bracing	(0)	(0)	(0)	(0)	(0)	
Other (specify)	(0)	(1)	(0)	(0)	(0)	

Part V. Additional Comments

In the space below, please write your comments on any topic associated with the use of intermediate diaphragms in PC girder bridges.

[Most damage happens at the bottom flange: A strike any where near the diaphragm shatters the beam: More damage between diaphragms: Damage is felt to be unrelated to type of diaphragms: Research proved that diaphragms are only necessary in the case of skewed and curved bridges: Corrosion is a problem in steel diaphragms]

Part VI. Intermediate Diaphragm Details and Specifications

Please send us a copy of your standard details and specifications for all types of intermediate diaphragms that are used for PC girder bridges by your state or agency. We are particularly interested in receiving information about structural-steel, intermediate diaphragms that have been developed by your state or agency and that can be used by bridge contractors as an alternate to RC or PC intermediate diaphragms in PC girder bridges which could be struck by over-height vehicles or loads.

Part VII. Survey Evaluation

Please indicate those questions that you had difficulty in answering by listing the survey part and the question numbers below (i.e., III-2 for Part III, Question 2).

Part VIII. Summary

Do you want to receive a copy of a summary of the survey results?

(35) Yes (35) No